The Role of DREAM/MMB-mediated mitotic gene expression downstream of mutated K-Ras in lung cancer

Die Rolle DREAM/MMB-vermittelter mitotischer Genexpression unterhalb von mutiertem K-Ras in Lungenkrebs

Doctoral thesis for a doctoral degree
at the Graduate School of Life Sciences,
Julius-Maximilians-Universität Würzburg,
Section Biomedicine

submitted by

Fabian Iltzsche

from

Riesa

Würzburg, 2017

Submitted on: ……..……..

Office stamp

Members of the *Promotionskomitee*:

Chairperson: **Prof. Dr. Jörg Schultz**

Primary Supervisor: **Prof. Dr. Stefan Gaubatz**

Supervisor (Second): **Dr. Katrin Paeschke**

Supervisor (Third): **Dr. Daniel J. Murphy**

Supervisor (Fourth): …….
(If applicable)

Date of Public Defence: ……..……

Date of Receipt of Certificates: …….

Substantial parts of this thesis were published in the following article:

Iltzsche F.*, Simon K.*, Stopp S*., Pattschull G.*, Francke S., Wolter P., Hauser S., Murphy DJ., Garcia P., Rosenwald A., Gaubatz S. (2017) „**An important role for Myb-MuvB and its target gene KIF23 in a mouse model of lung adenocarcinoma**"; *Oncogene*; 36(1):110-121

*These authors contributed equally to this work.

Table of Contents

1. Introduction

1.1. The mammalian cell cycle and its regulation

1.1.1. The mammalian cell cycle

The eukaryotic cell cycle is a complex process involving growth, replication of genetic material and division into daughter cells and is strictly controlled by a regulatory network which is - at least in parts - highly conserved from yeast to human (Morgen 2007). This precise regulation is crucial for proper cell proliferation and maintenance of genomic integrity as perturbations can lead to aberrant growth and tumorigenic developments.

The cell cycle comprises four major phases: the Gap-phases G1 and G2, the synthesis phase (S-phase) and mitosis (M-phase) (Vermeulen et al. 2003) (Fig. 1). The entirety of G1-, G2- and S-phase is also termed interphase. Upon external growth stimuli and intrinsic signals cells enter the cell cycle in early G1 and accumulate nutrients accompanied by cell growth in preparation for subsequent cell cycle events. If growth stimuli exceed a certain threshold a point of no return is achieved enforcing the cell to progress through the complete cell cycle (Pardee 1974). During the following S-phase cells duplicate their DNA and centrosomes before entering a second gap-phase (G2). In M-phase, which comprises the nuclear (mitosis) and cellular division (cytokinesis), the sister chromatids are separated and distributed into two daughter cells. Mitosis can be further divided into five stages: prophase, prometaphase, metaphase, anaphase and telophase. During prophase, chromatin condensed into chromosomes and nucleolus starts to disappear. In the subsequent prometaphase, the cell breaks down its nuclear membrane and centrosomes migrate apart, enabling the later definition of spindle poles for the spindle apparatus. Concomitantly, microtubules emanating from both sides of the spindle poles invade into the nuclear space and attach to the kinetochores, a specialized proteinaceous structure on chromatids. After alignment of chromosomes at the equatorial plate during metaphase, the cohesion between the chromosomes fades and sister chromatids migrate towards the spindle poles (anaphase). During the following telophase, chromosomes unwind into chromatin and the nuclear membrane reforms. In the final step of division, the cytokinesis, a contractile ring of actin and myosin filaments cleaves the cell into two emerging daughter cells. Afterwards, the daughter cells can re-enter the G1-phase to start a new division cycle or arrest in a non-proliferative state known as quiescence (G0-phase). Depending on growth stimuli, arrested cells are able to re-enter the cell cycle or remain in a resting state e.g. due to terminal differentiation or senescence.

To ensure accurate progression through the cell cycle and genomic integrity cells established a complex regulatory network with three principles (Morgen 2007). The G1/S checkpoint in late G1-phase marks a restriction point at which the cell has to decide whether to delay cell cycle, enter a resting phase or to progress. When cells bypass the restriction point they are committed to complete the division cycle. In response to DNA damage or replicative stress the checkpoint at G1/S boundary is

activated. Depending on the type of damage, the kinases ATM and ATR mediate a signaling cascade via the effector kinases Chk1/Chk2 and the phosphatase Cdc25A to block CDK activity which culminates in an arrest of cells in G1-phase (Musacchio and Salmon 2007). In order to maintain arrest, Chk1/Chk2 activates the tumorsuppressor p53 which in turn induces the expression of target genes like p21, an inhibitor of CDK complexes (Maya et al. 2001). The G2/M checkpoint at the G2/M boundary prevents cells from entering into mitosis with genomic DNA damage. By regulation of the kinase Wee1 and phosphatase Cdc25 cells control the activity of cyclin B-CDK1 complex which is required to promote mitotic entry (Kastan and Bartek 2004). Finally, prior transition from metaphase to anaphase the spindle assembly checkpoint (SAC) monitors the presence of unattached kinetochores to ensure accurate segregation of chromosomes. Activation of SAC inhibits the anaphase promoting complex/cylcosome (APC/C), a multi-subunit E3 ubiquitin ligase, until bipolar spindle microtubule-attachment at the kinetochores of sister chromatids and their orientation at the equatorial plate is sensed (Musacchio and Salmon 2007; Musacchio 2011).

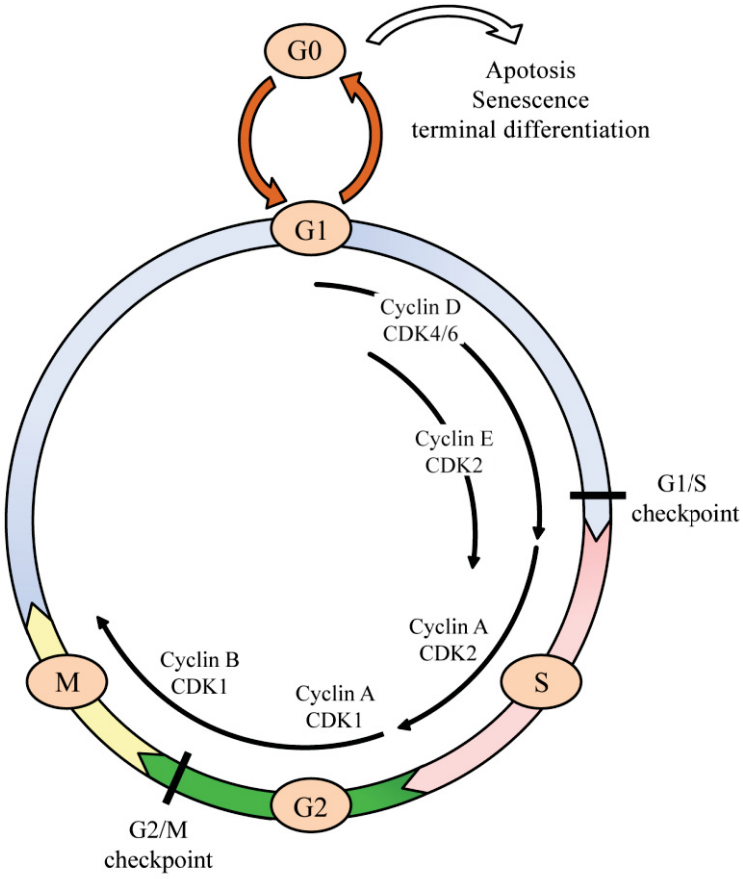

Figure 1: Simplified representation of the mammalian cell cycle
The cell cycle comprises of four major phases (S, M, G1, G2) and coordinates DNA duplication and segregation of replicated genomic material to emerging daughter cells. Thereby, progression through the cell cycle is controlled by an orchestra of oscillating Cyclin-CDK complexes. Checkpoints within the cell cycle are crucial instruments to monitor the correct progression. Cells that are no longer dividing withdraw from the cell cycle and enter into a non-proliferative state (G0). See text for detail.

1.1.2. Cyclins, Cyclin dependent kinases (CDKs) and CDK inhibitors (CKIs)

The accurate regulation of cell cycle involves a large number of proteins among cyclins and cyclin-dependent kinases (CDKs) play a fundamental role. CDKs are small heterodimeric serine/threonine kinases which are activated after formation of complexes with specific regulatory cyclin subunits (Morgan 1997, Morgan 2007). In its active form a cyclin-CDK complex initiates and coordinates cell cycle progression by transient and reversible phosphorylation of distinct target substrates (Errico et al. 2010). As soon as the complex is inactivated, substrates are rapidly dephosphorylated by specific phosphatases. So far more than 20 members of the CDK family are known of which CDK1, CDK2, CDK4 and CDK6 in combination with different cyclins are directly involved in cell cycle control (Malumbres and Barbacid 2005; Malumbres and Barbacid 2009; Lim and Kaldis 2013). In contrast to CDKs which are stably expressed throughout the cell cycle, most cyclins show an oscillating expression pattern in a cell cycle dependent manner.

Mitogenic stimuli induces the expression of D-type cyclins (D1, D2 and D3) which bind to CDK4 and CDK6 (Hunter and Pines 1994). The active cyclin-CDK complexes mediate the phosphorylation of retinoblastoma (Rb) family of transcriptional repressors hence driving the progression through G1 (Adams 2001). In late G1, E-type cyclins (E1 and E2) associate with CDK2 to promote the G1- to S-phase transition. In S-phase, cyclins of type A (A1 and A2) substitute cyclin E in their complex with CDK2 to function in initiation and completion of DNA replication (Girard et al. 1991; Ohtsubo et al. 1995). At the end of S-phase cyclin A forms a complex with CDK1 which remains stable to late G2/early mitosis. During the progression from G2- into M-phase cyclin A activity governs entry into mitosis until late prophase (Furuno et al. 1999). With the association of B-type cyclins (B1 and B2) with CDK1 in G2-phase the cells prepare for progression into mitosis and sustaining of mitotic state. Due to the rapid degradation of cyclin B, cells exit the M-phase and progress into G1 or the quiescent cell phase (Wheatley et al. 1997; Obaya and Sedivy 2002; Errico et al. 2010; Lim and Kaldis 2013).

There are two classes of CDK inhibitors (CKI) to restrain CDK activity. Members of the INK4 family ($p16^{INK4a}$, $p15^{INK4b}$, $p18^{INK4c}$ and $p19^{INK4d}$) target CDK4 and CDK6, thus affecting the progression from G1 into S-phase. The Cip/Kip family members ($p21^{Cip1}$, $p27^{Kip1}$ and $p57^{Kip2}$) inhibit cyclin D-, E-, A- and B-dependent kinase complexes which are required for G1- to S-phase and G2- to M-phase transition. In contrast to CKI, phosphorylation of CDKs by CDK activating kinases (CAK) enables full activation by improving the substrate binding and stability of complexes (Pavletich 1999).

1.1.3. The pRB/E2F pathway

On molecular level, the transition from G1 to S phase and initiation of DNA replication is regulated by cyclin-CDK-dependent phosphorylation of retinoblastoma (Rb) proteins (Adams 2001). In mammalian cells, three Rb family members are known (pRb, p107/Rbl1 and p130/Rbl2) to ensure the coordinated regulation of

progression through the cell cycle. They are also termed as “pocket proteins” according to their conserved pocket domain, through which they interact with viral oncoproteins like SV40 large T antigen or human papilloma virus E7 protein and transcription factors of the E2F family. The pocket region consists of two highly conserved domains (box A and B) that are separated by a spacer (Lipinski and Jacks 1999). Whereas pRb shares ~25 % sequence homology with its homologues, p107 and p130 are more closely related to each other (~ 54 % sequence identity) (Dick and Rubin 2013). All three Rb family members function as negative regulator of the cell cycle and play a crucial role on G1 progression through interaction with distinct E2F transcription factors, thus modulating their activity (Harbour et al. 1999).

E2F transcription factors are the best characterized targets of the pocket proteins and so far nine family members (E2F1-2, E2F3a/b, E2F4-8) are described in mammalian cells. E2F1-6 contain a heterodimerization domain enabling the binding of differentiation-regulated transcription factor-1 and 2 (referred as DP1 and DP2), hence increasing the stability of E2F-binding through a second DNA binding site (Sozzani et al. 2006; Giacinti and Giordano 2006). In contrast, E2F7-8 lack the DP-binding region and both factors increase DNA binding through a tandem repeat of the E2F DNA-binding domain (van den Heuvel and Dyson 2008). To mediate the interaction with pocket proteins of the Rb family, E2F1-5 contain a C-terminal transactivation domain which is absent in E2F6-8, thus acting in a Rb-independent manner.
Based on their regulatory function in cell cycle, E2Fs are subdivided into two groups either as activators or repressors of transcription. However, recent findings indicate that activator E2F proteins can take over repressive functions and vice versa (Chong et al. 2009; Lee et al. 2011; Weijts et al. 2012). Members of the activator group (E2F1-E2F3a) promote the cell cycle by regulation of genes required for G1/S transition and predominantly associate with pRb. In G0 and early G1-phase, the binding of hypophosphorylated pRB to the C-terminal transcription activation domain negatively controls the expression of E2F targets, hence inhibiting cell cycle progression (Rayman et al. 2002; Stengel et al. 2009). Upon mitogenic stimuli in G1-phase, cyclin D-CDK4/6 complexes sequentially phosphorylate pRb inducing the partial release of E2Fs to activate cyclin E and Cdc25a transcription. Cdc25 fosters CDK2 activation by removing inhibitory phosphate residues and thus the subsequent complex formation of cyclin E-CDK2. The complex in turn hyperphosphorylates pRb yielding in full release of E2F and expression of genes needed for transition into the next cell cycle stage (Fig.2) (Harbour et al. 1999; Harbour and Dean 2000; Bartek and Lukas 2001; Bracken et al. 2004).

In contrast to activators, members of the repressor group (E2F3b, E2F4-E2F8) inhibit gene expression. In quiescent (G0) cells and early G1-phase, E2F4-5 predominantly associate with the pocket proteins p107 and p130 and binding of complexes to E2F-regulated promoters hampers association of activators at these sites (Beijersbergen et al. 1994; Ginsberg et al. 1994; Hijmans et al. 1995; Moberg et al. 1996). Moreover, E2F4-5 complexes recruit chromatin-modifying enzymes like histone deacetylases

(HDAC) to promoters, thereby enabling silencing of gene transcription (Rayman et al. 2002). Upon CDK-mediated hyperphosphorylation of pocket proteins E2Fs are from the complex and relocate into the cytoplasm (Fig.2) (Verona et al. 1997; Gaubatz et al. 2001). E2F6 also functions as a transcriptional repressor but due to the lack of the pocket binding domain in a pRb independent manner (Morkel et al. 1997; Trimarchi et al. 1998; Gaubatz et al. 1998; Cartwright et al. 1998). Instead, E2F6 heterodimerizes with DP proteins and mediates target gene inhibition by interaction with Polycomb group proteins or in large multimeric complexes containing Max and Mga proteins (Ogawa et al. 2002). The least studied E2F family members, E2F7-8, are absent of a pocket protein binding domain and repress gene expression independent of DP protein heterodimerization but rather form homo- and heterodimers with each other (Moon and Dyson 2008; Li et al. 2008).

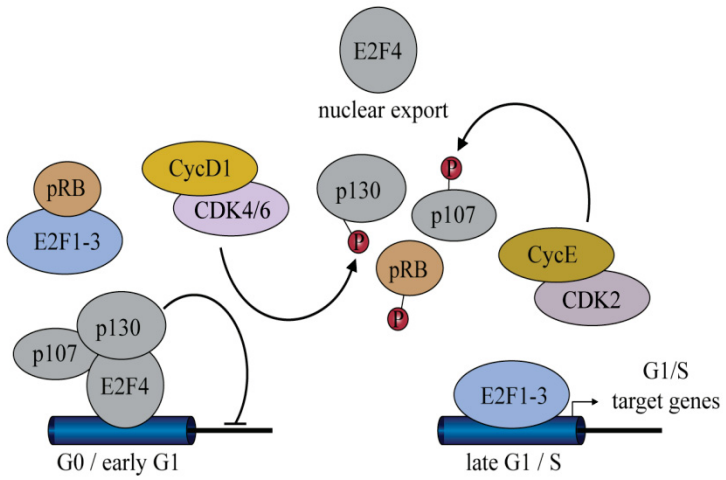

Figure 2: Schematic representation of G1-S control by E2F-pocket protein complexes
In GO/early G1, the expression of E2F target genes is repressed due to binding of unphosphorylated pRb to activating E2Fs and occupancy of promoters by repressive E2F-p107/p130 complexes. Mitogenic stimuli enforces the formation of cyclin/CDK-complexes which in late G1/S phosphorylate the pocket proteins yielding in release of E2Fs. The repressive E2Fs are then exported from the nucleus and activating E2Fs can bind to the promoters of respective target genes to recruit coactivators and induce expression of genes required for G1/S transition.
Figure adapted and modified after Bertoli et al. (2013)

1.2. The mammalian DREAM/MMB complex

In 2004, two groups independently identified an E2F/pRb repressor complex in the fly *Drosophila melanogaster*. The Brehm group purified a native multi-subunit complex named dREAM (Drosophila RBF, dE2F, and dMyb-interacting proteins (Fig. 3) that comprises of the pRb homologues (Rbf1 or Rbf2), dE2F2, dDP, the chromatin assembly factor 1 (CAF1/p55), dMyb (B-Myb) and three dMyb-interacting proteins (Mip40, Mip120, Mip130/TWIT) (Korenjak et al. 2004). In the Botchan group, a highly related complex was purified and termed Myb–MuvB (MMB) due to its strong homology to the worm *Caenorhabditis elegans* synthetic multivulva class B (synMuvB) genes. The MMB is similar to dREAM but associates with three additional subunits; dLin52, the histone deacetylase Rpd3 and the tumor suppressor L(3)MBT (Lewis et al. 2004). Although slightly different in composition, both

complexes are implicated in repression of developmental gene expression as well as activation of G2/M genes (Georlette et al. 2007). Furthermore, a testis-specific complex named tMAC (Meiotic Arrest Complex) was identified in Drosophila. In addition to the dREAM/MMB subunits mip40 and CAF1/p55, tMAC comprises the testis-specific proteins Always early (Aly), Tombola (Tomb), Cookie monster (comr) and Matotopetli (Topi). Mutations of tMac subunits *in vivo* results in reduced fertility or even sterility through meiotic arrest of cells during spermatogenesis (Beall et al. 2007; White-Cooper 2010)

Following the identification of dREAM/MMB in fly, a related complex termed DRM (DP, Rb, MuvB) was identified in *Caenorhabditis elegans* (Harrison et al. 2006). The complex contains the pRb homologue Lin35, Dpl-1, the E2F related protein Efl-1, Lin9, Lin37, Lin52, Lin53 as well as Lin54 and is involved in vulva differentiation (Fig. 3) (Ceol and Horvitz 2001).

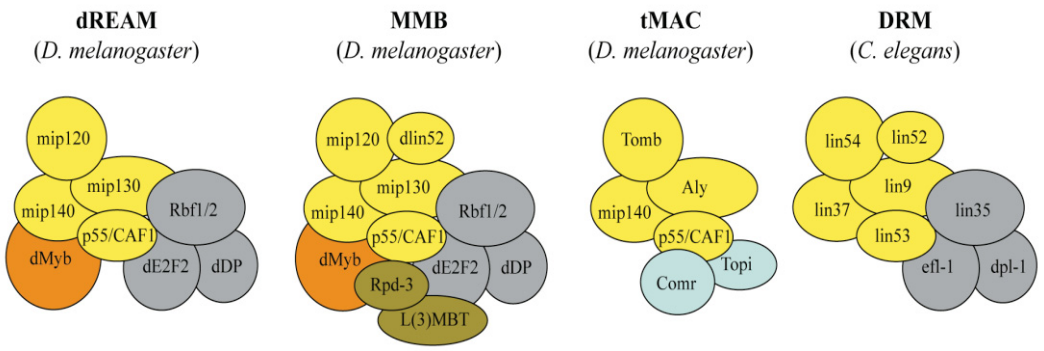

Figure 3: Summary of pRB/E2F complexes in different species
Conserved pRB/E2F complexes were found in fly and worm. Depending on the species and cellular context the core module (yellow) associates with different subunits (orange, grey, brown, blue). See text for detailed description.

In 2007, a multiprotein complex related to the dREAM/MMB and DRM complex was identified in mammalian cells named DREAM/LINC (Litovchick et al. 2007; Schmit et al. 2007; Pilkinton et al. 2007). Distinct to complexes found in fly and worm, the mammalian complex consist of a core module of five MuvB-like proteins (LIN9, LIN37, LIN52, LIN54 and RbAP48) and dynamically binds to subunits p130, DP1, E2F4 and B-MYB in a cell cycle dependent manner (Fig. 4A). In resting cells (G0, senescence) and early G1-phase the MuvB-core module associates with p130, DP1 and E2F4 forming DREAM, a repressive complex, which suppresses E2F target genes essential for G1/S transition. Upon growth stimulatory signals and entry into S-phase the MuvB core complex releases p130, DP1 and E2F4 and associates with the transcription factor B-MYB yielding MMB (Myb-MuvB) to promote the expression of late S-phase genes (Osterloh et al. 2007; Pilkinton et al. 2007; Sadasivam and DeCaprio 2013). In G2/M, MMB recruits the transcription factor FOXM1 to specific G2/M promoters to induce late cell cycle gene expression (Fig. 4B) (Sadasivam et al. 2012; Down et al. 2012).

Recently, a DREAM-like complex was discovered in the plant *Arabidopsis thaliana*, with function in periodic cell cycle gene expression and the establishment of a quiescent state (Fischer and DeCaprio 2015; Kobayashi et al. 2015).

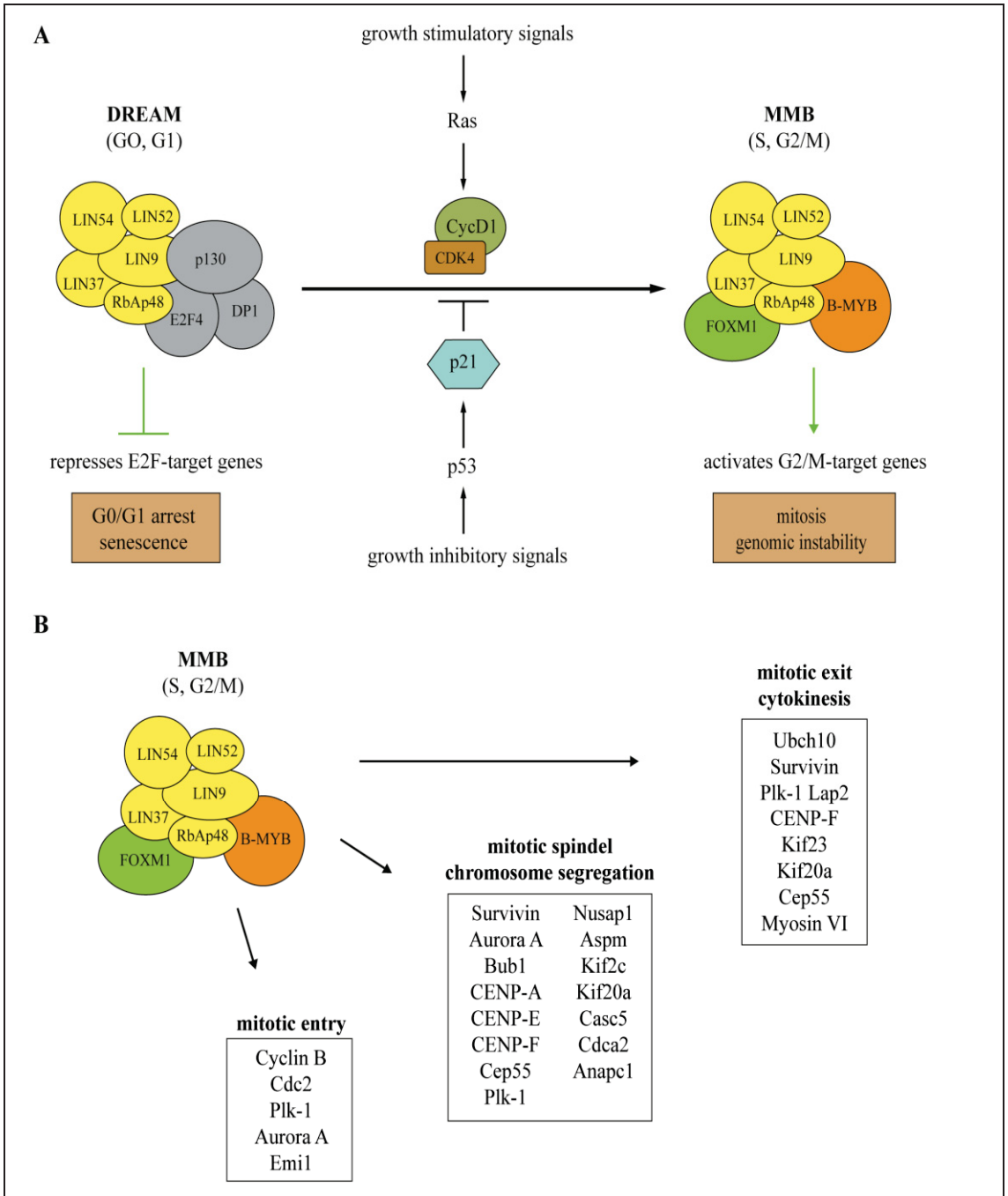

Figure 4: The mammalian DREAM/MMB complex
A) The mammalian DREAM/MMB complex associates with different subunits in a cell cycle dependent manner. In G0/early G1 the MuvB-core module (yellow) binds to the pocket protein p130 and E2F4/DP1 (grey) yielding DREAM, a repressor of E2F-target genes. Upon growth stimulatory signals, the MuvB core releases p130/E2F4/DP1 and associates in S-phase with the transcription factor B-Myb. In G2/M the transcription factor FoxM1 is recruited into the complex forming MMB, an activator of G2/M gene expression. Growth inhibitory signals can block the switch of between DREAM and MMB. **B**) The MMB complex is a key activator of genes required for mitotic entry, mitotic spindle, chromosome segregation, as well as mitotic exit and cytokinesis.

1.2.1. Gene regulation by DREAM/MMB

Knockdown experiments coupled with microarray analysis and next-generation sequencing (ChIP-on-ChIP, ChIP-Seq) in mouse/human fibroblast, in human cancer cell lines and embryonic stem cells revealed the crucial function of DREAM/MMB in cell cycle dependent gene expression. DREAM has been shown to be required for repression of E2F target genes in quiescent cells and depletion of various components of the complex by RNAi or mutation resulted in cell cycle-dependent de-repression of genes in G0 phase (Hurford et al. 1997; Litovchick et al. 2007). In contrast, MMB is a transcriptional activator of genes that are essential for progression through mitosis (Osterloh et al. 2007; Schmit et al. 2007; Pilkinton et al. 2007; Kittler et al. 2007; Knight et al. 2009; Schmit et al. 2009; Reichert et al. 2010; Sadasivam et al. 2012; Wolter et al. 2017). Its function as a key regulator of G2/M gene expression is evolutionarily conserved and has also been observed in zebrafish and flies (Katzen et al. 1998; Shepard et al. 2005; Georlette et al. 2007; Wen et al. 2008). After depletion of the core member Lin9 a host of genes involved in mitotic entry, mitotic spindle checkpoint and chromosome segregation as well as mitotic exit and cytokinesis were identified (Fig 4B) (Osterloh et al. 2007; Schmit et al. 2007; Pilkinton et al. 2007; Reichert et al. 2010; Sadasivam et al. 2012; Wolter et al. 2017) Similar, inhibition of Lin54 or the MMB-associated factor B-Myb led to decreased expression levels of late cell cycle genes yielding cytokinesis failures and mitotic arrest of cells (Kittler et al. 2007; Zhan et al. 2012; Sadasivam et al. 2012). Also in F9 embryonal carcinoma cells, MMB is involved in mitotic gene regulation (Knight et al. 2009). Knockdown of Lin9 or B-Myb in these cells causes mitotic arrest and decreased expression levels of Survivin and cyclin B. Furthermore, in embryonic stem cells (ESC), Lin9 was shown to be pivotal for normal cell cycle progression and genomic stability by activating genes with functions in mitosis and cytokinesis. RNAi-mediated depletion of Lin9 leads to downregulation of mitotic genes, upregulation of differentiation-specific genes as well as accumulation of cells in G2/M-phase and polyploidization. However, pluripotency markers like Oct4, Sox2 or Nanog are not altered after loss of Lin9 and ESC maintain alkaline phosphatase activity, a marker for undifferentiated cells (Esterlechner et al. 2013).

1.2.2. Transcriptional control of G2/M genes

Many genes regulated by DREAM/MMB contain common recognition sites in their promoters nearby the transcriptional start sites such as CHR (cell cycle genes homology region), CDE (cell cycle -dependent element) and CCAAT boxes. While CCAAT boxes are important for transcriptional activation, tandems of CDE and CHR are found to mediate transcriptional repression during G0/G1 (Müller and Engeland 2010). Thereby, CDE and CHR are located in close proximity only separated by a spacer of 4 nucleotide base pairs (Müller et al. 2012). Mutations in either CDE or CHR result in loss of transcriptional repression during G0/G1 confirming the cooperation of the tandem elements in cell cycle repression (Zwicker et al. 1995). However, expression of some genes (e.g. human cyclin B) is only controlled by CHR lacking functional CDE (Müller et al. 2012). Thus, genes containing a CDE/CHR

element are designated as class I genes whereas genes with only CHR are classified as class II genes (Müller and Engeland 2010). In contrast to CDE, CHR elements are involved in both repression and activation of genes.

In quiescent cells, the MuvB core member Lin54 has been shown to bind to CHR of the human cdc2 promoter and the DNA interaction of Lin54 is mediated through 2 cysteine-rich domains with the DNA consensus motif TTYRAA (Schmit et al. 2009; Marceau et al. 2016) Recently, more non-canonical CHR motifs have been identified to be occupied by Lin54 underlining the crucial role of CHR for transcriptional control (Müller et al. 2014; Marceau et al. 2016). The binding of DREAM to the Cdc2 promoter is supported by interaction of the subunits E2F4/p130 with the adjacent CDE that is supposed to stabilize the binding Lin54 to the CHR. Association of E2F4/p130 with CDE elements was also reported for other CDE-regulated promoters e.g. AurkB or Cyclin A2 (Zhu et al. 2004; Kimura et al. 2004). Binding of DREAM to CDE/CHR was also confirmed at mouse Cyclin B2 promoter; however the requirement for the CDE element in the human promoter is not essential for repression but can enhance binding affinity for DREAM (Müller et al. 2012). Furthermore, in proliferating cells MMB has been demonstrated to bind to CHR elements of late cell cycle gene promoters independently of the CDE (Müller et al. 2012; Sadasivam et al. 2012; Chen et al. 2012; Müller et al. 2016). With B-Myb and FoxM1 the MMB contains 2 more proteins with DNA-binding potential and in addition to CHR, other binding elements such as B-Myb binding sites (MBS) and forkhead binding sites (FBS) may mediate recruitment of the complex to target promoters (Knight et al. 2009; Schmit et al. 2009; Müller et al. 2012; Sadasivam et al. 2012). However, neither FBS nor MBS were found to be necessary for MMB recruitment. Computational analysis of genes bound by MMB or FOXM1 revealed a stronger enrichment at CHR sites than FBS within promoter regions concluding that FOXM1 is recruited to sites by MMB (Chen et al. 2012). Moreover, in F9 embryonal carcinoma cells MMB was found to bind to an isolated CDE/CHR element of the Ccnb2 promoter in the absence of an MBS site thus, emphasizing the crucial role of CHR as central promoter element in transcriptional regulation (Müller et al. 2014). Based on computational meta-analysis 95 % of late cell cycle genes contain a CHR (or CHR-like element) that is crucial for binding of DREAM and MMB. This underlines the role of CHR in DREAM/MMB-mediated gene repression and activation (Müller et al. 2014; Müller et al. 2016)

Several studies have shown that DREAM mediated gene repression is linked to the p53 pathway (Müller et al. 2012; Fischer et al. 2014; Fischer et al. 2015; Fischer et al. 2016; G. Müller et al. 2016). First described in 1979, p53 evolved as one of the most extensively studied protein which is frequently altered in more than 50 % of human tumors (Lane 1992; Vogelstein et al. 2000). The activation of p53 tumors suppressor by a variety of stress-inducing signals triggers the expression of a host of target genes that promote classical cellular responses including cell cycle arrest, DNA repair, senescence or apoptosis (Yee and Vousden 2005; Green and Kroemer 2009; Bieging et al. 2014). Notably, a p53-dependent indirect transcriptional repression of a majority

of genes has been demonstrated to occur via the p53-p21-DREAM-CDE/CHR pathway (Fischer et al. 2014; Engeland 2016). As described for Survivin, CDC25C and PLK1, p53-induced expression of p21 leads to assembly of DREAM which is guided to the CDE/CHR recognition sites within the promoter regions yielding in transcriptional repression (Fischer et al. 2015). Moreover, repression through the p53-p21-cyclin/CDK-DREAM-CDE/CHR pathway is implied to be a general mechanism in cell cycle control (Fischer, Grossmann, et al. 2016). In response to DNA damage, the activating MMB complex has been shown to revert to the repressive DREAM in a p53-dependant manner in normal cells (Mannefeld et al. 2009). In contrast, p53-negative cells (that cannot arrest in G1 and are dependent on a functional G2 checkpoint) fail to switch to DREAM. Hence, MMB promotes checkpoint recovery and premature mitotic entry due to continuous mitotic gene expression.

In addition to p53, the kinase DYRK1A has been shown to have a crucial function in DREAM assembly (Litovchick et al. 2011; Guiley et al. 2015). The kinase specifically phosphorylates the MuvB core member Lin52 on Serine residue 28 thus, preventing interaction of MuvB core with p130. Hence, formation of the repressive DREAM is disturbed. As a consequence, cells fail to enter a quiescent state or oncogenic RAS-induced senescence. Intriguingly, the DYRK1A-DREAM connection revealed a new link between the Hippo/YAP signaling pathway and cell cycle control. ShRNA screens identified the YAP-regulating kinase LATS1/2 which phosphorylates DYRK1A and that in turn promotes assembly of DREAM (Tschöp et al. 2011; Dick and Mymryk 2011; Ehmer and Sage 2015). Therefore, alterations in the Hippo signaling pathway such as low expression levels of LATS2 or inactivation of the upstream kinase MST1/2 may contribute to chromosomal instability by undermining DREAM-mediated gene repression. Furthermore, LATS2-deficient MEFs exhibit multiple mitotic defects such as centrosome fragmentation, cytokinesis failures and multinucleated cells.

1.2.3. Function of DREAM/MMB in cells and *in vivo*

In recent studies the physiological role of DREAM/MMB has been elucidated. *In vivo*, functional Lin9 is essential for early murine embryonic development and inactivation is embryonic lethal. Lin9-null embryos fail to maintain the inner cell mass (ICM) *in vitro* and die shortly after implementation (Reichert et al. 2010). Similar effects were found in B-Myb-deficient mice which emphasize the important role of both genes during embryonic development (Tanaka et al. 1999). In adult mice, conditional knockout of Lin9 resulted in atrophy of the intestinal epithelium and led to rapid mortality among animals (Reichert et al. 2010). Tissue analysis revealed a loss of proliferating intestinal epithelial cells and accumulation of abnormal nuclei, indicating that Lin9 is required for proper execution of mitosis in dividing adult tissues. In mouse and human fibroblasts loss of Lin9 causes severe mitotic defects (e.g. multipolar spindle formation or centrosome amplification) yielding in multinucleated cells, induction of $p16^{INK4a}$ and $p21^{Wafl}$ and premature senescence (Reichert et al. 2010; Hauser et al. 2012). Thereby, the induction of senescence is mediated independently by the pRB and p53 tumor suppressor pathway as

demonstrated in experiments with SV40 large T antigen, which binds and disrupts the function of both tumor suppressors. Moreover, MEFs with non-functional pocket proteins (p107, p130) fail to repress transcription due to inability of DREAM complex formation. Instead MMB is preferentially assembled in these cells leading to elevated expression levels of mitotic genes (Forristal et al. 2014). Furthermore, the repressive DREAM is crucial for chondrocyte proliferative control and endochondral ossification as mice with deficient DREAM complex die shortly after birth and display failures in bone morphogenesis (Cobrinik et al. 1996; Forristal et al. 2014).

1.2.4. DREAM/MMB and tumorigenesis

Chromosomal instability (CIN) is found in almost all cancers (Negrini et al. 2010; Shen 2011). CIN is assumed to cause aneuploidy which arises in 90 % of solid tumors and 85 % of hematopoietic neoplasias (Weaver and Cleveland 2006; Thompson et al. 2010; Giam and Rancati 2015). Although an association of CIN and aneuploidy has been observed in several cancers (e.g. in lung, colon or brain) the question whether aneuploidy is cause or consequence of tumorigenesis is intensively discussed (Lengauer et al. 1997; Haruki et al. 2001; Yoon et al. 2002; Weaver and Cleveland 2006; Thompson et al. 2010).

So far the role of MMB in cancer is not fully understood but there are strong indications that deregulation contributes to genomic instability, a hallmark of cancer (Holland and Cleveland 2009; Hanahan and Weinberg 2011). In a recent report, long-term depletion of the MMB members Lin9, Lin54 or B-Myb in human and mouse fibroblast was shown to induce cellular senescence, a fail-safe mechanism to prevent tumorigenesis that is dependent on the p53 and pRB tumor suppressor pathways (Hauser et al. 2012). Notably, Lin9-deficient cells which overcome senescence by inactivation of p53 or pRB adapt to the loss of Lin9 and become highly aneuploid, thus enabling cells for oncogenic transformation and growth in an anchorage-independent manner. Concurrently, mitotic gene expression in these adapted cells is no longer dependent on Lin9 expression (Hauser et al. 2012). In contrast to complete loss of Lin9, heterozygous Lin9 expression resulted in transformation cells *in vitro* (Reichert et al. 2010). Furthermore, while $Lin9^{fl/+}$ mice are not predisposed to spontaneous tumorigenesis, haploinsufficient mice were more prone to lung tumor formation in a mouse model of NSCLC expressing a constitutively active c-raf-1 kinase under the control of the human SP-C promoter (BXB-Raf) (Reichert et al. 2010). In this model, heterozygous mice exhibit a shortened life span suggesting that Lin9 may function as haploinsufficient tumor suppressor. A direct role of MMB subunit B-Myb in cancer is not yet fully established but there a multiple indications that it could act as tumor promoting factor. Mutation of dMyb in the fly *Drosophila* have been described to causes defects in cell cycle progression and genomic stability (Manak et al. 2002; Fung et al. 2002). Similar, in zebrafish the loss-of-function mutation in B-Myb led to mitotic defects and increased cancer susceptibility (Shepard et al. 2005). Furthermore, amplification of B-Myb is often found in liver, ovarian and prostate carcinomas and in cutaneous T-cell lymphomas (Zondervan et al. 2000; Tanner et al. 2000; Mao et al. 2003; Bar-Shira et al. 2002). In neuroblastoma, the

constitutive expression of B-Myb prevents neural differentiation and elevated expression levels are associated with poor prognosis (Raschellá et al. 1995; Raschellà et al. 1999). Most lately, a critical role of B-Myb in breast cancer was demonstrated (Thorner et al. 2009; Tao et al. 2014). The precise mechanism of B-Myb-induced genome instability remains unknown. However, a recent published study identified a B-Myb complex containing clathrin and filamin (Myb–Clafi complex) which facilities precise clathrin localization at the mitotic spindle, thereby stabilizing kinetochore fibers and so may contribute to chromosomal stability (Yamauchi et al. 2008). The MMB associated transcription factor FoxM1 is overexpressed in various human malignancies including colon, breast, lung, kidney, ovary and bladder cancer as demonstrated by gene expression analyzes of public available microarray data (Pilarsky et al. 2004). In glioblastoma, a correlation between high expression levels of FoxM1 and the tumorigenicity of glioma cells was found (Liu et al. 2006). Moreover, in breast cancer, overexpression of FoxM1 strongly correlates with poor prognosis (Bektas et al. 2008).

In addition to B-Myb and FoxM1, mitotic genes are frequently expressed at elevated levels in a large number of tumor types and their upregulation is often highly correlated with aggressiveness, survival and tumor recurrence (Liang et al. 2014; Sotillo et al. 2007; Diaz-Rodríguez et al. 2008; O'Hare et al. 2016; Weaver et al. 2016). Many of these genes are part of recently published chromosomal instability signatures that predict the clinical outcome of several cancers including brain, breast and lung tumors independent of the cell cycle score (Carter et al. 2006; Chibon et al. 2010; Cheng et al. 2013). Remarkably, a significant number of genes included in the CIN signature lists such as Top2α, Nusap1, Ccnb2 and kinesins are directly controlled by MMB or its associated factors. Thus, MMB might promote tumorigenesis by activation of genes with critical functions in G2/M

1.3. Aim of this project

The contribution and relationship of MMB to tumorigenesis is largely unknown and has not been tested directly so far.

Therefore, the first aim of this thesis was to determine the requirement of MMB-mediated mitotic gene expression in adenocarcinoma lung cancer cells by inhibition of the MuvB core subunit Lin9 or the associated transcription factor B-Myb. In addition, the relationship with the tumor suppressor p53 was further investigated. The second project goal was to advance the understanding of MMB to tumorigenesis *in vivo*. Hence, a conditional Lin9 knockout mouse model of lung cancer driven by K-Ras and loss of p53 was established. Cell lines derived from tumors of this mouse model were used in order to study the importance of Lin9 for lung cancer development in more detail.

2. Materials and Methods

2.1. Materials

2.1.1. Chemical stocks and reagents

Unless otherwise noted, chemicals were purchased from AppliChem, Invitrogen, Carl Roth, Fluka or Sigma Aldrich.

A Agarose [Peqlab]
Ammonium acetate
Ammonium hydroxide
Ammonium persulfate (APS)

B Bovine serum albumin fraction V (BSA)

C Chloroform 99%
p-Coumaric acid
Crystal violet

D Diethylpyrocarbonate (DEPC), approx. 97%
Dimethylsulfoxide (DMSO), >99,9%
Dithiothreitol (DTT) [Invitrogen]
dNTPs (dATP, dCTP, dGTP, dTTP, 2mM each) [Promega]
Doxycycline
Dynabeads® Protein G [Life Technologies]

E Minimum Essential Medium Eagle (EMEM) powder
Eosin Y Solution Aqueous
Ethanol 99,8%
Ethidium bromide
Ethylenediaminetetraacetic acid (EDTA)

F Formaldehyde 37%

G Glacial acetic acid
D-Glucose
Glutaraldehyde 25 % in H_2O
Glycine

H Hematoxylin Solution, Gill No. 3
HEPES
Hoechst 33258, 10 mg/ml
Hydrogen peroxide
4-Hydroxytamoxifene (4-OHT)

I Immobilized Protein G (Pierce)
ImmoMount [Shandon]
ImmunoPure Immobilized Protein A (Pierce)

K Ketavet 100 mg/ml [Pfizer]

L Lithium chloride ultra
Low melting agarose
Luminol

M Methanol

N Nonfat dry milk powder
Nonidet P 40

P Paraformaldehyde
Paraplast
peqGOLD TriFast [Peqlab]
Phenylmethylsulphonyl fluoride (PMSF), 100 mM in isopropanol [Roche]
Polybrene
Ponceau S solution
Potassium ferricyanide
Potassium ferrocyanide
Propidium iodid (PI), 1 mg/ml
Protease Inhibitor Cocktail P8340 (PIC)
ProtoGel 30 % [Biozym]

R Random primer, 0.5 µg/µl [Roche]
Roti® Histokitt

S Salmon sperm ssDNA
Sodium butyrate
Sodium deoxycholate
Sodium dodecyl sulfate (SDS)

T Tetramethylethylenediamine (Temed) 99%
Tissue-Tek® O.C.T. Compound
Tris
Triton X-100
Tween 20

X X-Gal (5-bromo-4-chloro-3-indolyl-β-D-galactopyranoside)
Xylazine 2 % [CP-Pharma]
Xylene

2.1.2. Antibiotics

Antibiotic	Final concentration	Purpose
Ampicillin	100 µg/ml in LB-medium	DH5α (E.coli)
Blasticidin S	10 µg/ml in DMEM	KPR8
Puromycin	2,5 µg/ml in DMEM	KPL1 lung tumor cell line KPL2 lung tumor cell line

2.1.3. Enzymes

Enzyme	Company
ABsolute™ QPCR SBR Green Mix	Thermo Scientific
RevertAid Reverse Transcriptase (200 U/µl)	Thermo Scientific
RiboLock RNase-Inhibitor (40 u/µl)	Thermo Scientific
Proteinase K (10 mg/ml)	AppliChem
RNase A (10 mg/ml)	Sigma-Aldrich®
T4-DNA-Ligase (400 u/µl)	New England Biolabs
Pfu DNA Polymerase (2.5 u/µl)	Thermo Scientific
Phusion High-Fidelity DNA polymerase (2 U/µl)	Thermo Scientific
His Taq Polymerase [15U]	prepared in Gessler Lab
Restriction endonucleases	Thermo Scientific New England Biolabs

2.1.4. Adeno-virus for infection experiments

The adenoviral vector with Cytomegalovirus (CMV) promoter driving the expression of the Cre-recombinase protein for the mouse infection experiments, Ad5CMVCre (Cat #: VVC-U, Viral Vector Core Facility of the University of Iowa), was a generous gift from Dr. Daniel Murphy.

2.1.5. Molecular kits and Protein/DNA markers

2.1.5.1. Kits

Kits	Company
DAB Substrate Kit	BD Pharmingen™550880
VECTASTAIN Elite ABC Kit (Rabbit IgG)	Vector Labs PK-6101
VECTASTAIN Elite ABC Kit (Rat IgG)	Vector Labs PK-4004
Absolute™ QPCR SYBR Green Mix	Thermo Scientific
GeneJET Gel Extraction Kit	Thermo Scientific

GeneJET PCR Purification Kit	Thermo Scientific
QIAquick PCR Purification Kit	Quiagen
PureLink HiPure Plasmid Midiprep Kit	Life Technologies
PureLink HiPure Plasmid Maxiprep Kit	Life Technologies

2.1.5.2. Markers

Marker	Company
GeneRuler™ DNA Ladder 1 kb	Thermo Scientific
GeneRuler™ DNA Ladder 100 bp	Thermo Scientific
PageRuler™ Prestained Protein Ladder	Thermo Scientific

2.1.6. Buffers

2.1.6.1. General buffers

5x Loading buffer (in 1x TAE)	15 % Ficoll 0.05 % Bromophenol blue 0.05 % Xylene cyanol 0.05 M EDTA
2x HEPES buffered saline (HBS)	280 mM NaCl 1.5 mM Na_2HPO_4 50 mM HEPES-KOH, pH 7.05
Miniprep solution S1	50 mM Tris-HCl, pH 8.0 10 mM EDTA, pH 8.0 100 µg/ml RNase A
Miniprep solution S2	200 mM NaOH 1 % SDS
Miniprep solution S3	3.1 mM Potassium acetate adjust pH to 8.0 with glacial acetic acid
10x Phosphate buffered saline (PBS)	137 mM NaCl 3 mM KCl 6.4 mM Na_2HPO_4 1.5 mM KH_2PO_4 adjust pH to 7.4 with HCl
50x TAE	200 mM Tris-acetate 250 mM glacial acetic acid 500 mM EDTA, pH 8.0
10x TE	100 mM Tris-HCl, pH 7.5 10 mM EDTA, pH 8.0

1x Tris buffered saline (TBS)	50 mM Tris-HCl, pH 7.4 150 mM NaCl
10x TES	0.1 M Tris-HCl. pH 7.5 10 mM EDTA, pH 8.0 2 M NaCl
10x ReproFast buffer	100 mM $(NH_4)_2SO4$ 200 mM Tris-HCl, pH 8.8 100 mM KCl 20 mM $MgSO_4$ 1 % BSA 1 % Triton X-100 filter sterile

2.1.6.2. Buffers for whole cell lysate

TNN buffer	50 mM Tris-HCl pH 7.5 120 mM HCl 5 mM EDTA, pH 8.0 0.5 % (v/v) Nonidet (NP-40) 10 mM $Na_4P_2O_7$ 2 mM Na_3VO_4 100 mM NaF ad 500 ml H_2O DTT 1 mM (add freshly) PIC 1:500 (add freshly) PMSF 1:1000 (add freshly)
Bradford solution	50 mg Coomassie Brilliant Blue G250 23.75 ml ethanol 50 ml 85 % (v/v) *ortho*-phosphoric acid ad 500 ml H_2O filter twice

2.1.6.3. Buffers for immunoblotting

Stacking gel buffer	0.5 M Tris-HCl, pH 6.8
Separating gel buffer	1.5 M Tris-HCl pH 8.8
Acrylamid buffer for SDS gels (Protogel)	30 % (w/V) acrylamide 0.8 % (w/v) N,N'-methylenbisacrylamide
3x Electrophoresis sample buffer (3x ESB)	300 mM Tris-HCl, pH 6.8 15 mM EDTA, pH 8.0 150 mM DTT 12 % (w/v) SDS

	15 % (w/v) glycerol 0.03 % (w/v) bromophenol blue
10x SDS running buffer	144 g glycine 30 g Tris 10 g SDS ad 1 l H_2O
Ponceau S	0.1 % Ponceau S 5 % glacial acetic acid
1x Blotting buffer	0.6 g Tris base 2.258 g glycine 150 ml methanol ad 1 l H_2O
TBST	0.05 % Tween in 1x TBS
Blocking solution	3 % (w/v) milk powder in 0.05 % TBST or 5 % (w/v) BSA in 0.05 % TBST (for cell signaling antibodies)
Chemoluminescence solution	10 mL 100 mM Tris-HCl, pH 8.5 55 µl 250 mM luminol 22 µl 90 mM *p*-coumaric acid 3 µl 30 % H_2O_2

2.1.6.4. Buffers for chromatin immunoprecipitation (ChIP)

Cell lysis buffer	5 mM PIPES, pH 8.8 85 mM KCl 0.5 % (v/v) Nonidet (NP-40) PIC 1:500 (added freshly) PMSF 1 mM (added freshly) store at 4 °C for several months
Nuclei lysis buffer	50 mM Tris-HCl, pH 8.1 10 mM EDTA, pH 8.0 1 % SDS PIC 1:500 (added freshly) PMSF 1 mM (added freshly)
Dilution buffer	0.01 % SDS 1.1 % Triton X-100 1.2 mM EDTA, pH 8.0 16.7 mM Tris-HCl, pH 8.2 167 mM NaCl PIC 1:500 (added freshly) PMSF 1 mM (added freshly) store at 4 °C for several months

LiCl wash buffer	0.25 M LiCl 0.5 % (v/v) Nonidet (NP-40) 0.5 % Sodium deoxycholate (DOC) 1 mM EDTA, pH 8.0 10 mM Tris-HCl, pH 8.0 PIC 1:500 (added freshly) PMSF 1 mM (added freshly) store at 4 °C for several months
Blocking buffer	3 ml dilution buffer 30 µl BSA (100 mg/ml) 30 µl ssDNA (10 mg/ml) prepared freshly
Elution buffer	50 mM Tris, pH 8.0 1 % SDS 10 mM EDTA, pH 8.0

2.1.6.5. Buffers for flow cytometry (FACS)

Sodium citrate	38 mM in 1x PBS

2.1.6.6. Buffers for immunohistochemistry

4 % PFA	4 % PFA in 1x PBS adjust pH to 7.0 with NaOH
Citrate buffer	100 mM, pH 6.0
Blocking solution	3 % BSA in 1x PBS
Differentiation solution	5 ml glacial acetic acid ad 500 ml H_2O
Bluing agent	100 ml tap water 1.5 ml ammonium hydroxide ad 500 ml H_2O

2.1.6.7. Buffers for ß-Galactosidase staining

Formalin solution	4.05 ml Formaldehyde 37 % w/w 0.6 ml 25 % Glutaraldehyde ad 75 ml 1x PBS store on ice
X-Gal reaction buffer	35 mM potassium ferricyanide 35 mM potassium ferrocyanide 2 mM $MgCl_2$ 0.02 % Nonidet P-40

	0.01 % sodium deoxycholate 1 mg/ml X-Gal in DMF

2.1.6.8. Buffers for genomic DNA extraction (HotSHOT)

1x Base buffer	25 mM NaOH 0.2 mM EDTA, pH 8.0 adjust pH to 12.0 with NaOH
1x Neutralization buffer	40 mM Tris-HCl, pH 5.0

2.1.7. Antibodies

2.1.7.1. Primary antibodies

Internal No	Antibody	Company	Origin	Application and dilution
#33	p130 (C-20)	Santa Cruz sc-317	rabbit polyclonal	WB 1:1000 ChIP: 4 µg
#79	B-Myb (N-19)	Santa Cruz sc-724	rabbit polyclonal	ChIP: 4 µg
#104	IgG	Sigma I5006	rabbit polyclonal	IP 1 µg/ml protein ChIP: 4 µg
#149	B-Myb (LX015.1)	Watson (Tavner et al., 2007)	mouse monoclonal	WB 1:5
#158	α-tubulin	Sigma T6074	mouse monoclonal	WB 1:10000 IF 1:200
#163	Lin9	Abcam ab62329	rabbit polyclonal	IP: 1 µg/ml protein WB 1:1000
#185	Ki-67	Thermo Scientific RM-9106	rabbit polyclonal	IHC 1:200
#196	ß-Actin (C4)	Santa Cruz sc-47778	mouse monoclonal	WB 1:10000
#224	TopIIa (F12)	Santa Cruz sc-365916	mouse monoclonal	WB 1:1000
#231	Survivin (71G4B7)	Cell Signaling 2808	rabbit monoclonal	WB 1:1000
#232	CENPF	Abcam ab5	rabbit polyclonal	IHC 1:2500
#233	*p*-B-Myb (Phospho T487)	Abcam ab76009	rabbit monoclonal	IHC 1:600 WB 1:1000
#234	Nusap1	Gift of Geert Carmeliet, against protein sequence	rabbit polyclonal	WB 1:1000 IHC 1:1500

		QENQENQ DPRDTAEV (Raemaekers et al. 2003)		
#237	Cyclin B1 (H-433)	Santa Cruz sc-752	rabbit polyclonal	IHC 1:100
#289	Phospho-p44/42 MAPK (ERK1/2)	Cell Signaling 4376	rabbit monoclonal	IHC 1:400

2.1.7.2. Secondary antibodies

Specificity	Company	Application and dilution
Anti-mouse HRP	GE Healthcare	WB 1:5000
Anti-Protein A HRP	BD Bioscience	WB 1:5000
Anti-rabbit HRP	Invitrogen	WB 1:5000 IHC 1:200

2.1.8. Plasmids

Internal No	Plasmid name	Description
#746	pBabe-H2B-GFP	GFP control for retroviral transfections
#210	pBabe-puro-empty	Empty vector control for retroviral transfection
#924	pBabe-puro-CreER^{T2}	Retroviral expression vector for inducible Cre-recombinase
#1348	pCMV-VSV-G	Envelope plasmid for producing lentiviral particles
#1386	psPAx2	Lentiviral packaging plasmid
#1376	pInducer10-shB-Myb 1620	Lentiviral expression vector for murine shRNA against B-Myb (5'- AAGCAGAGAGACAACAGATGTA-3')

2.1.9. Primers

2.1.9.1. Primers for cloning

Primer nucleotides were purchased from Metabion or Eurofins MWG.

Internal No	Target gene	Sequence (5' to 3')	Directionality
SG 1161	mir30	CTAAAGTAGCCCCTTGAATTCCGAG GCAGTAGGCA	sense
SG 1164		CAGAAGGCTCGAGAAGGTATATTGC TGTTGACAGTGAGCG	antisense
SG1620	97-mer template shB-Myb	TGCTGTTGACAGTGAGCGaagcagagaga caacagatgtaTAGTGAAGCCACAGATGT AtacatctgttgtctctctgctcTGCCTACTGCCT CGGA	sense

Restriction sites (EcoRI GAATTC / XhoI CTCGAG) are underlined, shRNA sequences are lowercased.

2.1.9.2. Primers for quantitative RT-PCR

Internal No	Target gene	Sequence (5' to 3')	Directionality
SG 783	HPRT	TCCTCCTCAGACCGCTTTT	sense
SG 784		CCTGGTTCATCATCGCTAATC	antisense
SG 1015	p21	AACATCTCAGGGCCGAAA	sense
SG 1016		TGCGCTTGGAGTGATAGAAA	antisense
SG 1030	Nusap1	TCTAAACTTGGGAACAATAAAAGGA	sense
SG 1031		TGGATTCCATTTTCTTAAAACGA	antisense
SG 1038	Cenpf	AGCAAGTCAAGCATTTGCAC	sense
SG 1039		GCTGCTTCACTGATGTGACC	antisense
SG 1200	Kif20a	AAGGACCTGTTGTCAGACTGC	sense
SG 1201		TGAGGTGTCCGCCAGTCGAGC	antisense
SG 1941	Kif23	CTGTTGCCGTTGAAATGAGA	sense
SG 1942		GGCTGTCAGTTCAAGGTTTCTT	antisense
SG 1005	CCNB1 (CyclinB1)	CGCTGAAAATTCTTGACAACG	sense
SG 1006		TCTTAGCCAGGTGCTGCATA	antisense
SG 961	Birc5	CCCGATGACAACCCGATA	sense
SG 962		CATCTGCTTCTTGACAGTGAGG	antisense
SG 785	Lin9	TTGGGACTCACACCATTCCT	sense
SG 786		GAAGGCCGCTGTTTTTGTC	antisense
SG 820	B-Myb	TTAAATGGACCCACGAGGAG	sense
SG 821		TTCCAGTCTTGCTGTCCAAA	antisense

SG 1274 SG 1275	Cdc6	TCCGTGTGTGGACGTAAAAC GGAGTGTTGCACAGGTTGTC	sense antisense
SG 1948 SG 1949	Kif14	AACACCTGTCTCTTTGCTTATGG TCATTAAGCCCCATCATCGT	sense antisense
SG 1946 SG 1947	Kif4	GCATGACTGCAACCATTGAT TGGTATCTGGGCTGCTTTG	sense antisense
SG 1942 SG 1943	Kif2C	GCCCGCTTACTGTGACAGAC TTTATTCAGTGGGCGTTTCC	sense antisense
SG 1944 SG 1945	KifC1	AGGAGCGGAGCACACTGA CTTCTGTGGCCTGAAACCTC	sense antisense
SG 1028 SG 1029	Plk1	TTGTAGTTTTGGAGCTCTGTCG AGTGCCTTCCTCCTCTTGTG	sense antisense

2.1.9.3. Murine primers for chromatin immunoprecipitation (ChIP)

Internal No	Target gene	Sequence (5' to 3')	Directionality
SG 976 SG 977	GAPDH promoter	ATTTCCCCTGTTCTCCCATT GACATCCAGGACCCAGAGAC	sense antisense
SG 1044 SG 1045	Nusap1 promoter	GTTTTGAGCCGCTCTGTTTT CATCGCGTTCTGCAATCTC	sense antisense
SG 1046 SG 1047	Cenpf promoter	AAGTGAGCGGGAGGGAAG GACCAGCACGAGCGATTC	sense antisense
SG 1050 SG 1051	Aspm promoter	GCTGTAGCGAGGAGGTTCC TTTTGCTCGGTTCAAATATCG	sense antisense

2.1.9.4. Primers for genotyping

Internal No	allele	Sequence (5' to 3')	Product size (bp)
SG 722 SG 893	floxed (fl) Lin9	GCAAAAGCTGCAAGTCCTCT CCTGGCTGCCTAGCATTTAC	fl Lin9 770 wt 541 Δfl Lin9 289
SG 1556 SG 1557	floxed (fl) p53 for tails	GGTTAAACCCAGCTTGACCA GGAGGCAGAGACAGTTGGAG	fl p53 390 wt 270
SG 1499 SG 1500	floxed stop cassette (LSL) Ras for tails	TCTCGACCAGCTTCTGATGGAA CAACCTCCCCTTCTACGAGCG	LSL 645
SG 2031 SG 2032	floxed stop cassette	GTCTTTCCCCAGCACAGTGC CTCTTGCCTACGCCACCAGCTC	LSL 500 wt 622

SG 2033	(LSL) Ras for tumors	AGCTAGCCACCATGGCTTGAGT AAGTCTGC	ΔLSL 650

2.1.10. siRNA sequences

siRNA against	Sequence (5' to 3')	Target and Reference
Control (ctrl)	UAGCGACUAAACACAUCAA	Non-targeting
Lin9	GCUACUUACAGAGUAACUUUC	Murine Lin9, Knight et al., 2009
B-Myb	GCCCAUAAAGUCCUGGGUAAC	Murine B-Myb, Knight et al., 2009

2.1.11. Media and additives

2.1.11.1. Media for cell culture

DMEM (4.5 g Glucose/L-Glutamine)	Gibco®, Life Technologies
Fetal Calf Serum (FCS)	Gibco®, Life Technologies
GlutaMAX™	Gibco®, Life Technologies
Opti-MEM®	Gibco®, Life Technologies
Penicillin/Streptomycin (10 U/µl each)	Cambrex/Lonza
Trypsin/EDTA (0.05 %)	Gibco®, Life Technologies
Trypsin/EDTA (0.25 %)	Gibco®, Life Technologies
TrypLE™ Express	Gibco®, Life Technologies
10x DMEM	Sigma-Aldrich
Mouse FibrOut™ 9, for tumors	CHI Scientific

2.1.11.2. Media for soft agar assay

2x DMEM (50 ml)

10 ml 10x DMEM
1.85 ml 1 M Na_2CO_3 ,autoclaved
10 ml FCS
5 ml 200 mM GlutaMAX™
450 mg D-Glucose (dehydrated)
0.5 ml Penicillin/Streptomycin
ad 50 ml H_2O

1.4 % low melting agarose for base layer, autoclaved

0.7 % low melting agarose for top layer, autoclaved

2.1.11.3. Media for bacterial cell culture

Luria Bertani (LB) Agar	40 g powder in 1 l H_2O, autoclaved
Luria Bertani (LB) Medium	25 g powder in 1 l H_2O, autoclaved

2.1.12. Cell lines

All cell lines were cultured in DMEM media with 10 % FCS and 1 % Penicillin/Streptomycin.

2.1.12.1. Human cell lines

Cell line	Description
HEK293	Human embryonic kidney cell line for generating stable cell lines by lentiviral infection
PlatE	Retroviral packaging cell line for generating stable cell lines by retroviral infection

2.1.12.2. Murine cell lines

Cell line	Description
KPR8	primary lung adenocarcinoma cell line (*K*-Ras mutated and restorable wild type p53), maternal cell line was a gift from Tyler Jacks (Feldser et al. 2010)
KPR8-pInducer10-shB-Myb 1620	primary lung adenocarcinoma cell line with inducible shB-Myb expression, this work
KPL1	primary lung tumor cell line (*K*-Ras mutated, p53 deficient and partial Lin9 ko), established in lab
KPL1-pbabe-empty	primary lung tumor cell line with empty vector (e.v.) as control
KPL1-pbabe-CreER^{T2}	primary lung tumor cell line with 4-OHT-inducible Cre-recombinase expression
KPL2	primary lung tumor cell line (*K*-Ras mutated, p53 deficient and partial Lin9 ko) established in lab
KPL2-pbabe-empty	primary lung tumor cell line with empty vector (e.v.) as control
KPL2-pbabe-CreER^{T2}	primary lung tumor cell line with 4-OHT-inducible Cre-recombinase expression

2.1.13. Transfection reagents

Transfection reagent	Cell line	Purpose
MetafectenePro (Biontex)	KPR8	siRNA transfection
Calcium phosphate	PlatE Hek293	Plasmid transfection

2.1.14. Bacterial strains

E.coli DH5α or XL1-blue competent cells for transformation of plasmid DNA

2.1.15. Mouse strains

All strains were maintained on a C57BL/6 background. The B6.129-*K*ras^{tm4Tyj} mice were a generous gift from Dr. Daniel Murphy, whereas B6.129P2-Trp53^{tm1Brn}/J mice were purchased at the Jackson Laboratory (Bar Harbor, ME, USA). The C57BL/6-Lin9^{tm1SGau} mouse strain was established in lab (Reichert et al. 2010)

B6.129-*K*ras^{tm4Tyj} — mice carrying a latent point mutation of *K*-Ras (G12D). Cre-recombinase-mediated deletion of a transcriptional termination sequence (loxP-stop-loxP, LSL) results in oncogenic protein expression.

B6.129P2-Trp53^{tm1Brn}/J — mice carrying conditionally targeted Trp53 locus (floxed p53). Cre-recombinase-mediated deletion of exons 2-10 results in non-functional protein expression.

C57/Bl6-Lin9^{tm1SGau} — mice carrying conditionally targeted Lin9 allele (floxed Lin9). Cre-recombinase-mediated excision of exon 7 results in frame shift abolishing functional protein expression.

For infection experiments mice were inter-crossed yielding the following mutant strains:

K-Ras$^{LSL-G12D/+}$; p53$^{fl/fl}$ — mice carrying a removable stop cassette (LSL) for a mutant *K*-Ras allele (G12D) and floxed p53 alleles

K-Ras$^{LSL-G12D/+}$; p53$^{fl/fl}$; Lin9$^{fl/+}$ — mice carrying a floxed stop cassette for a mutant *K*-Ras allele (G12D), floxed p53 alleles and one floxed Lin9 allele

K-Ras$^{LSL-G12D/+}$; p53$^{fl/fl}$; Lin9$^{fl/fl}$ — mice carrying a floxed stop cassette for a mutant *K*-Ras allele (G12D), floxed p53 alleles and floxed Lin9 alleles

2.1.16. Devices

Device	Company
Agarose gel electrophoresis system	Peqlab
Bioruptor®	Diagenode
Centrifuge 5417R, 5804 and 5414D	Eppendorf
Megafuge 1.0 R	Heraeus
Flow cytometer Cytomics FC500	Beckman Coulter
Frigocut 2800E Microtome Cryostat	Leica
Upright Microscope DMI6000B	Leica
Confocal Microscope Eclipse Ti	Nikon Instruments
Mx3000 qPCR System	Agilent technologies
NanoDrop 2000	Thermo Scientific
SDS-PAGE Gel Electrophoresis system	BIORAD
Thermocycler	Biometra
Hyrax M40 microtome	Zeiss
SMZ1500 Stereomicroscope	Nikon
Ultrospec™ 2100 pro Spectrophotometer	Amersham Bioscience
Microm EC 350 tissue embedding center	Thermo Scientific
STP 120 Spin Tissue Processor	Thermo Scientific
GS Gene Linker® UV chamber	BIORAD

2.2. Methods

2.2.1. Cell culture

2.2.1.1. Passaging of cells

Eukaryotic cells were grown and maintained in a tissue culture incubator at 37 ºC and 5 % carbon dioxide (CO2). For passaging, cells were washed once with 1x PBS prior to incubation either with Trypsin/EDTA (0.05 %) or TrypLE™ Express until cells detaches from the dish. The enzymatic reaction of the trypsin was stopped by adding fresh culture media. Cells were seeded at the desired density onto new cell culture dishes.

2.2.1.2. Cryopreservation and thawing of cells

For freezing cells, an almost confluent dish was washed with 1x PBS prior trypsination until detachment. The reaction was stopped with 10 ml fresh media and cells were pelleted for 3 minutes at *259 g*. The supernatant was discarded; cells were resuspended in 1 ml pre-chilled media with 10 % DMSO, transferred into labeled cryotubes and stored at -80 °C (short term) or in liquid nitrogen (long term).

For recovery, the cryotubes were quickly warmed up in a water bath at 37 °C. Subsequently, the cell suspension was added to 9 ml warm fresh media and

centrifuged for 3 minutes at 259 *g*. The supernatant was discarded; cells were resuspended in 10 ml media and seeded onto new cell culture dishes

2.2.1.3. Counting cells

The cell number was determined using a modified Neubauer chamber. Cells in 4 large squares were counted and the number of cells per ml in suspension was calculated according to the formula

Cells/ml = (Cells counted/ number of counted large squares) x 10^4

2.2.1.4. Cell treatment with different reagents

In avoidance of stress from seeding, cells (except doxycycline treated) were allowed to recover 24 h and were fed with fresh medium before treatment. For UV treatment, media was removed for short time.

4-OHT	To induce the $CreER^{T2}$ recombinase which is fused to an estrogen binding domain receptor, cells were treated with 500°nM 4-Hydroxytamoxifen (4-OHT) for indicated time.
Doxycycline	Lentiviral shRNA expression was induced by adding the desired concentration of doxycycline for indicated time.
Mouse FibrOut™ 9 for tumors	To prevent fibroblastic overgrowth during primary cell culture, 500 ml media was supplemented with 1 ml FibrOut™ 9 solution and cells were fed for 1 week.

2.2.1.5. Establishing of tumor cell lines

Lung tumors from Adeno-Cre virus infected *K*-$Ras^{LSL\text{-}G12D/+}$; $p53^{fl/fl}$; $Lin9^{fl/fl}$ mice were dissected under aseptic conditions, washed in ice cold 1x PBS and transferred into the cell culture hood. Each tissue piece was placed into a 10 cm cell culture dish and minced with sterile razor blades in 1 ml Trypsin/EDTA (0.25 %). Cells were trypsinized for 30 min in a tissue culture incubator at 37 ºC. The reaction was stopped by adding 10 ml fresh media to the dish; tissue was broken up by vigorous pipetting and cell suspension was transferred into a 15 ml falcon tube. Untrypsinized tumor chunks and debris were allowed to sediment for 5 minutes. Supernatant and sediment were plated separately on 10 cm dishes in 10 ml media supplemented with Mouse FibrOut™ 9 for tumors. Cells were cultured until confluency was reached, genotyped and stored for further processing.

2.2.1.6. Transient transfection

2.2.1.6.1 Plasmid transfection with calcium phosphate

For transient transfection with calcium phosphate, cells were fed 4 h before transfection with fresh media. Next, plasmid DNA (20-30 µg) was mixed with 50 µl 2.5 M $CaCl_2$ in a final volume of 500 µl sterile H_2O and precipitated by adding

slowly under gently vortexing to 500 µl 2x HBS solution. Carefully, the mixture was evenly distributed among the cells and dish was incubated for 8-16 h in the cell culture hood. The following day, fresh media was applied and cells were incubated until further use.

2.2.1.6.2 siRNA transfection with MetafectenePro

To introduce small interfering RNA (siRNA), mammalian cells were seeded ensuring 30-40 % confluency the following day and fed with fresh media prior transfection. For transfection with 50-150 nM siRNA, respective amount of siRNA were diluted in a final volume of 200 µl Opti-MEM®, mixed gently and incubated for 5 minutes. Meanwhile, a 5-fold ratio MetafectenePro (relative to the siRNA-volume used) was diluted in a separate tube in the same volume Opti-MEM®, mixed gently and incubated for 5 minutes. The siRNA-solution was added to the transfection reagent, mixed gently by pipetting and incubated for 20 minutes at room temperature (RT) for complex formation. Finally, the mixture was evenly distributed among the cells. After 8 h incubation media was replaced by fresh one. Cells were harvested 48-72 h post-transfection and processed for RNA or protein analysis (see section 2.2.2.1 and 2.2.3.1)

2.2.1.7. Cell infection

2.2.1.7.1 Retroviral infection of cells

Production of ecotropic viral supernatant was performed by transient transfection of PlatE cells with the gene of interest using calcium phosphate (section 2.2.1.6.1). The virus-containing supernatant was harvested, filtered through 0.45 µm filter and used immediately for cell infection. For higher infection efficiency, 8 µg/ml polybrene was added. The target cell lines were incubated overnight with viral supernatant. The following day, cells were allowed to recover in fresh media for 8 h before a second infection round was started. Target cells were selected for the appropriate antibiotic and tested for positive infection.

2.2.1.7.2 Lentiviral infection of cells

Lentiviral virus production was carried out in a biosafety level 2 environment with high precaution. A confluent 10 cm dish of HEK293 cells was split 1:4 a day before and media was renewed 4 h prior transfection. Therefore, 9 µg of the lentiviral vector shRNA construct was transfected together with 6.75 µg psPAX2 (packaging vector) and 4.5 µg pCMV-VSV-G (envelope vector) via calcium phosphate (section 2.2.1.6.1). After incubation overnight, media was replaced by 8 ml new DMEM supplemented with 5 mM sodiumbutyrate. Viral supernatant was collected after 24 h, filtered through 0.45 µm filter and target cell lines were infected with 4 ml supernatant in the presence of 8 µg/ml polybrene. After 8 h, 4 ml fresh media was added and cells were cultured for further 12-16 h. Cells were recovered for 8 h in fresh media following treatment with appropriate antibiotics. Infection process was repeated up to 5 times depending on the cell line.

2.2.1.8. Cell cycle determination by Flow cytometry (FACS)

Determination of the cell cycle phase was done by quantitatively assessing the DNA content of a cell using the intercalating dye Propidium Iodide (PI). Therefore, cells were trypsinized, centrifuged for 5 minutes at *250 g* at 4 °C and washed with cold 1x PBS before fixation overnight with 1 ml 80 % ethanol at -20 °C. Before measurement, cells were pelleted for 10 minutes at *390 g* and washed once with cold 1x PBS. Cells were resuspended in 500 µl 38 mM sodium citrate, mixed with 25 µl RNase and kept 1 h at 37ºC in the dark. Shortly before analysis, cells were stained with15 µl PI and measured in a Cytomics FC500 Flow cytometer.

2.2.1.9. Colony formation assay

For investigating the effect of shRNA induction on cell growth an *in vitro* survival based assay was performed. Therefore, cells were seeded in low density and treated with different drugs (doxycycline or 4-OHT). Every 3rd day, fresh media and drugs were applied. After 10 days, cells were fixed for 10 minutes with 3.7 % formaldehyde (in H_2O) at RT under gentle shaking, washed with tap water and air-dried. Colonies were stained with 0.1 % crystal violet (in 20% ethanol) for 20 minutes at RT, washed 3 times with tap water until they appear clear and air-dried. For quantification, the dye was extracted with 5 ml 10 % acetic acid by agitation for 20 minutes at RT, diluted 1:4 in H_2O and absorbance was measured at 590 nm using 10 % acetic acid as reference.

2.2.1.10. Soft agar assay

Transformation potential of cells was assessed in an anchorage independent growth assay. Therefore, 1x10^4 cells were resuspended in 2 ml DMEM containing 0.35 % low melting agarose supplied with respective drug, seeded in triplicate into six-well plates onto a 2-ml layer of solidified 0.7 % low melting agarose in complete medium. Following a 14 days incubation period, formed colonies were recorded and foci number was scored.

2.2.2. Molecular biological methods

2.2.2.1. RNA isolation

Total RNA from cells was extracted with RNA isolation reagent TriFast. After aspirating media, 1 ml Trifast was added. Cells were scraped, transferred into a 1.5 ml tube and incubated for 5 minutes at RT. Next, 200 µl Chloroform was added and mixture was vortexted thoroughly for 1 minute. Subsequent centrifugation for 10 minutes at *12000 g* in a cooling centrifuge results in formation of 3 phases. The upper aqueous phase containing RNA was transferred into a new reaction tube and mixed with 2 volumes ethanol and 0.1 volume 5 M ammonium hydroxide. RNA precipitation was enhanced by keeping tubes for 1 h at -20 °C. Samples were centrifuged for 10 minutes at *12000 g* at 4 °C. The pellet was washed twice with

75 % ethanol (in DEPC), dried and resuspended in 25 µl RNase free water. Purity and concentration of the RNA was determined in a NanoDrop 2000 spectrophotometer.

2.2.2.2. Reverse transcription (RT-PCR)

For transcription of RNA into cDNA, 2 µg RNA in a final volume of 9.5 µl DEPC water were mixed on ice with 0.5 µl random primers. After denaturing at 70 °C for 5 minutes, samples were kept at 4 °C and the following mixture was added:

5 µl 5x RevertAid reaction buffer

6.25 µl dNTP

0.5 µl RiboLock RNase inhibitor

0.5 µl RevertAid Reverse Transcriptase

2.75 µl DEPC water

The solution was pipetted once up and down and incubated for 1 h at 37 °C. Heat inactivation for 15 minutes at 70 °C stopped the synthesis process. Until use, cDNA was stored at -20 °C.

2.2.2.3. Quantitative real-time PCR (qRT-PCR)

To determine the quantitative amount of specific mRNA compared to a housekeeping gene, the following set-up was used and measured in triplicate:

PCR mix

12.5 µl Absolute™ QPCR SYBR Green Mix

0.5 µl forward primer (10 µM)

0.5 µl reverse primer (10 µM)

1 µl cDNA or precipitated chromatin

ad 25 µl H_2O

Thermal profile set-up:	activation	95 °C	15 min
	amplification	95 °C	0.5 min
	(40 cycles)	60 °C	1 min
		95 °C	15 min
	dissociation	95 °C	1 min
		60 °C	0.5 min
		95 °C	0.5 min

The relative expression of a specific mRNA compared to a housekeeping gene was calculated according to the formula:

$$2^{-\Delta\Delta CT}$$

with $\Delta CT = CT_{\text{gene of interest}} - CT_{\text{housekeeping gene}}$

with $\Delta\Delta CT = \Delta CT_{\text{sample}} - \Delta CT_{\text{reference}}$

The standard deviation of ΔΔCT was calculated with:

$$s = \sqrt{s_1^2 + s_2^2}$$

with s_1 = standard deviation of gene of interest

with s_2 = standard deviation of housekeeping gene

The margin of error for $2^{-\Delta\Delta CT}$ was determined by the formula:

$$2^{-\Delta\Delta CT \pm s}$$

and the error used for error bars was calculated with

$$2^{-\Delta\Delta CT + s} - 2^{-\Delta\Delta CT}$$

2.2.2.4. Isolation of plasmid DNA from bacteria

2.2.2.4.1 Mini preparation

Extraction of plasmid DNA from bacteria in small scale was performed of single colonies of transformed *E.coli*. Therefore, colonies were picked and incubated overnight in 3 ml ampicillin-enriched LB media at 37 °C at 160 rpm on a platform shaker. Next day, 1.5 ml bacterial culture were pelleted for 2 minutes at *13200 g* at RT and resuspended in 150 µl miniprep solution S1. For cell lysis, 150 µl miniprep solution S2 was added, samples were gently inverted 5 times and incubated 5 minutes at RT. The reaction mix was neutralized with 150 µl miniprep solution S3 and cell suspension was centrifuged for 10 minutes at *13200 g*. The cleared supernatant (~ 400 µl) was transferred into a fresh reaction tube, mixed with 800 µl absolute ethanol and vortexed thoroughly. Precipitated DNA was pelleted by spinning for 10 minutes at *13200 g* and washed with 500 µl 70 % ethanol. After a second centrifugation step for 10 minutes at *13200 g* supernatant was discarded, pellet dried and dissolved in 20 µl TE buffer. Plasmid DNA concentration and purity was determined with a NanoDrop 2000 spectrophotometer.

2.2.2.4.2 Midi/Maxi preparation

A single colony was picked from an LB agar plate and incubated for 6-8 h in 2 ml ampicillin-enriched LB media. For inoculation either 100 ml (Midiprep) or 200 ml (Maxiprep) LB media containing ampicillin, up to 1 ml of the pre-culture was used. After overnight incubation at 37 °C at 160 rpm on a platform shaker, bacterial cultures were harvested by centrifugation for 10 minutes at *3200 g* at RT and plasmid DNA was extracted with PureLink HiPure Plasmid Midi-/Maxiprep Kit according to

the manufacture's instruction. Concentration and purity was determined with a NanoDrop 2000 spectrophotometer and samples were stored at -20 °C.

2.2.2.5. Isolation of plasmid DNA fragments from agarose gels

After digestion of plasmid DNA with respective restriction endonucelases, fragments were loaded on 0.8-2 % agarose gels containing ethidiumbromide (0.35 µg/ml) following separation by electrophoresis for 1-2 h at 100 V. Desired bands were excised under UV light with a clean scalpel and DNA was extracted with GeneJET Gel Extraction Kit according to manufacturer's protocol.

2.2.2.6. Isolation of genomic DNA from tumor slides

Genomic DNA from tumor slides was isolated under a stereomicroscope by scraping the material with forceps into 1 ml pure xylene. Samples were centrifuged for 5 minutes at full speed in a tabletop centrifuge at RT and washed twice with 1 ml absolute ethanol. Genomic DNA from the obtained pellet was further processed (see section 2.2.2.7) and genotyped (see section 2.2.2.8).

2.2.2.7. Extraction of genomic DNA (HotSHOT)

For preparation of genomic DNA (gDNA) for subsequent genotyping PCR, tails were lysed in 75 µl base buffer for 30 minutes at 95 °C. After heating, samples were cooled down for 5 minutes and 75 µl of neutralizing buffer was added. For isolated tumor material the amount of each solution was adjusted to the sample size and heating step was reduced to 15 minutes.

2.2.2.8. Genomic DNA PCR

For genotyping of tails, 1-5 µl of the final gDNA were used for each PCR reaction according to the following program

PCR mix	PCR program (30 cycles)	
1-5 µl gDNA	94 °C	5 min
2.5 µl 10x ReproFast buffer	94 °C	30 sec
2.5 µl dNTPs (2 mM)	56-64 °C	0.5-1 min
1 µl forward primer (10 µM)	72 °C	1 min
1 µl reverse primer (10 µM)	72 °C	5 min
0.2 µl His Taq polymerase (15 U)	4 °C	hold
ad 25 µl H_2O		

For genotyping of isolated tumor material, 5 µl of the final gDNA were used for each PCR reaction according to the following program

PCR mix	PCR program (35 cycles)	
5 µl gDNA	95 °C	1 min
4 µl 5x Phusion HF buffer	95 °C	15 sec
2 µl dNTPs (2 mM)	58-67 °C	30 sec
1 µl forward primer (10 µM)	72 °C	30 sec
1 µl reverse primer (10 µM)	72 °C	10 min
0.2 µl Phusion DNA polymerase (2 U)	4 °C	hold
ad 20 µl H_2O		

2.2.2.9. Cloning of lentiviral shRNAs

Potential shRNA sequences for the gene of interest were predicted using the Designer of Small Interfering RNA tool (DSIR, http://biodev.extra.cea.fr/DSIR/DSIR.html) and selected for several criteria described in Dow et al. (2012). Positive candidates were purchased as 97 bp long cloning template in a mir30-based format and restriction sites were introduced by PCR according to the following reaction:

PCR mix	PCR program (30 cycles)	
50 µM DNA (97 bp oligo)	94 °C	2 min
5 µl Pfu polymerase buffer	94 °C	0.5 min
5 µl dNTPs (2 mM)	54 °C	0.5 min
1 µl forward primer (10 µM)	72 °C	1 min
1 µl reverse primer (10 µM)	72 °C	10 min
0.5 µl DMSO	4 °C	hold
0.5 µl Pfu polymerase (1.25 U)		
ad 50 µl H_2O		

The expected band (138 bp) was purified in an agarose gel, extracted (see section 2.2.2.10) and digested with EcoRI/XhoI restriction endonucleases for 2-3 h at 37 °C. The column purified fragment was ligated into the cut pInducer10 vector and tested for its knockdown efficiency.

2.2.2.10. Agarose gel electrophoresis

Size-separation and concurrent purification of restriction digests or PCR products for analytical or preparative purpose was conducted by electrophoresis in agarose gels. Therefore, the respective amount of agarose powder was added to 1x TAE yielding gels of 0.8-2 % concentration. The solution was boiled in a microwave until complete dissolution of the agarose, mixed with ethidiumbromide (0.35 µg/ml final concentration) and solidified in a gel chamber. DNA samples were mixed with 5x loading buffer and loaded into pockets of the gel. As a size marker 100 bp or 1 kb DNA ladder was used. Electrophoresis ran for 1-2 h at 100 V, DNA bands were

visualized in a UV transilluminator, photographed and - if necessary - excised for further processing.

2.2.2.11. Restriction digestion

Digestion of plasmid DNA or PCR fragments was performed with appropriate restriction endonucelases and their recommended buffer for 1-4 h at 37 °C. A standard restriction reaction includes the following components:

PCR mix

0.5-5 µg DNA

5 µl 10x restriction endonuclease buffer

5-10 U restriction endonuclease

ad 20-50 µl H_2O

Digested DNA fragments were purified by gel electrophoresis or column purification using GeneJET PCR Purification Kit or QIAquick PCR Purification Kit according to manufacturer's protocol.

2.2.2.12. Ligation

In a standard ligation, DNA fragments were used in a molar ratio of 1:3-5 (vector to insert). For a final volume of 10 µl, ~50 ng vector were mixed with 1 µl 10x T4 ligase buffer and 0.5 µl T4 DNA ligase, the respective amount of insert and H_2O. The reaction was incubated for 1 h at room temperature with subsequent heat inactivation of the enzyme for 15 minutes at 65 °C.

2.2.2.13. Transformation of E.coli

For transformation of plasmid DNA, chemically competent D5Hα *E.coli* bacteria were used. After thawing, 50 µl bacteria were mixed with 5 µl ligation sample solution, mixed gently and chilled on ice for 10 minutes. DNA uptake was achieved by heating bacteria for 45 seconds at 42 °C in a heating block. Immediately, suspension was cooled on ice and 500 µl pre-warmed LB media was added. The approach was incubated for 1 h at 37 °C in a heat shaker with moderate agitation. Bacteria were pelleted for 1 minute at full speed in a tabletop centrifuge. Except a small rest, the supernatant was discarded; bacteria were resuspended and spread over an ampicillin-containing LB agar plate. Plates were kept at 37 °C overnight and single colonies were picked for plasmid isolation.

2.2.2.14. Sequencing

Sequencing of samples was done by LGC genomics or Eurofins and DNA was prepared according to the company's specifications.

2.2.3. Biochemical methods

2.2.3.1. Whole cell lysates

Cells were washed with ice cold 1x PBS, collected with a plastic cell scraper and transferred into a 1.5 ml reaction tube. After centrifugation for 5 minutes at *950 g* at 4 °C supernatant was aspirated and pellet was lysed in adequate volume of TNN lysis buffer for 30 minutes on ice. Cell debris was removed by spinning for 10 minutes at *20000 g* in a cooling centrifuge; clear supernatant was transferred into fresh reaction tube and protein concentration determined with Bradford solution (see section 2.2.3.2). Lysates were used immediately for subsequent analysis or flash frozen and stored at -80 °C until use.

2.2.3.2. Quantification of protein by Bradford method

Protein concentration was determined according to the method described by Bradford (1976). After incubation of 1 µl whole cell lysate with 1 ml Bradford solution for 5 minutes in the dark, extinction was measured at 595 nm and compared to a standard BSA dilution series.

2.2.3.3. Western Blot

The Western blot is a technique for the detection of specific proteins in a protein mixture. In brief, the desired amount of whole cell lysate was boiled with the same volume of 3x ESB and loaded on SDS gel for size separation (see section 2.2.3.5) and subsequent immunoblotting (see section 2.2.3.6)

2.2.3.4. Immunoprecipitation

During Immunoprecipitation a specific protein is purified from a cell lysate or extract. Therefore, 0.5-1 mg of whole cell lysate was mixed with respective antibodies. During the 4 h incubation period at 4 °C, gentle agitation of the lysate allows the target antigen to bind to the immobilized antibody. Pre-washed magnetic Dynabeads (50 µl) were added and further incubated for 1-2 h in the cold room. Beads were collected with a magnet, washed 5 times in pure TNN buffer and dried with a Hamilton syringe. Samples were resuspended in 30 µl 3x ESB, boiled at 95 °C for 5 minutes and loaded on a SDS gel (see section 2.2.3.5) or stored at -20 °C. In addition, 5-10 % of protein amount was used as input for immunoprecipitation.

2.2.3.5. SDS polyacrylamide gel electrophoresis (SDS-PAGE)

Separation of proteins was performed using discontinuous SDS-gel electrophoresis described by Laemmli (1970).Therefore, a separating gel (ranging from 8-14 %) was casted, and covered after polymerization with a stacking gel (5 %). In the table below, the composition of 1.5 mm gels is summarized:

Separating gel	8 %	10 %	12.5 %	14 %
H_2O (µl)	3894	3344	2656	2244
Separating gel buffer (µl)	2035	2035	2035	2035
20 % SDS (µl)	60.5	60.5	60.5	60.5
10 % APS (µl)	55	55	55	55
30 % Acrylamide (µl)	2200	2750	3438	3850
TEMED (µl)	5.5	5.5	5.5	5.5

Stacking gel	5 %
H_2O (µl)	1000
Bromphenol blue	50
Stacking gel buffer (µl)	1000
20 % SDS (µl)	60
10 % APS (µl)	40
30 % Acrylamide (µl)	500
TEMED (µl)	4

Electrophoresis was conducted in 1x SDS running buffer for 20 minutes at 80 V to allow migration of proteins into the stacking gel. Subsequently, current was increased to 35 mA/gel until desired resolution was achieved.

2.2.3.6. Immunoblotting

Proteins were transferred onto PVDF membranes in a BIORAD wet blot chamber. In brief, PVDF membrane was immersed in 100 % methanol for activation and equilibrated for a few minutes in blotting buffer. Meanwhile, sponges, Whatman paper and SDS gel were soaked in pre-chilled blotting buffer. After assembly of the blot (order: sponge, Whatman paper, PVDF membrane, SDS gel, Whatman paper, sponge), the "sandwich" was transferred into a wet blot chamber and filled with ice cold blotting buffer. In addition, a cooling device was added to prevent excessive heat development and protein degradation. Depending on the protein size, transfer was performed for 1-2 h at constant voltage (100 V). Successful and equal protein transfer was visualized by incubation of the membrane in Ponceau S solution.

Prior incubation with primary antibodies overnight at 4 °C, membranes were blocked for 1 h either in 3 % nonfat dry milk powder in TBST or 5 % BSA in TBST to reduce unspecific binding. Unbound antibody was removed by washing 3 times with TBST for 10 minutes followed by incubation with respective secondary antibodies for 1 h at RT. Membranes were rinsed with TBST (3 times. 10 minutes), chemoluminescent solution was added and specific bands were detected after exposition to ECL-films.

2.2.3.7. Chromatin immunoprecipitation (ChIP)

The enrichment of DREAM at target gene promoters was assessed in ChIP assays. In detail, approximately $2x10^7$ cells in 20 ml medium were cross-linked by adding 540 µl 37 % formaldehyde dropwise to the dishes and incubated at RT for 10 minutes under slowly shaking. The reaction was stopped by addition of 2.5 ml 1 M glycine and further incubation for 5 minutes. The medium was poured off, cells were washed twice with ice cold 1x PBS, scraped into 15 ml polystyrene falcon tubes and centrifuged for 5 minutes at *300 g* in a cooling centrifuge. According to its size, the pellet was lysed in 10 times lysis buffer for 15 minutes and centrifuged for 5 minutes at *3865 g* at 4 °C. The supernatant was removed carefully and nuclei were lysed in 900 µl nuclei lysis buffer on ice for additional 10 minutes. The chromatin was sheared on ice for 8 minutes using a BioRuptor sonificator (Diagenode) with 30 sec on/ 30 sec off cycle and high intensity yielding fragments of 250-1000 bp in length. After sonication, suspension was spun for 10 minutes at *18000 g* in a cooling centrifuge to remove cell debris and the size of the chromatin was examined. Therefore, 2 µl 5 M NaCl and 1 µl RNase A were mixed with 50 µl of the chromatin suspension and agitated overnight at 65 °C with moderate shaking. The following day, 2 µl Proteinase K were added, chromatin was incubated for 2 h in a shaking heat block at 55 °C and the fragment size was analyzed on a 1.2 % agarose gel. The remaining chromatin was diluted 1: 10 with dilution buffer and immunoprecipitations (IP) were set up with 2 ml chromatin suspension each. A 1 % input of the amount taken for the IP was removed and stored at 4°C until further processing. For immunoprecipitation the targets of interest, 4 µg of specific antibodies were added and incubated overnight on a rotating wheel at 4 °C. The antibody-protein-DNA complexes were purified using 50 µl of pre-blocked magnetic Protein-G Dynabeads for 1-2 h at 4 °C. The beads were collected on a magnet for 90 seconds and washed 7 times with 1 ml LiCl buffer. To reduce background the beads were incubated after the 5^{th} washing step for 10 minutes on a rotating wheel in the cold room. After washing, the beads and input samples were eluted with 100 µl of elution buffer for 15 minutes at room temperature under vigorous shaking. A second elution step with 150 µl was performed and both supernatants were combined. Reverse cross-linking was achieved by adding 10 µl 5 M NaCl and 5 µl RNase A to the supernatants following heat incubation overnight at 65 °C with slowly shaking. After addition of 1 µl proteinase K for 2 h at 55 °C proteins were removed from the eluted chromatin. Moreover, proteinase K digestion eliminates nucleases from the purified DNA, preventing its degradation. To separate DNA from protein fragments, samples were purified with Qiagen PCR Purification Kit according to the manufacturer's protocol and eluted in 50 µl of provided elution buffer. Purified chromatin (1 µl) was analyzed with quantitative PCR or stored at -20 °C until further processing.

2.2.4. Immunohistochemical methods

2.2.4.1. Preparation of paraffin sections

For preparation of lung paraffin sections, the mouse was sacrificed by cervical dislocation and chest was opened to expose the lung. Blood was removed by perfusing the lung with 3-5 ml 1x PBS. After instillation of 4 % PFA fixation solution, the lung was removed, washed in 1x PBS and kept in fixative at 4 °C overnight at a horizontal shaking platform. Organs were washed twice in 1x PBS and once in 0.9 % NaCl for 10 minutes each followed by incubation in 50 % and 70 % ethanol for 1 h each on a rotating wheel at RT. Tissue samples were stored in fresh 70°% ethanol at 4 °C until further processing.

Serial dehydration of the organs was performed automatically overnight in a Tissue Spin Processor according to the following steps:

Reagent	Time
70 % ethanol	1 h
80 % ethanol	1 h
90 % ethanol	1 h
95 % ethanol	1.5 h
100 % ethanol (2 times)	1 h
Xylene (2 times)	1.5 h
Paraffin (2 times)	2 h

After the last dehydration step, tissue samples were embedded in paraffin using a Microm EC 350 modular tissue embedding center. The blocks were allowed to solidify and stored at 4 °C. Paraffin blocks were sectioned into 5 µm (for immunohistochemical applications) or 10 µm thick slices (for tumor gDNA isolation) with a Hyrax M40 microtome.

2.2.4.2. H&E staining

For staining, dry slides were deparaffinized 2 times in xylene for 10 minutes and rehydrated in an ethanol dilution series (100 %, 95 %, 80 %, 70 %, 50 %) for 3 minutes each. After rinsing in H_2O, nuclei were stained in hematoxylin solution for 4 minutes followed by washing with running tap water for 4 minutes. Slides were differentiated (4x 10 sec) and blued (20 seconds) before counterstained with 0.1 % eosin solution for 1 minute and rinsed with water to remove excess stain. Samples were dehydrated in serial ethanol dilutions (70 %, 95 %, 100 %) for 3 minutes each, 2 times xylene for 10 minutes and sealed with Roti® Histokitt. Images of the lungs were acquired with an Upright Microscope DMI6000B and evaluated for their total tumor burden with ImageJ software.

2.2.4.3. Antibody staining of tissue sections

Paraffin slides were deparaffinized in xylene (5 minutes) and rehydrated in an ethanol dilution series (100 %, 95 %, 80 %, 70 %, 50 %) for 3 minutes each. Endogenous peroxidase activity was blocked by incubating in 3 % H_2O_2 (in 1x PBS). Samples were then washed 3 times in 1x PBS for 5 minutes each. For antigen retrieval, slides were boiled in 10 mM sodiumcitrate buffer (pH 6.0) for 2 minutes, cooled to RT and rinsed 3 times with 1x PBS for 5 minutes. Unspecific staining was minimized by blocking with 3 % BSA (in 1x PBS) or appropriate sera followed an overnight incubation with primary antibody at 4 °C in a humidified chamber. Next morning, excess antibody was washed away with 1x PBS (3 times, 2 minutes) and secondary antibody was applied for 1 h at RT in a humidified chamber. If necessary, staining was enhanced with biotinylated antibodies and manufacturer's instructions were implemented. Immunostaining was visualized by reaction of 3,3'-Diaminobenzidine (DAB substrate Kit) for 5-10 minutes with antibody-coupled peroxidases yielding a brown precipitate. The slides were rinsed 3 times in H_2O for 2 minutes and were counterstained with hematoxylin. Samples were dehydrated in serial ethanol dilutions (70 %, 95 %, 100 %) for 3 minutes each, 2 times in xylene for 10 minutes and mounted with Roti® Histokitt. Images were acquired with a Confocal Microscope Eclipse Ti or an Upright Microscope DMI6000B and processed with ImageJ.

2.2.4.4. β-Galactosidase staining of lung tissue

For ß-Galactosidase assay the mouse was sacrificed 3 days after infection with adeno-LacZ virus by cervical dislocation, chest was opened and lung was cleared from blood by perfusion with 3-5 ml 1x PBS. The lung was fixed by intratracheal instillation of 5 ml cold formalin solution, soaked for 30 min in fixative on ice and subsequently perfused with 20 ml 1x PBS. Organs were embedded in Tissue-Tek® O.C.T. Compound, frozen overnight at -80 °C and sections of 20 µm thickness were cut with a Leica 2800E Frigocut Microtome Cryostat. Sections were rinsed twice with 1x PBS containing 2 mM $MgCl_2$ for 10 min at 4 °C before incubation with X-Galactosidase reaction buffer at 37 °C in the dark. After 3 h, slides were rinsed with 1x PBS until yellow color of solution disappeared and sealed with Roti® Histokitt. Images of the lungs were acquired with an Upright Microscope DMI6000B and evaluated for the presence of blue precipitates.

2.2.5. Mouse husbandry

All animal experiments were carried out according to regulatory guidelines and protocols that were approved by an institutional committee (Tierschutzkommission der Regierung von Unterfranken).

2.2.5.1. Mouse facility

Mice were kept in an open cage system in type II polycarbonate cages, fed with standard rodent diet and health monitoring of sentinel mice was performed every 3-6 months. Preservation of strains was done continuously by breeding respective pairs in a ratio of 1:2 (male to female). Pups were weaned after 3 weeks, genotyped and separated from their parents before achieving maturity. All animals were registered with identity number (ear clip), gender, genotype, date of birth and parental breeding pair name. With exception of virus-infected mice, animals were sacrificed with CO_2. As this can induce capillary hemorrhages in certain tissues, e.g. lung, cervical dislocation was used for infected mice.

2.2.5.2. Anesthesia of mice

Prior infection, animals were anesthetized with Ketamine/Xylazine. Therefore, 200 µl Xylazine and 600 µl Ketavet were mixed with 0.9 % NaCl in a 1:4 ratio (v/v) and 150-200 µl suspension per 25 g body weight were administered with a 25 gauge needle intraperitoneally to the mice (corresponding 6-8 mg/kg body weight Xylazine and 90-120 mg/kg body weight Ketamine).

2.2.5.3. Infection of animals

Infection of mice was performed in a biosafety level 2 environment with high precaution. First, Adeno-Cre or Ad-LacZ virus was precipitated with calcium phosphate enhancing adenoviral uptake into bronchial tissue. The desired amount of virus ($1x10^5$ plaque forming units per mouse for Ad-Cre or $1x10^7$ plaque forming units per mouse for Ad-LacZ) was added to EMEM pH 7.86. Under gently agitation, $CaCl_2$ was added dropwise to a final concentration of 4 mM and the mixture was incubated for 30 minutes at RT. Male and female mice of an age of 6-8 weeks were anesthetized and viral precipitate (45 µl) was administered via intranasal instillation. Animals were placed back into the cage and regularly monitored until their recovery from anesthesia.

2.2.6. Statistical analysis

Statistical significance was calculated using Student's t-test or Chi Square test with post-hoc Fisher's Exact test and determined as significant according to following P-values: *: $p<0.05$; **: $p<0.01$; ***: $p<0.001$, ****: $p<0.0001$. All statistical analyses were performed with GraphPad Prism 6 (GraphPad Software, Inc., La Jolla, CA, USA).

3. Results

3.1. Gene regulation by MMB in lung cancer cells

In many human cancers the inactivation of p53 by mutation and/or deletion is a common event discovered in more than 50 different cancer types e.g. of lung, brain or breast (Vogelstein et al. 2000; Reilly et al. 2000; Olivier et al. 2010; Liu et al. 2016). In the absence of p53 the MMB complex, a master regulator of mitosis, was shown to be activated after DNA damage. Hence, promoting the over-activation of mitotic genes might be a critical step in tumorigenesis caused by chromosomal instability (Carter et al. 2006; Mannefeld et al. 2009; Bakhoum et al. 2014; Bakhoum and Compton 2012). The aim of this part is to analyze the regulation of mitotic gene expression by MMB and its relationship to the tumor suppressor p53 by the use of depletion assays in a K-Ras-driven lung tumor cell line with restorable p53 expression. This will help to understand the function of MMB during tumorigenesis and may identify cellular targets for therapeutic therapies.

3.1.1. Mitotic genes are targets of MMB in lung cancer cells

In order to analyze the regulation of mitotic genes by MMB in lung cancer a primary cell line (KPR8) isolated from lung adenocarcinoma of K-Ras$^{LA2\text{-}G12D/+}$; p53$^{LSL\text{-}+/LSL\text{-}+}$; Rosa^{CreERT2} mice was used (Feldser et al. 2010) (Fig. 5A) In addition to the expression of mutant K-Ras^{G12D} the cell line harbors wildtype p53 alleles which expression is abolished by a transcriptional and translational inhibitory element ("STOP cassette"). Thus, alleles are functionally equivalent to null alleles. Upon treatment with 4-hydroxytamoxifene (4-OHT), a Cre recombinase fused to the estrogen receptor (CreER^{T2}) can be activated resulting in the excision of the "STOP cassette" and re-expression of p53.

It is known from previous studies that MMB acts as activator of mitotic gene expression (Schmit et al. 2007; Mannefeld et al. 2009) in mammalian cells. Therefore, in the first experiment it was investigated whether MMB is also required for activation of mitotic gene expression in KPR8 cells. To do so, the MMB units Lin9 and B-Myb were inhibited for 48 h by small interfering RNA (siRNA). The expression of genes which were identified as MMB targets in a genome-wide microarray analysis after Lin9 inhibition was analyzed by rt-qPCR (Reichert et al. 2010). Genes were selected due to their strong downregulation in the microarray and the availability of according primers for analysis in the lab. Transient inhibition of Lin9, a core member of the MMB complex, or the transcription factor B-Myb, a subunit of MMB associated during S-phase, reduced the expression of 6 kinesins and 5 other MMB genes (Nusap1, Cenpf, Plk1, Birc5, CyclinB1) with different functions in mitosis (Fig. 5B). This finding imply that mitotic genes are targets of the MMB in lung cancer cells, a fact which previous studies also demonstrated for other cell lines like HeLa, T98G or HEK293 (Schmit et al. 2007; Reichert et al. 2010). Interestingly, cell cycle analysis by flow cytometry (PI-FACS) revealed that depletion of Lin9 or B-Myb resulted in higher proportions of cells with fractional DNA content (SubG1 peak) as compared to cells transfected with a control siRNA (Fig. 5C). This indicates

for a strong requirement of functional MMB to prevent apoptosis. In conclusion, data from both experiments suggest that mitotic genes are regulated by MMB in lung cancer cells and emphasize the importance of MMB for cell viability.

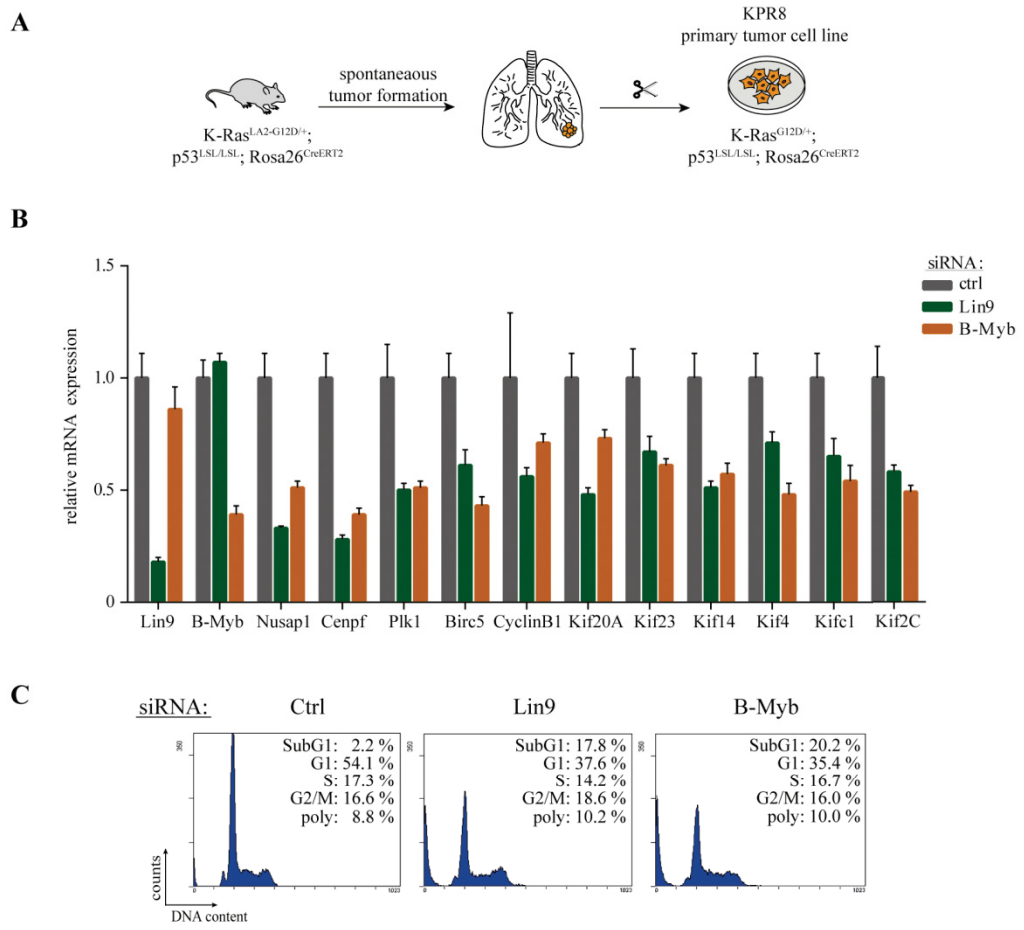

Figure 5: Regulation of mitotic genes by MMB in lung cancer cells
(**A**) Establishment of murine primary lung cancer cell line KPR8, gift by Tyler Jacks. (**B**) MMB units Lin9 and B-Myb were inhibited for 48 h by small interfering RNA (siRNA) in KPR8 cells. Gene expression was determined by real-time quantitative PCR (rt-qPCR). Two independent experiments were analyzed in triplicate, one representative experiment is shown.The error bars of the representative experiment were calculated of triplicates according to section 2.2.2.3 (**C**) KPR8 cells were treated as in (B) and cell cycle was analyzed by flow cytometry (PI-FACS). Three independent experiments were conducted, one representative experiment is shown.

3.1.2. Lentiviral inhibition of MMB subunit B-Myb decreases mitotic gene expression

To further explore the contribution of MMB to mitotic gene regulation a lentiviral vector expressing doxycycline-inducible small hairpin RNAs (shRNA) directed at B-Myb was introduced into KPR8 cells. Upon treatment with doxycycline the reverse transactivator (rtTA3), which is constitutively expressed, binds at its corresponding response element and a red fluorescent protein (RFP) is co-expressed together with the shRNA (Fig. 6A). Without induction no RFP fluorescence was detected in KPR8 cells indicating that the pInducer-system was tightly regulated. On the other hand,

addition of doxycycline for 48 h resulted in a dose-dependent expression of RFP with highest signals after treatment with 5 µg/ml doxycycline (Fig. 6B). Furthermore, the efficiency of inhibition of B-Myb mRNA expression by shRNA was measured by real-time quantitative PCR (rt-qPCR). Treatment with 1-5 µg/ml doxycycline resulted in dose-dependent knockdown of B-Myb mRNA levels yielding a 56 % reduction of mRNA expression after treatment with the highest concentration (Fig. 6C). Next, to confirm if B-Myb was also depleted on protein levels treated cells were lysed and subjected for immunoblot analysis. Addition of increasing doxycycline concentrations resulted in a distinct knockdown of B-Myb protein in KPR8 cells as depicted in figure 6D. Single clones of KPR8 cells stably expressing shRNA directed at B-Myb were isolated enhancing the knockdown efficacy of B-Myb on mRNA level up to 71 %. As expected from previous experiments with siRNA, the mitotic MMB target genes Nusap1, Cenpf and Birc5 were downregulated by half (Fig. 6E). Furthermore, reduced protein expression levels of Nusap1, Survivin (Birc5) and Top2A, another MMB target, could be confirmed by immunoblotting as shown in figure 6F. Taken together, these findings support the notion that MMB regulates mitotic genes in lung cancer cells.

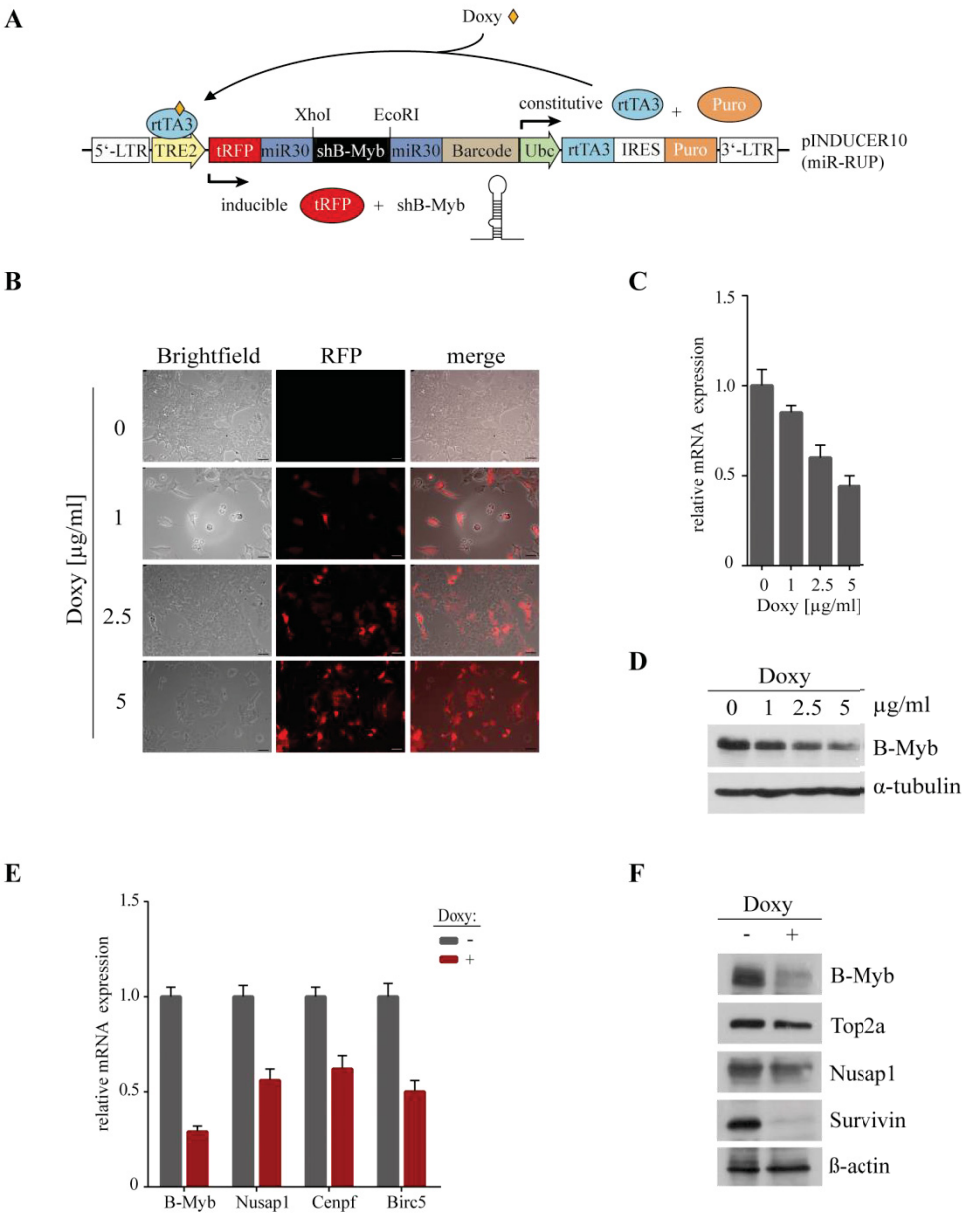

Figure 6: Lentiviral inhibition of B-Myb results in downregulation of MMB targets
(**A**) Scheme of lentiviral pInducer10 vector encoding for mir30 based shRNA against B-Myb. Doxycycline (Doxy) -induced binding of constitutively expressed reverse tetracycline transactivator (rtTA) to corresponding response element induces expression of shRNA and red fluorescent protein (tRFP). (**B**) KPR8 cells stably infected with pInducer vector encoding inducible B-Myb-specific shRNA were treated for 48 h with indicated concentrations of doxycycline. Expression of RFP was detected by microscopy. Scale bar: 75 µm (**C**). Knockdown of B-Myb was determined on mRNA level in cells treated as in (B) by rt-qPCR. (**D**) In KPR8 cells treated as in (B) knockdown of B-Myb was confirmed on protein level by immunoblotting. Tubulin was used as loading control. (**E**) A single clone of KPR8 cells stably expressing inducible shRNA against B-Myb was established and treated with 5 µg/ml doxycycline for 48 h. The knockdown of MMB target gene expression on mRNA level was validated by rt-qPCR Three independent experiments were analyzed in triplicate, one representative experiment is shown. The error bars of the representative experiment were calculated of triplicates according to section 2.2.2.3. (**F**) In cells treated as in (D) protein level of MMB target genes after B-Myb depletion were determined by immunoblotting. Actin was used as loading control

3.1.3. Impaired proliferation after B-Myb depletion in lung cancer cells

To investigate the biological relevance of B-Myb inhibition in KPR8 cells flow cytometry cell cycle analysis was performed. Treatment with 5 µg/ml doxycycline for 48 h induced robust expression of shRNA against B-Myb as deduced by co-expression of RFP. In addition, B-Myb depleted cells exhibited a greater proportion of cells in G2/M phase and with 4 N DNA content (Fig. 7A) which indicates for an impairment of proper mitosis. Only a small amount of fractionated cells were detected. Next, the influence of B-Myb knockdown on proliferation was determined. Therefore, cells were seeded at low density, treated with doxycycline for 10 days and colonies were visualized with crystal violet. KPR8 cells with an empty pInducer vector, containing a stuffer sequence instead of shRNA, were used as control. A strong reduction in colony formation was observed after B-Myb depletion whereas cells expressing the empty vector showed no effect on proliferation (Fig. 7B). Moreover, to explore the clinical relevance of this finding, the capability of KPR8 cells for oncogenic transformation after B-Myb inhibition was analyzed. To do so, cells were seeded in soft agar at low density and anchorage-independent cell growth as a sign for transformation was determined. Indeed, suppression of B-Myb significantly reduced colony size and number (Fig. 7C). In order to minimize the amount of doxycycline used for induction, cells were infected and selected alternately for 3 times with the shRNA containing vector and effects on proliferation were analyzed. Similar to results above strong growth inhibition was observed even at lowest concentration of 1 µg/ml doxycycline (Fig. 7D).

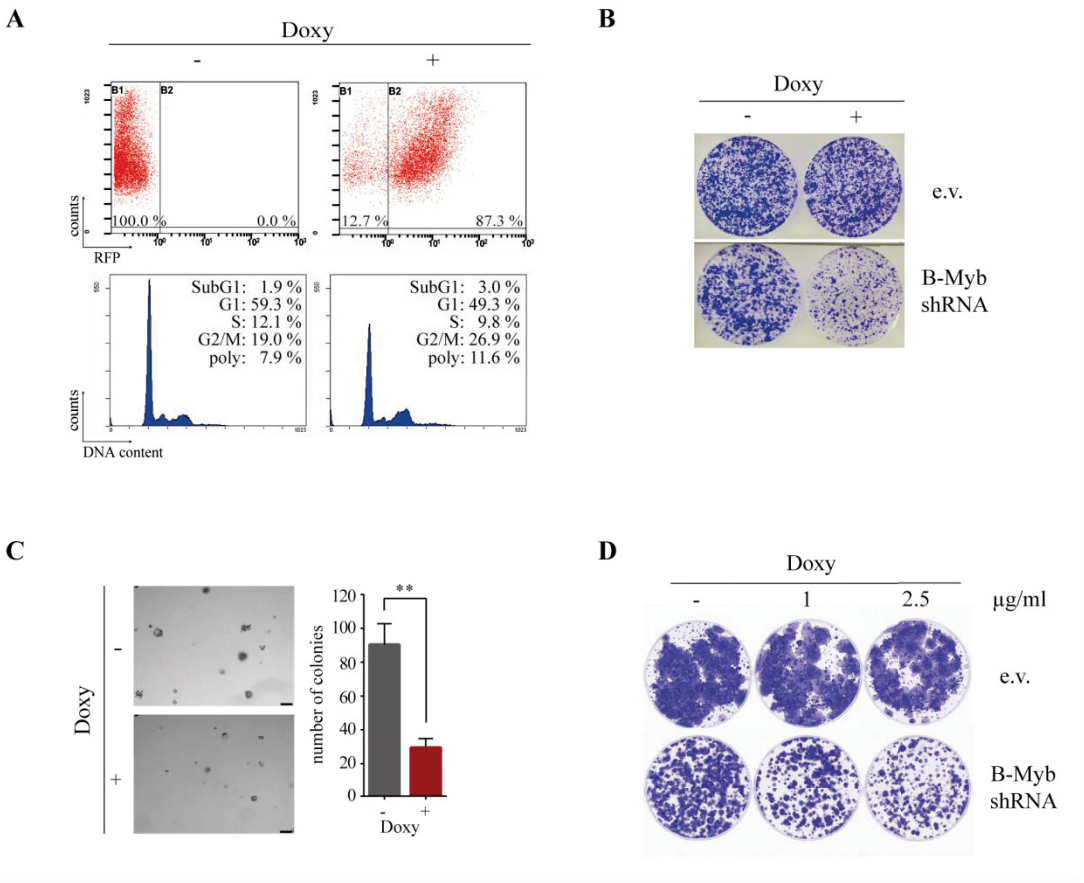

Figure 7: Depletion of MMB impairs proliferation in KPR8 lung cancer cells
(**A**) KPR8 cells stably infected with pInducer10 vector encoding inducible B-Myb-specific shRNA were treated for 48 h with 5 µg/ml doxycycline. Induction of RFP expression and cell cycle distribution was determined by flow cytometry. Three independent experiments were conducted and one representative experiment is shown. (**B**) KPR8 cells with inducible B-Myb-specific shRNA were seeded at low density and treated with 5 µg/ml doxycycline for 10 days. An empty pInducer10 vector (e.v.) was used as control. Cells were fixed and visualized by crystal violet staining revealing impaired proliferation after MMB depletion. (**C**) Soft-agar assays were conducted to analyze anchorage-independent growth of KPR8 cells after 14 days of doxycycline-induced depletion of B-Myb. Three independent experiments were analyzed in triplicate. Mean + SD is given. **: $P < 0.01$ (student's t-test) (**D**) In cells infected up to 5 times with pInducer10 encoding B-Myb-specific shRNA proliferation was examined after 10 days of induction with low concentrations (1-2.5 µg/ml) of doxycycline. An empty pInducer10 vector was used as control.

3.1.4. Restoration of p53 suppresses mitotic gene expression

In a previously published report it was found that B-Myb failed to dislocate the MuvB core in p53 mutant cells and this contributed to elevated G2/M gene expression after DNA damage (Mannefeld et al. 2009). Hence, it was of interest to elucidate the role of p53 in regulation of mitotic genes in KPR8 lung cancer cells. As described at the beginning, the expression of wildtype p53 in the used K-Ras^{G12D}-driven cell line is abolished by a translational "STOP cassette" that can be removed by inducible CreER^{T2} recombinase (Fig. 8A). Treatment of KPR8 cells with 4-OHT activates the expression of CreER^{T2} recombinase. Hence, the translational "STOP cassette" is removed yielding in re-expression of functional p53. The influence of p53

on MMB target gene expression was then analyzed by rt-qPCR. Treatment with 4-OHT for indicated time points (0-72 h) restored the p53 alleles and cyclin-dependent kinase inhibitor $p21^{CIP1}$, a well-known target gene of p53, was strongly activated after restoration. In contrast, mitotic mRNA levels of 6 MMB targets (Nusap1, Plk1, Cenpf, Birc5, Kif20a and CyclinB1) were downregulated in a time-dependent manner. First reduction in mitotic gene expression was observed after 12 h of p53 induction. Within 24 h an average knockdown of mRNA levels of ~50 % was observed and enhanced further after prolonged p53 expression (Fig. 8B). In addition, expression of phospho-B-Myb, a marker for active B-Myb protein, was detected by immunoblotting with an antibody against phosphorylation on threonine 487 by cyclinA/CDK2 and decreased rapidly after p53 reactivation (Fig. 8C) suggesting that progression through the cell cycle arrested. Consistent with this observation, a halt in proliferation with time depicted by an increase of cells in G1 phase was confirmed by flow cytometry after induction of p53 (Fig. 8D). Taken together, these results indicate that MMB-dependent genes are repressed after restoration of the tumor suppressor and act downstream the p53 pathway.

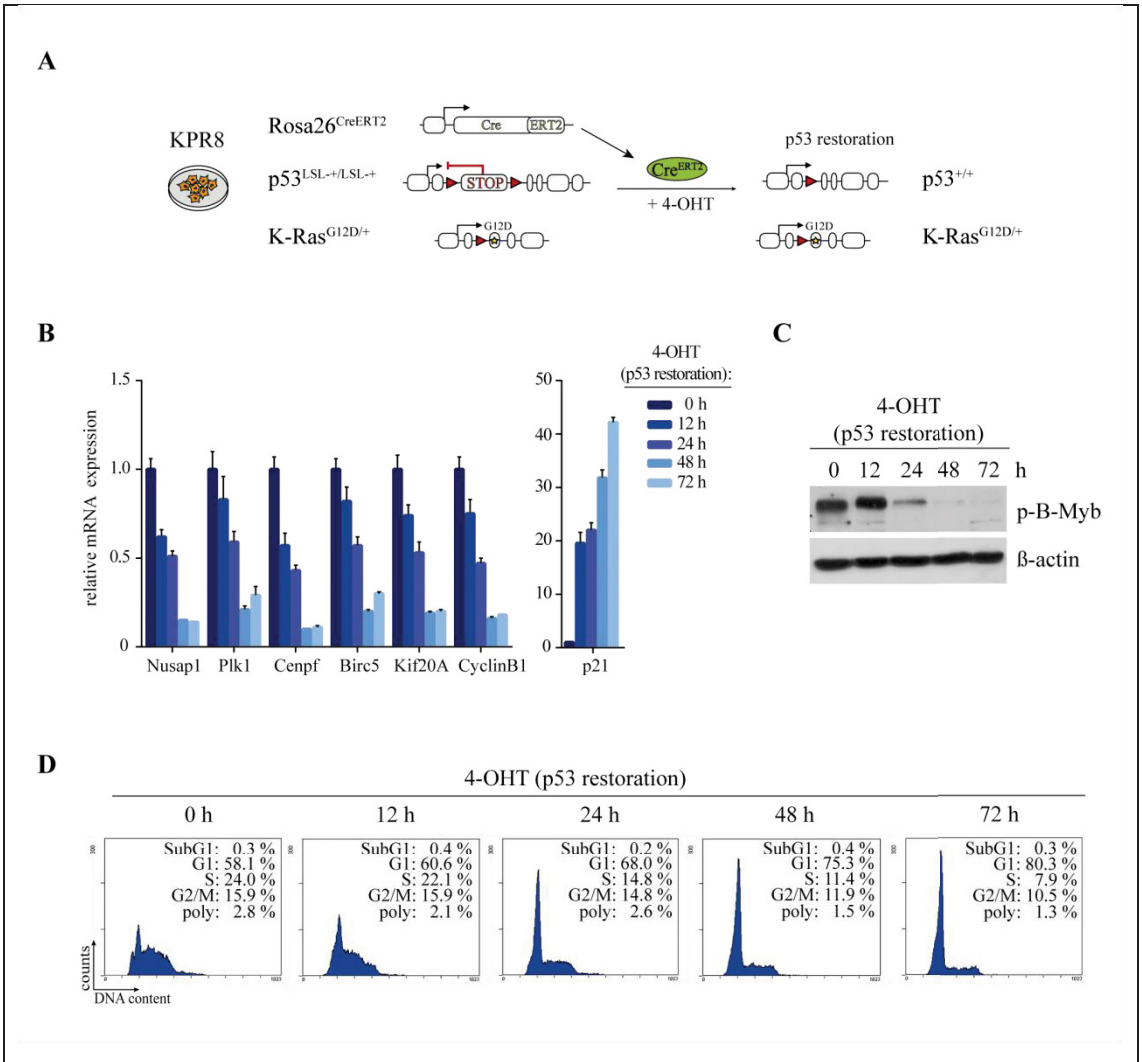

Figure 8: Restoration of p53 represses MMB gene expression.
(**A**) Treatment of KPR8 cells with 500 nM 4-hydroxytamoxifene (4-OHT) activates Cre recombinase and results in restoration of p53 function by deletion of "LoxP-STOP-LoxP (LSL) cassette" on p53 alleles. (**B**) After addition of 500 nM 4-OHT to medium of KPR8 cells for indicated time points the

expression of mitotic MMB target genes was evaluated by rt-qPCR. The increasing expression of p53 target gene p21 was used as sensor for p53 restoration. Three independent experiments were analyzed in triplicate, one representative experiment is shown. The error bars of the representative experiment were calculated of triplicates according to section 2.2.2.3. (**C**) In cells treated as in (B) the expression of active, phosphorylated B-Myb (T487) was analyzed by immunoblotting. As loading control ß-actin was used. (**D**) The fraction of cells in the different cell cycle phases was determined by flow cytometry (PI FACS) in KPR8 cells treated as in (B). Three independent experiments were conducted and one representative experiment is shown.

3.1.5. Restoration of p53 promotes formation of repressive DREAM complex

Previous studies reported that the MuvB core associated with different subunits in a cell cycle dependent manner to regulate gene transcription. Specifically, the pocket protein p130, E2F4 and DP1 bind to MuvB in quiescent cells (G0) and during G1-phase to form the repressive DREAM complex. In contrast, upon entrance into S-phase the association of p130/E2F4/DP1 is lost and B-Myb binds to the MuvB core yielding MMB. In later S-phase the transcription factor FoxM1 is recruited into the MMB complex (MMB-FoxM1) (Schmit et al. 2007; Litovchick et al. 2007; Mannefeld et al. 2009; Sadasivam and DeCaprio 2013). Having shown that p53 restoration resulted in cell cycle arrest it was of interest to determine the effect of p53 reactivation on the composition of MMB. To do so, co-immunoprecipitation assays were performed in KPR8 cells (Fig.9A). After treatment of cells with 4-OHT for 30 h to induce the re-expression of p53 the lysates were immunoprecipitated with a Lin9 antibody, a member of the MuvB core. The antibody-protein complexes were washed and binding was disrupted by heat shock treatment. The association of p130 or B-Myb to the MuvB core was then analyzed by western blot. As respective controls immunoglobulin G (IgG) was used. Treatment with 4-OHT for 30 h resulted in a strong association of p130 to the MuvB core. Conversely, B-Myb was released from the complex indicating that restoration of p53 promoted formation of the repressive DREAM complex (Fig. 9B). To support the notion, ChiP assay were conducted. Therefore, chromatin of 4-OHT treated KPR8 cells was isolated and subjected for immunoprecipitation with B-Myb and p130 antibodies. Subsequently, the binding of the proteins to 3 MMB target gene promoters (Nusap1, Cenpf, Aspm) and 1 reference promoter (Gapdh) was analyzed with rt-qPCR. An IgG antibody was used as respective control. ChIP assays with B-Myb and p130 antibodies on promoters of MMB targets Nusap1, Cenpf and Aspm confirmed that binding of p130 was strongly fostered whereas binding of B-Myb decreased after p53 induction. As expected, weak binding of all 3 proteins to the promoter of the reference gene Gapdh was detected (Fig. 9C). In conclusion, these findings suggest that the MMB is the predominant complex in the absence of functional p53 and is required to drive elevated expression of mitotic genes in lung cancer cells.

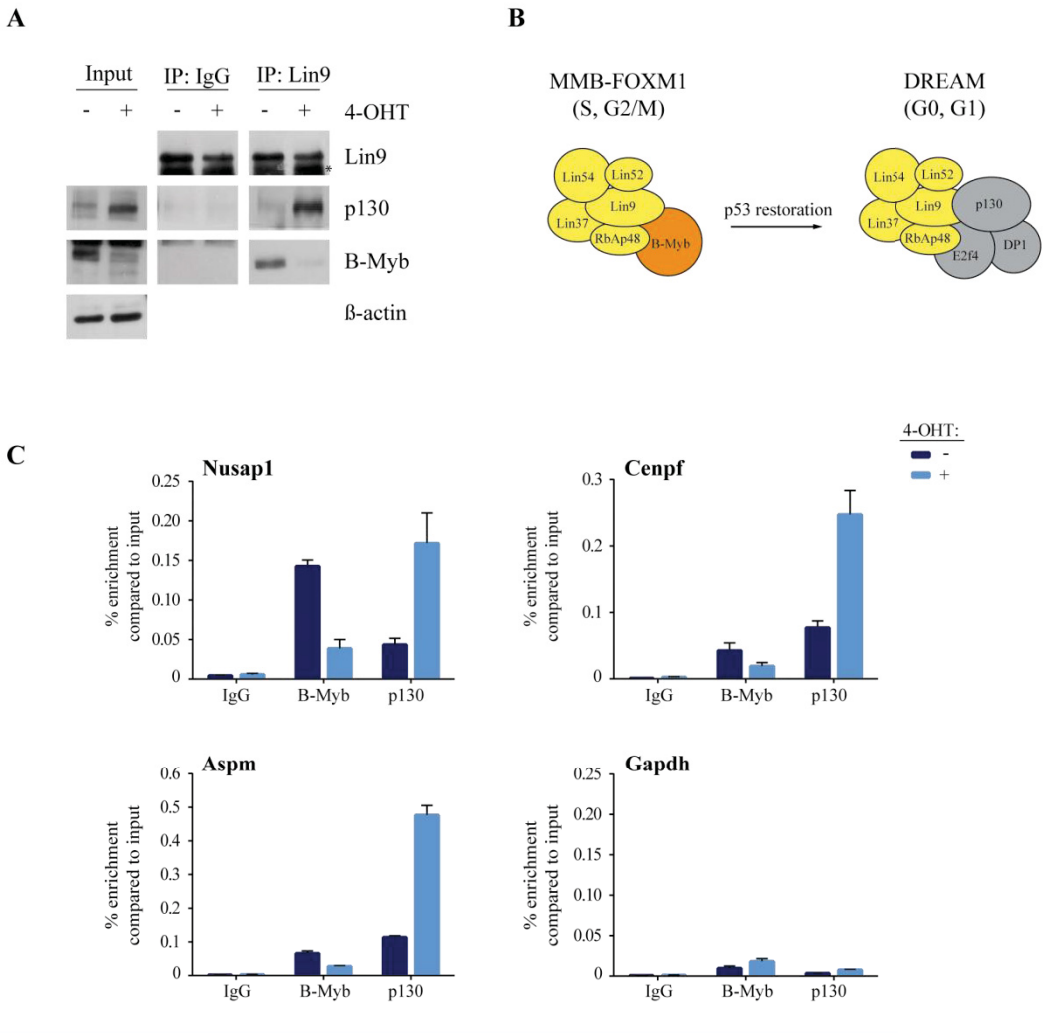

Figure 9: Restoration of p53 induces formation of repressive DREAM complex
(**A**) KPR8 cells were treated with 500 nM 4-OHT for 30 h to induce re-expression of p53 and lysates were immunoprecipitated with a Lin9 specific antibody. An IgG antibody was used as control. Binding of B-Myb and p130 to Lin9 or IgG was confirmed by immunoblotting. (**B**) Upon restoration of p53, the active MMB complex switches to the repressive DREAM complex (**C**) KPR8 cells were treated with 500 nM 4-OHT for 30 h and chromatin was immunoprecipitated with B-Myb or p130 antibody. Immunoglobulin G (IgG) antibody was used to discriminate for unspecific binding. Enrichment of proteins on promoters of mitotic MMB targets was determined by rt-qPCR in 3 independent experiments. The Gapdh promoter was used as reference gene. The error bars were calculated according to section 2.2.2.3.

3.2. Role of MMB in lung tumorigenesis *in vivo*

The MMB complex is a transcriptional activator and essential regulator of mitotic genes. Although expression of MMB target genes is elevated in a variety of cancer and MMB has been extensively characterized biochemically (Müller et al. 2012; Schmit et al. 2007; Osterloh et al. 2007; Pilkinton et al. 2007) its role during tumorigenesis *in vivo* is still unknown and has to be elucidated. Hence, the aim of this part is to investigate the contribution of MMB to tumorigenesis by depletion of Lin9, a core unit of the complex, in a mouse model of non-small cell lung cancer (NSCLC) to achieve a better understanding of lung tumor initiation and progression.

3.2.1. Intranasal instillation of adenoviral vectors *in vivo*

A well-established NSCLC mouse model driven by oncogenic K-Ras and loss-of-function p53 was selected to investigate the role of MMB in tumorigenesis. Mice bearing a mutant K-Ras allele (K-Ras$^{LSL\text{-}G12D/+}$) were crossed with conditional p53 knockout mice (p53$^{fl/fl}$) and offspring positive for the described alleles were selected by genotyping PCR exhibiting band pattern as shown in figure 10A.

First, to establish adenoviral delivery of virus particles *a test* infection experiment was conducted. According to the method described by DuPage et al. (2009), $5*10^7$ plaque forming units (PFU) of a LacZ containing adenoviral vector was administered intranasal to anesthetized mice, yielding in expression of ß-galactosidase protein in infected cells. Three days after infection, mice were sacrificed. Dissected lungs were fixed, embedded and cryopreserved. Beta-galactosidase activity was visualized in frozen lung sections by staining with X-Gal, an artificial galactose linked to a substituted indole, resulting in formation of a blue insoluble dye (Fig. 10B). As expected, only few cells stained blue and were distributed sporadically over the lung reflecting single infection events (Fig. 10C). Thus, intranasal instillation with adenoviral particles is a suitable tool to infect epithelial lung cells *in vivo* for investigation of initiation and progression of tumors by single events.

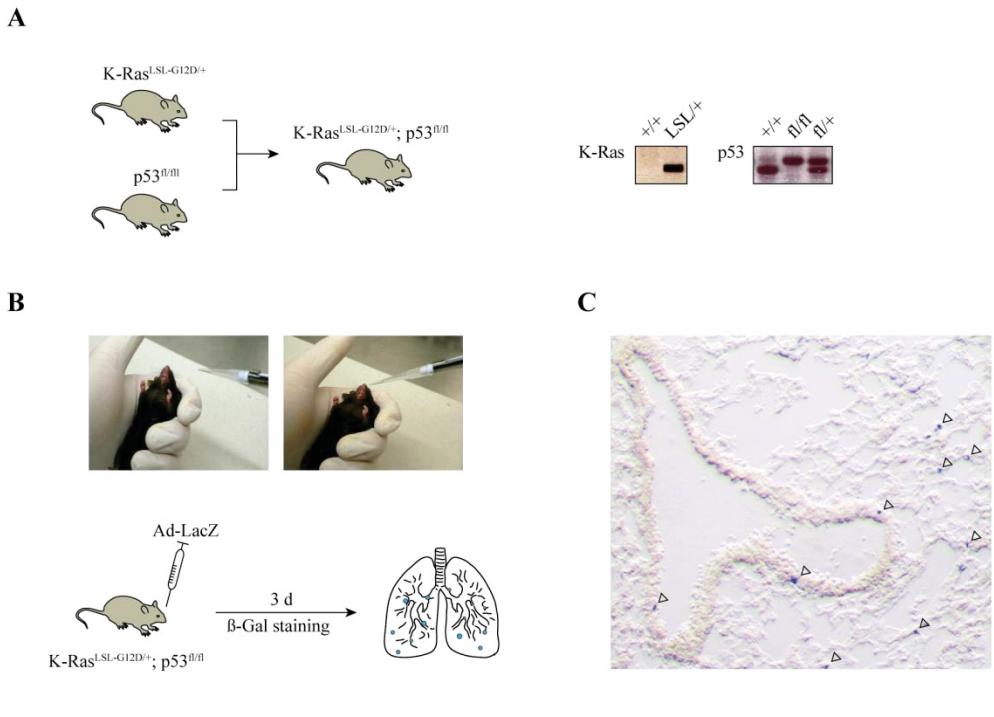

Figure 10: Infection of epithelial lung cells with adenoviral LacZ by intranasal instillation
(**A**) Inducible K-Ras$^{LSL-G12D/+}$ mouse strain was crossed with conditional p53$^{fl/fl}$ strain to obtain K-Ras$^{LSL-G12D/+}$; p53$^{fl/fl}$ mice. Genotype was determined by genomic PCR with primers for the LoxP-STOP-LoxP cassette (LSL) on K-Ras allele and floxed alleles of p53. (**B**) Intranasal infection with $5*10^7$ plaque forming units (PFU) of an adenoviral LacZ vector in anaesthetized K-Ras$^{LSL-G12D/+}$; p53$^{fl/fl}$ mice. After 3 days ß-galactosidase staining was performed on cryostat sections. Pictures were taken in the lab during experiment. (**C**) Representative sample of a lung section after infection with Ad-LacZ. Epithelial lung cells expressing LacZ stained blue after formation of precipitate in a ß-galactosidase assay Arrowheads indicate LacZ positive cells.

3.2.2. Lung tumor induction in a mouse model of NSCLC

Next, it was investigated whether lung tumor formation could be induced in the aforementioned mouse model. To address that question, K-Ras$^{LSLG12D/+}$; p53$^{fl/fl}$ mice were infected with $1*10^5$ plaque forming units (PFU) of an adenoviral Cre-recombinase and tumor progression was evaluated (Fig. 11A). Upon controlled Cre-mediated recombination of LoxP sites the transcriptional and translational "STOP cassette" on the K-Ras locus is excised which resulted in the expression of oncogenic K-Ras^{G12D}. Concurrently, expression of functional p53 is abolished by deletion of exons 2-10 (Fig. 11B). Thirteen weeks post-infection, mice were sacrificed dissected and lungs were removed. Organs were cleaned of remaining blood and kept in fixative (PFA) overnight. After dehydration by serial ethanol dilution lungs were embedded in paraffin. Lung sections were stained with H&E for clearer discrimination of cytoplasm or nuclei and evaluated for tumor formation. Within 13 weeks after infection mice developed a spectrum of tumors which were classified by a four-stage grading system (based on Nikitin et al. 2004; DuPage, Dooley, and Jacks 2009; Jackson et al. 2001) (Fig. 11C). Lesions were categorized as grade I (atypical adenomatous hyperplasia, AAH) if they showed uniform nuclei without any nuclear atypia. In lesions of grade II (adenomas) nuclei were slightly enlarged and prominent

nucleoli were visible. Adenocarcinomas were classified as grade III and presented a greater cytological atypia with enlarged, pleomorphic nuclei and a higher frequency of abnormal mitotic figures as compared to adenomas. Tumors of grade IV (invasive adenocarcinomas) harbored all the features of grade III and exhibited highly invasion of stromal cells (desmoplastic reaction) as well as invasive edges bordering blood vessels and lymphatic vessel. Taken together, these findings confirm that controlled activation of oncogenic K-Ras and loss of p53 induces tumor formation in epithelial lung cells.

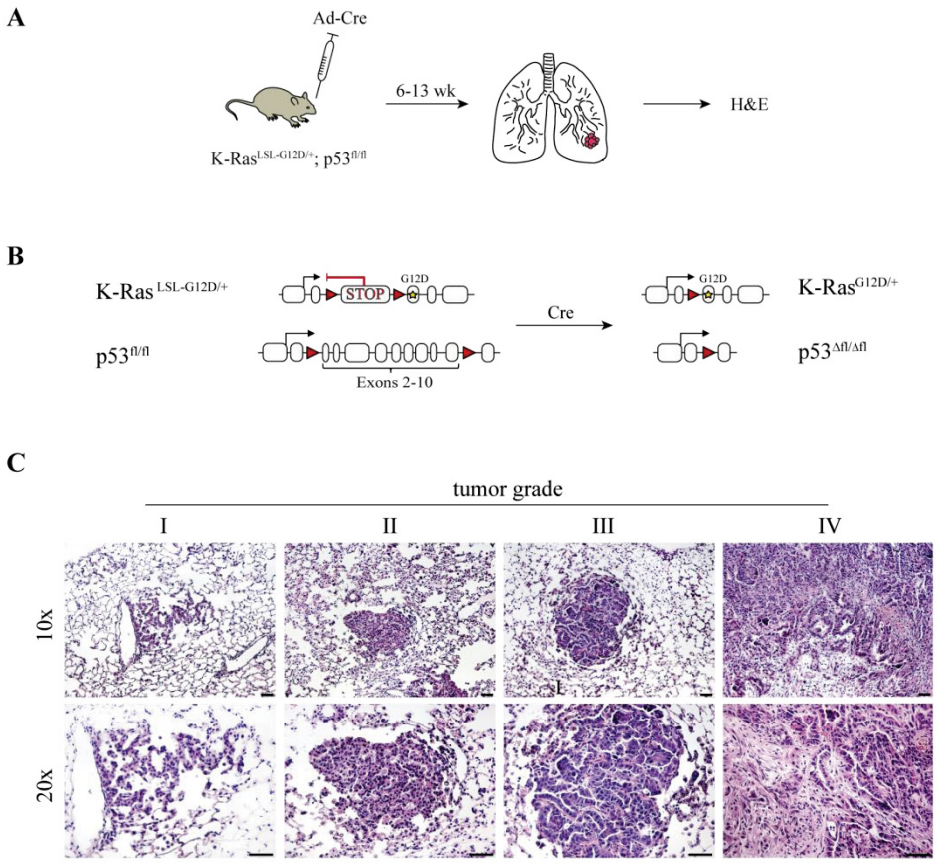

Figure 11: Induction of tumorigenesis after activation oncogenic K-Ras and loss of p53
(**A**) After infection of K-Ras$^{LSL-G12D/+}$; p53$^{fl/fl}$ mice with 1*10^5 plaque forming units (PFU) of an adenoviral Cre recombinase (Ad-Cre) tumor progression was analyzed by H&E staining of formalin fixed paraffin embedded (FFPE) lung sections. (**B**) Cre recombinase expression after infection with Ad-Cre mediates oncogenic K-Ras^{G12D} activation and deletion of p53. (**C**) Representative histological samples of tumors observed in hematoxylin and eosin (H&E) stained lung sections of K-Ras$^{LSL-G12D/+}$; p53$^{fl/fl}$ mice . Grade 1: atypical adenomatous hyperplasia; Grade II: adenomas; Grade III: adenocarcinomas; Grade IV: invasive adenocarcinomas; original magnification 10x (upper panel) or 20x (lower panel). Scale bar 50 µm.

3.2.3. Mitotic genes are expressed at elevated levels in lung tumors

After it was shown that lung tumors arise due to activation of oncogenic K-Ras and in the absence of p53 the expression pattern of MMB target genes in tumors should be clarified. To do so, 13 weeks after infection of K-Ras$^{LSL-G12D/+}$; p53$^{fl/fl}$ mice with

$1*10^5$ PFU of AdCre lung paraffin sections were prepared as described in section 2.2.2.. For immunohistochemical analysis, lung sections were rehydrated and antigens were retrieved by heat in citric solution. After incubation with antibodies against phosphorylated B-Myb (*p*-B-Myb) or mitotic MMB-target genes (Nusap1, Cenpf, CyclinB1) binding reaction was visualized by DAB staining and expression patterns were analyzed (Fig. 12A). Elevated levels of active B-Myb expression was observed in tumors demonstrated by staining with an antibody that detects B-Myb phosphorylated on threonine 487 by cyclin A/CDK2 during S phase. In contrast, no *p*-B-Myb expression was detected in normal lung tissue suggesting for a role of MMB subunit B-Myb during lung tumorigenesis. This observation was strongly supported by immunohistochemistry with antibodies against the MMB targets Nusap1, Cenpf and CyclinB1, all having functions during mitosis. In comparison to normal lung tissue, adenocarcinoma depicted strong expression of indicated genes (Fig. 12B). Thus, these data demonstrate that mitotic genes are highly expressed in lung tumors and MMB may be the driver for overexpression.

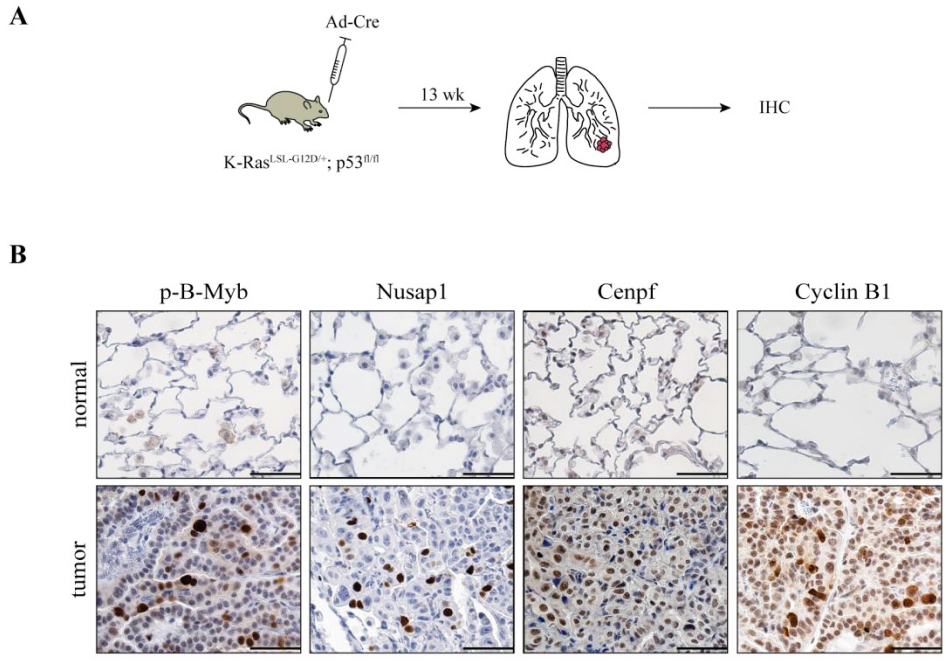

Figure 12: Mitotic genes are expressed at elevated levels in tumors of NSCLC
(**A**) K-Ras$^{LSL-G12D/+}$; p53$^{fl/fl}$ mice were infected with $1*10^5$ PFU of Ad-Cre. Thirteen weeks after tumor initiation lungs were isolated and FFPE samples prepared for immunohistochemical analysis. (**B**) Lung tumor and adjacent normal lung tissue were stained with antibodies against active B-Myb (phosphor T487) and mitotic MMB target genes Nusap1, Cenpf and Cyclin B1. Scale Bar: 50 µm

3.2.4. Establishment of a NSCLC mouse model with conditional Lin9

After incidence of elevated expression of mitotic MMB target genes was confirmed in lung adenocarcinomas, it was of interest to know if knockdown of MMB activity could inhibit tumor formation *in vivo*. To directly test the contribution to lung tumorigenesis the above described double-mutant K-Ras$^{LSL-G12D/+}$; p53$^{fl/fl}$ mice were crossed with conditional Lin9 (Lin9$^{fl/fl}$) mice (Fig. 13A). In latter one, exon 7 of Lin9

locus was flanked by LoxP sites resulting in deletion upon Cre-mediated recombination and the expression of a truncated non-functional protein due to a frameshift (Reichert et al. 2010). Genotype of littermates was determined by PCR. In an attempt to identify an optimal time point that might generate a modest number of lesions in the lung K-Ras$^{LSL-G12D/+}$; p53$^{fl/fl}$; Lin9$^{fl/+}$ mice were infected with 1*10^5 PFU of an adenoviral Cre-recombinase achieving simultaneous activation of oncogenic K-Ras as well as loss of p53 and Lin9 (Fig. 13B and 13C). At 6 weeks after infection mice developed nodules of AAH and small adenomas. Single lesions were observed in lungs 13 weeks following infection suggesting this time point as optimum for further evaluations of tumors (Fig. 13D)

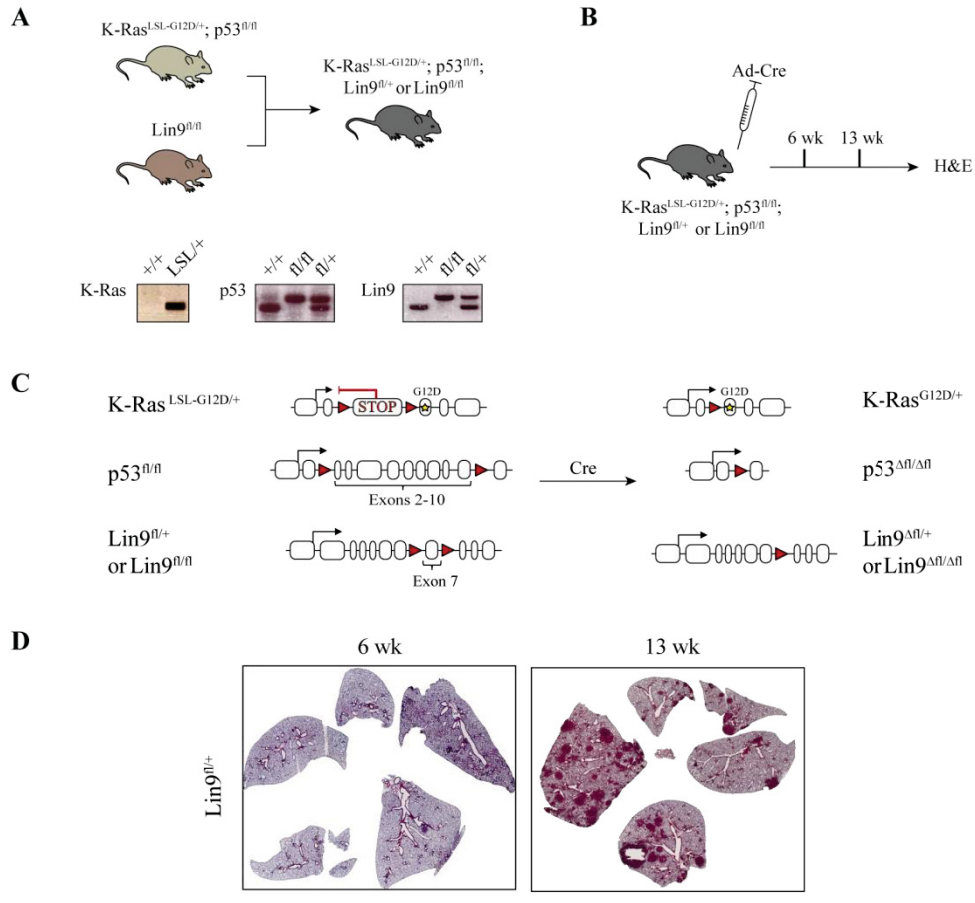

Figure 13: Mouse model to investigate the contribution of MMB to lung tumorigenesis
(**A**) Inducible K-Ras$^{LSL-G12D/+}$; p53$^{fl/fl}$ mouse strain was crossed with conditional Lin9$^{fl/fl}$ strain to obtain K-Ras$^{LSL-G12D/+}$; p53$^{fl/fl}$; Lin9$^{fl/+}$ and K-Ras$^{LSL-G12D/+}$; p53$^{fl/fl}$; Lin9$^{fl/fl}$ mice. Genotype was determined by genomic PCR with primers for the LoxP-STOP-LoxP cassette (LSL) on K-Ras allele or LoxP sites on alleles of p53 and Lin9. (**B**) After infection with 1*10^5 PFU of Ad-Cre mice were sacrificed after 6 or 13 weeks and lungs were subjected to histological analysis by H&E staining (**C**) Adenoviral infection with Ad-Cre initiates the activation of oncogenic K-Ras^{G12D} and expression of non-functional p53 and Lin9. (**D**) K-Ras$^{LSL-G12D/+}$; p53$^{fl/fl}$; Lin9$^{fl/+}$ mice were killed at indicated time points and histological sections were examined for the presence of tumorigenic lesions.

3.2.5. Deletion of MMB core member Lin9 reduces tumor burden

The experiments shown in Figure 14 indicate that the knockout of MMB core member Lin9 does not prevent the initiation of lung tumorigenesis. Next the impact of Lin9 deletion on tumor burden was quantified. Simultaneous activation of mutant K-Ras and deletion of p53 and Lin9 was induced with $1*10^5$ PFU of adenoviral Cre-recombinase in K-Ras$^{LSL\text{-}G12D/+}$; p53$^{fl/fl}$; Lin9$^{fl/fl}$ mice (Fig. 14A). As internal control K-Ras$^{LSL\text{-}G12D/+}$; p53$^{fl/fl}$ mice with wildtype alleles of Lin9 were used. K-Ras$^{LSL\text{-}G12D/+}$; p53$^{fl/fl}$; Lin9$^{fl/+}$ with only one functional allele remaining served as additional control. At 13 weeks after infection mice were sacrificed. Gross inspections of the lungs suggested a lower incidence for tumors (white bulky spots on lung surface) in K-Ras$^{LSL\text{-}G12D/+}$; p53$^{fl/fl}$; Lin9$^{fl/fl}$ mice as compared to controls. In contrast, K-Ras$^{LSL\text{-}G12D/+}$; p53$^{fl/fl}$ Lin9$^{+/+}$ and K-Ras$^{LSL\text{-}G12D/+}$; p53$^{fl/fl}$; Lin9$^{fl/+}$ mice showed a similar number of lesions (Fig. 14B). To further verify these observations, histological lung sections were stained with H&E and inspected under the microscope. Tumor burden was evaluated by calculating the ratio of tumor area to total lung area. Indeed, K-Ras$^{LSL\text{-}G12D/+}$; p53$^{fl/fl}$; Lin9$^{fl/fl}$ mice had a significantly lower tumor burden as measured by the relative tumor area. Moreover, in comparison to K-Ras$^{LSL\text{-}G12D/+}$; p53$^{fl/fl}$; Lin9$^{+/+}$ mice, tumors were less advanced and a shift in tumor grade was observed. In contrast, animals heterozygous for Lin9 showed a slight increase in tumor burden as compared to K-Ras$^{LSL\text{-}G12D/+}$; p53$^{fl/fl}$; Lin9$^{+/+}$ (Fig. 14C and 14D). In conclusion, depletion of Lin9 significantly impairs the development of lung tumors indicating a requirement of Lin9 for tumorigenesis in NSCLC *in vivo*.

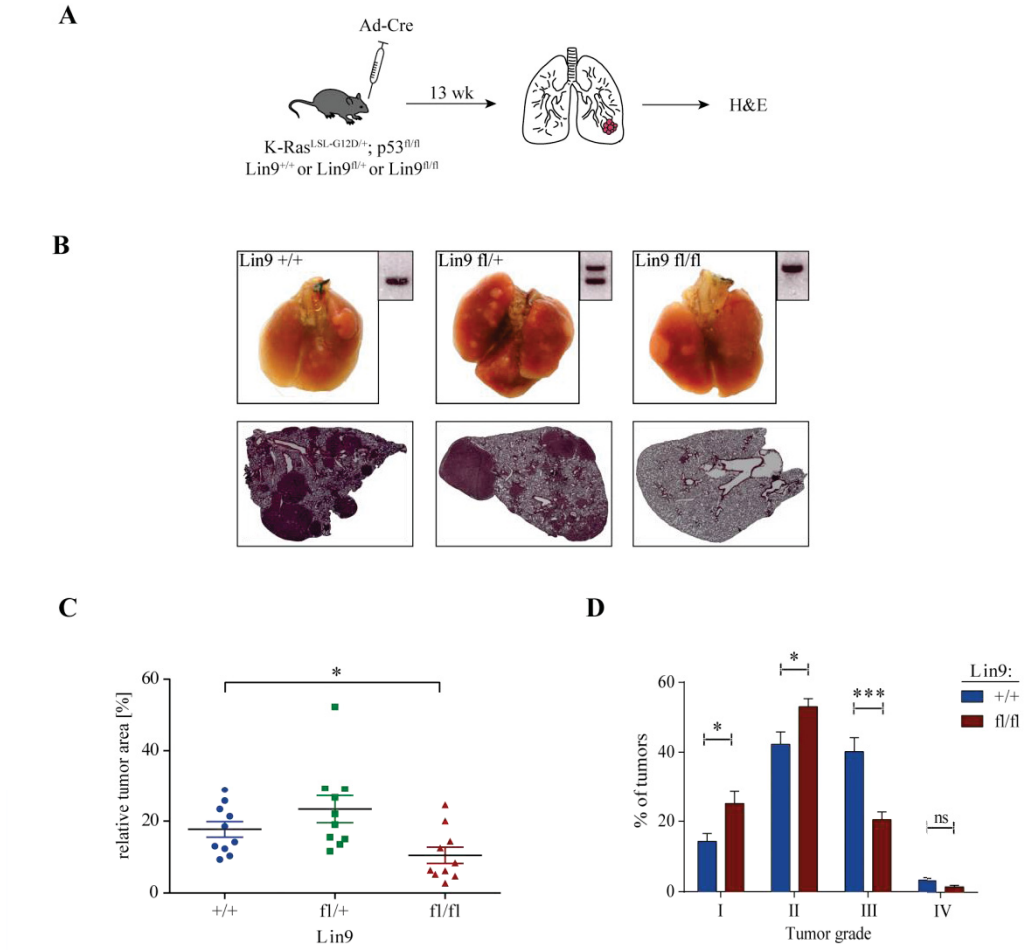

Figure 14: Requirement of Lin9 in a NSCLC mouse model
(**A**) K-Ras$^{LSL-G12D/+}$; p53$^{fl/fl}$; Lin9$^{fl/fl}$ mice were infected with 1*10^5 PFU of Ad-Cre and histological examined 13 weeks after tumor initiation. K-Ras$^{LSL-G12D/+}$; p53$^{fl/fl}$ mice with either Lin9$^{+/+}$ or Lin9$^{fl/+}$ served as internal controls. (**B**) Lungs of K-Ras$^{LSL-G12D/+}$; p53$^{fl/fl}$; Lin9$^{fl/fl}$ mice and internal controls (Lin9$^{+/+}$; Lin9$^{fl/+}$) were depicted. Gross inspections of the lungs showed white bulks with varying size identified as lesions (upper panel) in all genotypes. Representative histological lung sections stained with H&E (lower panel). Representative images of Lin9 genotyping of genomic tail DNA is shown. Upper band: floxed allele, lower band: wildtype allel. (**C**) The tumor area in relation to total lung area of H&E stained sections was quantified. Two sections of each lung were analyzed and average tumor area was measured for each individual animal. Symbols represent individual analysis of tumor area in each mouse. Mean ± S.E.M. is given. (**D**) Distribution of tumor grades was examined in H&E stained lung sections of K-Ras$^{LSL-G12D/+}$; p53$^{fl/fl}$; Lin9$^{+/+}$ (n = 708 tumors form 10 mice) and K-Ras$^{LSL-G12D/+}$; p53$^{fl/fl}$; Lin9$^{fl/fl}$ mice (n = 647 tumors of 10 mice). Error bars represent S.E.M.. Statistical significance for all panels was determined as *: $P < 0.05$, ***: $P < 0.001$; ns: not significant

3.2.6. Reduced mitotic gene expression and proliferation in tumors after loss of Lin9

In order to assess the effect of Lin9 deletion on the expression of MMB target genes and proliferation in tumors immunohistochemical staining of lung sections of K-Ras$^{LSL-G12D/+}$; p53$^{fl/fl}$; Lin9$^{fl/fl}$ mice at week 13 after infection was conducted (Fig. 15A). Tumors of K-Ras$^{LSL-G12D/+}$; p53$^{fl/fl}$; Lin9$^{+/+}$ mice were used as respective controls. Expression levels were divided into low, middle and high staining. In K-

Ras$^{LSL-G12D/+}$; p53$^{fl/fl}$; Lin9$^{fl/fl}$ mice 40.9 % of tumors showed a low expression of Nusap1, a protein required for spindle microtubule organization during mitosis and known target of the MMB. This expression level corresponded to an increase of 15.6 % in comparison to K-Ras$^{LSL-G12D/+}$; p53$^{fl/fl}$; Lin9$^{+/+}$ mice although no statistical significance was reached. Moreover, the amount of tumors with medium and high protein expression decreased after loss of Lin9 about 11.3 % (medium expression) and 4.3 % (high expression). A more pronounced effect on protein expression was observed by staining with Ki-67 antibody, a marker of proliferation. In comparison to controls, a significant 3-fold shift to tumors with lower protein expression was observed after Lin9 deletion. In addition, the amount of tumors with medium Ki-67 expression decreased significantly (1.7-fold) and high expression levels were lowered slightly (9.6 % in K-Ras$^{LSL-G12D/+}$; p53$^{fl/fl}$; Lin9$^{fl/fl}$ versus 14.1 % in K-Ras$^{LSL-G12D/+}$; p53$^{fl/fl}$; Lin9$^{+/+}$) (Fig. 15B). Due to lack of a suitable antibody for IHC the Lin9 expression in tumors could not be analyzed. Taken together, although statistical significance was only reached for proliferation marker Ki-67, the shift in Nusap1 expression may support the notion that MMB drives tumorigenesis by activation of mitotic targets and loss of MMB core member Lin9 impairs proliferation of lung tumors *in vivo*.

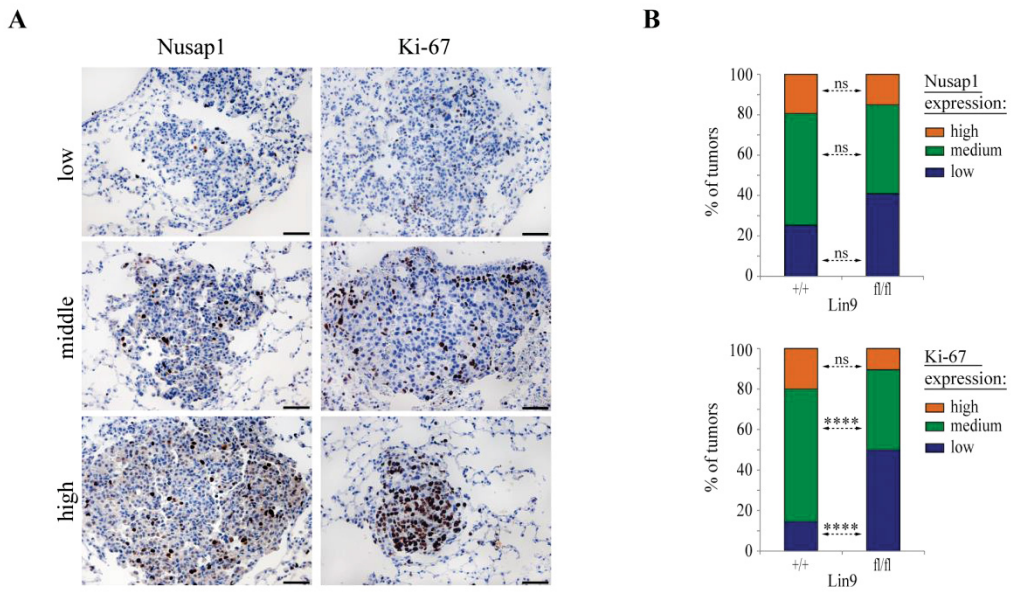

Figure 15: Depletion of MMB impacts gene expression in lung tumors
(**A**) Immunohistochemical staining of Nusap1 and Ki-67 in lung tumors of K-Ras$^{LSL-G12D/+}$; p53$^{fl/fl}$; Lin9$^{+/+}$ and K-Ras$^{LSL-G12D/+}$; p53$^{fl/fl}$; Lin9$^{fl/fl}$ mice 13 weeks after infection. Representative tumor samples with low, middle and high gene expression levels were given. Scale bar: 50 µm. (**B**) Quantification of cells positive for Nusap1 (low: <1 %; middle: 1-10 %; high: >10 %) and Ki-67 (low: <10 %; middle: 10-25 %; high: >25 %) in lung tumors. For each genotype, tumors from 3 different mice were analyzed. For Ki-67 71 (Lin9$^{+/+}$) and 52 (Lin9$^{fl/fl}$) tumors and for Nusap1 170 (Lin9$^{+/+}$) and 159 (Lin9$^{fl/fl}$) tumors were analyzed. Statistical significance was determined (Chi Square test) as ****P < 0.0001, ns: not significant

3.2.7. Incomplete inactivation of Lin9 after adenoviral Cre-infection *in vivo*

Next, to assess the efficiency of recombination mediated by adenoviral Cre-recombinase the status of conditional alleles was determined. To do so, tumor material from embedded lung sections of mice 13 weeks post-infection was isolated under the microscope by scraping with forceps. After deparaffinization, purified tumor material was analyzed by genomic PCR (Fig. 16A). In all 13 tumors a band corresponding to the recombined allele (Δfl) of Lin9 was detected but also retention of a floxed allele was observed indicating that recombination was incomplete. Furthermore, efficient deletion of the "STOP cassette" (ΔLSL) of the K-Ras allele could be confirmed. An additional weak signal for unrecombined, floxed allele (LSL) was detected in tumors L2-L8 and L11-L13 which was assumed to be contamination from surrounding normal lung material (Fig. 16B). In conclusion, these data suggest that there is a strong dependency of Lin9 for tumor development as well as an enormous selection pressure against the complete loss of Lin9. A functional MMB seems to be essential for K-Ras induced lung tumorigenesis. Therefore, only tumors which escape the deletion of Lin9 are capable to progress.

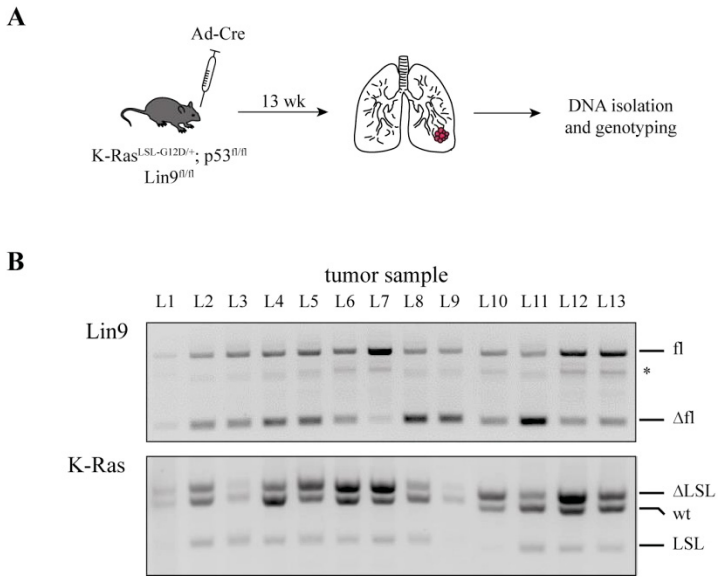

Figure 16: Incomplete recombination of Lin9 in tumors of a NSCLC model
(**A**) Tumorigenesis was initiated in K-Ras$^{LSL-G12D/+}$; p53$^{fl/fl}$; Lin9$^{fl/fl}$ mice by infection with 1*10^5 PFU of Ad-Cre. After 13 weeks, tumor material from paraffin embedded lung sections was isolated by scraping with forceps and subjected for genotyping by genomic PCR. (**B**) Determination of allelic status of isolated tumor samples by genomic PCR revealed incomplete recombination of floxed Lin9 allele. Oncogenic K-Ras^{G12D} activation was confirmed with respective primers. fl, LSL: unrecombined allele; Δfl, ΔLSL: recombined allele; wt: wildtype allele; * background band

3.2.8. Deletion of remaining Lin9 allele *in vitro* impairs proliferation

As an incomplete recombination of Lin9 alleles was detected in all tumors *in vivo,* the effect of ablation of the remaining allele was further investigated. For this purpose, primary cell lines (KPL1 and KPL2) from lung adenocarcinomas were established 13 weeks after infection of K-Ras$^{LSL-G12D/+}$; p53$^{fl/fl}$; Lin9$^{fl/fl}$ mice (Fig. 17A). As

expected, incomplete recombination of Lin9, demonstrated by the presence of a floxed, unrecombined allele, and efficient deletion of the "STOP cassette" on oncogenic K-Ras allele was confirmed in both cell lines by genomic PCR (Fig. 17B). To directly test the requirement of Lin9 for proliferation, the cell lines were stably infected with a retroviral vector expressing a hormone-inducible CreER^{T2} recombinase. Addition of 4-OHT to KPL1-CreER^{T2} and KPL2-CreER^{T2} cells resulted in activation of Cre-recombinase and efficient ablation of remaining floxed Lin9 allele (Fig. 17C). Moreover, Cre- mediated deletion of Lin9 strongly impaired proliferation of KPL1-CreER^{T2} cells indicating a requirement for Lin9 for proliferation of lung cancer cells *in vitro*. In contrast, no effect on proliferation was observed in control KPL1 cells transfected with an empty vector and treated with 4-OHT (Fig. 17D).

Upon single treatment with 4-OHT for 48 hours, efficient recombination of the residual floxed Lin9 allele was observed in KPL1-CreER^{T2} cells as demonstrated by an increase in intensity of the Δfl band. Interestingly, with increasing passage number the unrecombined Lin9 allele (fl) returned and after passage 4 the ratio between floxed and recombined allele was almost equal. In control KPL1 cells stably transfected with an empty vector no effect was observed (Fig. 17E). Collectively these findings indicate that there is a high selection pressure on cells against the loss of Lin9 and undergirds the importance of MMB for lung tumorigenesis.

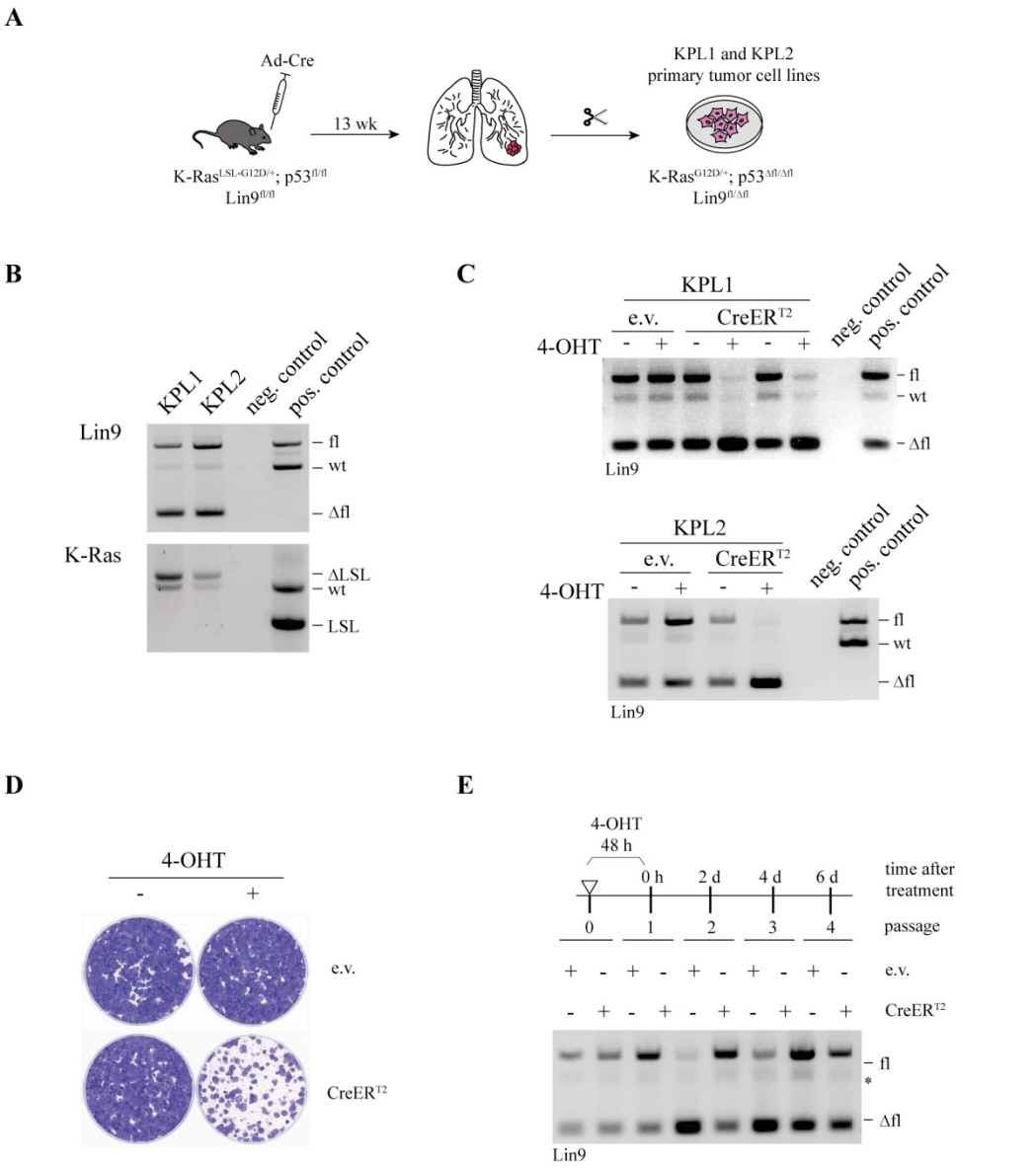

Figure 17: NSCLC-derived cell lines are dependent on Lin9
(**A**) K-Ras$^{LSL-G12D/+}$; p53$^{fl/fl}$; Lin9$^{fl/fl}$ mice were infected with 1*10^5 PFU of Ad-Cre to initiate tumorigenesis. Fresh tumors were isolated after 13 weeks and murine primary lung cancer cell lines (KPL1, KPL2) were established. (**B**) Both cell lines were genotyped by genomic PCR and showed retention of a floxed Lin9 allele as well as oncogenic K-Ras^{G12D} activation. (**C**) Cell lines were stably transfected with a CreER^{T2} vector encoding an inducible Cre recombinase. An empty vector (e.v.) was used as control. Cells were treated with 500 nM 4-OHT for 48 h to induce Cre-mediated excision of floxed Lin9 allele. Recombination was confirmed by genomic PCR. (**D**) KPL1-CreER^{T2} or KPL1 cells transfected with the empty vector were treated with 500 nM 4-OHT for 48 h. After 10 days cells were fixed and stained with crystal violet to visualize impaired proliferation. (**E**) KPL1- CreER^{T2} cells were treated with 500 nM OHT for 48 h and cultured for 6 days. KPL1 cells with empty vector were used as controls. After each passage cells were genotyped for Lin9 allelic status by genomic PCR.
For all panels: fl, LSL: unrecombined allele; Δfl, ΔLSL: recombined allele; wt: wildtype allele; * background band

4. Discussion

Lung cancer is the most frequent cancer worldwide accounting for 1.6 million deaths in 2012 and has a 5-year overall survival rate of 10-15% (Stewart and Wild 2014). It is divided into 2 major groups whereof 10-15 % is assigned as small cell lung cancer (SCLC) and 80-85 % as non-small cell lung cancer (NSCLC) (Molina et al. 2008; American Cancer Society 2017). Among NSCLC constitutive activation of K-Ras was found in 20-40 % of all cancers with about 80 % having an activating mutation at codon 12. K-Ras encodes a small GTPase that has essential roles in many cellular functions including proliferation, differentiation, cytoskeletal remodeling and apoptosis (Inoue and Nukiwa 2005). Activation of Ras mediates signal transduction into several downstream pathways (Downward 2003; Takashima and Faller 2013; Fang 2015). Most notably the stimulation of the RAF-MEK-ERK pathway, the PI3K-AKT-mTOR pathway and the RALGDS (that are guanine nucleotide exchange factors for RAL) pathway activate numerous target proteins required for transcription, cell-cycle progression and survival. Furthermore, Ras-dependent induction of Phospholipase Cε (PLCε) has influence on calcium signaling within the cell. The multiple proliferative signals generated by oncogenic Ras triggers the expression of cyclin D1 and the suppression of the CKIs (p21, p27), thus yielding in activation of cyclin D4/6 and subsequent progression through the cell cycle (Pylayeva-Gupta, Grabocka, and Bar-Sagi 2011). Direct targeting of Ras proteins with small molecule inhibitors is challenging so far mainly due to the high binding affinity of Ras to GDP/GTP (Cox et al. 2014). Although, therapeutic approaches have emerged including alteration of plasma membrane localization of Ras, modulation of its posttranscriptional modification, interference with downstream pathways or induction of synthetic lethality an effective anti-Ras therapy in clinic is not yet available (van der Hoeven et al. 2013; Cho et al. 2013; Fang 2014; Fang 2015). Moreover, many tumors in Ras mutant cancers are heterogeneous and have a high recurrence rate due to accumulation of further driver mutations (e.g. loss of p53) and hence, crosstalk and feedback activations of signaling pathways (Vogelstein et al. 2013; Fang 2015). Therefore, co-targeting of multiple cancer-associated pathways might be an effective therapy approach in oncogenic Ras-induced cancers. As a key activator of G2/M gene expression, MMB regulates various proteins with mitotic functions and might be an interesting candidate for co-therapy.

To understand the role of MMB in K-Ras driven lung cancer I investigated the requirement of MMB to mitotic gene expression in adenocarcinoma lung cancer cells. In RNAi depletion assays the influence on gene regulation and cell proliferation was analyzed. Moreover, the relationship of MMB to the tumor suppressor p53 was assessed in lung cancer cells with restorable p53 function. Furthermore, I elucidate the requirement of MMB to tumor formation *in vivo*. To this end, I established a conditional knockout of the conserved MMB key subunit Lin9 in a NSCLC mouse model driven by oncogenic K-Ras and loss of p53. I demonstrate that MMB target genes are highly expressed in adenocarcinomas of NSCLC and that MMB contributes to tumorigenesis *in vivo*.

So far, previous reports have shown that Lin9 is essential for early embryonic development and the viability of adult mice (Reichert et al. 2010). In this study, deletion of Lin9 inhibited tumor formation *in vivo* in a K-Ras-driven model of NSCLC with p53-negative background. (Fig. 14B und 14C) Notably, tumor development was not suppressed completely after Lin9 knockout and analysis of allelic status revealed an unrecombined Lin9 allele within isolated tumors (Fig. 16B). Additional Cre-recombinase-mediated deletion of the remaining allele in tumor derived cell lines confirmed the requirement of functional Lin9 for proliferation (Fig. 17D). Taken together, these findings indicate for an essential role of Lin9 in K-Ras driven lung cancer and ague for a strong selection pressures on tumors against the loss of Lin9. Hence, only tumors that retain a functional Lin9 allele are able to progress. These results are consistent with previous reports using conditional mice deficient for tumor essential genes. For instance, in a lung tumor mouse model driven by K-Ras and loss of Rac1 all tumors displayed an incomplete inactivation of Rac1 (Kissil et al. 2007). Only cells that escape inactivation of both alleles of Rac1 were found to be able to progress efficiently in tumorigenesis. Similar results were reported for JNK, a kinase of the MAP kinase signaling cascade pathway, and CK1α, the activation kinase of the Fas-associated death domain (FADD) protein (Cellurale et al. 2011; Bowman et al. 2015). However, due to the technical method used only material of large tumors was isolated for genotyping. Hence, the incomplete recombination of Lin9 could only be verified for a subset of tumors especially for those at later stages during tumor development. To further analyze the contribution of Lin9 to initiation it would be necessary to determine the allelic status of early lesions and small tumors e.g. after isolation of tumorigenic material by laser capture microdissection. In future experiments it will be interesting to investigate whether incomplete recombination might be circumvented by the use of other knockout tools. The here used adenovirus is only transiently expressed within infected cells. Thus, it might be that with degradation of the Cre-expressing vector the concentration of functional recombinase is decreased within the cell and thereby, the probability of partial recombination events is increased. In contrast to adenovirus, lentiviral vectors are integrated into the genome and expressed continuously (depending on the integration site). Hence, the permanent inhibition of Lin9 might efficiently suppress lung cancer development. However, lentiviral infection is technically more sophisticated than adenoviral infection as virus is delivered by intratracheal instillation. Recently, with the discovery of the clustered regularly interspaced short palindromic repeat (CRISPR/Cas9) system a new promising knockout tool has emerged. Originally used as bacterial defense system, it has been modified to facilitate genetic manipulations in a variety of cell types and organisms (Horvath and Barrangou 2010; Hsu et al. 2014).
Interestingly, heterozygous knockout of Lin9 resulted in a slightly increased tumor burden (Fig. 14C). Although it was not statistically significant it might suggest that Lin9 can behave as an oncogene as well as a haploinsufficient tumor suppressor in the same tumor type. This finding corroborates with a previous study of conditional Lin9 knockout (Reichert et al. 2010). Therein, Lin9 heterozygous MEFs are shown to have a weaker spindle checkpoint than Lin9 wildtype MEFs and prematurely exit

mitosis after nocodazole treatment. This in turn facilitates anchorage-independent growth which is a sign for oncogenic transformation. Moreover, in a BXB-Raf-induced NSCLC mouse model Reichert and colleagues demonstrated that Lin9 heterozygosity accelerates tumor formation and reduced overall survival. Similar as described for Lin9, the ß-catenin regulator Axin2 has been found to function in opposing roles in colorectal cancer development. Depending on mutations in the adenomatous polyposis coli (APC) tumor suppressor, Axin2 can inhibit (i.e. in $APC^{+/+}$ cells) or promote (i.e. in APC mutated cells) colorectal cancer (Yochum 2012). In human gastrointestinal tumors, the krüppel-like transcription factor KLF4 has been demonstrated to possess tumor suppressor-like properties and mediates cell cycle arrest at least partially via p21. In contrast, KLF4 has been identified as oncogenic driver of squamous cell carcinoma and breast cancer (Rowland and Peeper 2006; reviewed in Tetreault et al. 2013).

Mechanistically, the suppressive effect of Lin9 knockout on tumor growth can be explained by the function of MMB in proliferating cells. As a key activator of mitotic genes, MMB has been reported to regulate the expression of genes required for mitotic entry, mitotic spindle checkpoint and chromosome segregation as well as mitotic exit and cytokinesis (Osterloh et al. 2007; Schmit et al. 2007; Pilkinton et al. 2007; Kittler et al. 2007; Knight et al. 2009; Schmit et al. 2009; Reichert et al. 2010; Sadasivam et al. 2012; Wolter et al. 2017). RNAi-mediated inhibition of either the MMB core subunit Lin9 or the MMB-associated transcription factor B-Myb in a primary lung adenocarcinoma cell line reduced the expression of genes with function in mitosis (Fig. 5A). Similarly, a lentiviral-based inducible shRNA system was established that effectively depleted B-Myb and resulted in suppression of mitotic gene expression after induction with doxycycline (Fig. 6E,-D). All analyzed genes were previously identified in a genome-wide microarray analysis in Lin9 knockout MEFs as MMB regulated genes (Reichert et al. 2010; Esterlechner et al. 2013; Fischer et al. 2013). Therefore, the data of this thesis suggest a requirement of MMB for activation of G2/M phase-specific genes in lung cancer cells. This is in line with a number of studies in human and murine somatic cells where MMB was found to activate G2/M phase-specific genes (Osterloh et al. 2007; Pilkinton et al. 2007; Schmit et al. 2007; Knight et al. 2009; Esterlechner et al. 2013). For instance, Nusap1, a spindle-associated protein that is mainly expressed at the G2/M transition and declines rapidly after cell division (Raemaekers et al. 2003). Being primarily nucleolar during interphase it localizes at the central spindle microtubules during mitosis. It has a crucial role in spindle microtubule organization and inhibition results in aberrant mitotic spindles, defective chromosome segregation, cytokinesis failures and deformed nuclei. *In vivo*, Nusap deficiency in mice leads to early embryonic lethality due to improper chromosome alignment (Vanden Bosch et al. 2010). The kinetochore associating protein Cenpf localizes to the nuclear envelope at the transition of G2 to mitosis and abruptly degrades at the end of mitosis. RNAi-mediated suppression disturbs kinetochore assembly, chromosome alignment and segregation as well as cytokinesis (Chan et al. 1998; Holt et al. 2005). Moreover,

Cenpf has been found to be involved in the recruitment of the checkpoint proteins Mad1 and BubR1 to sustain a robust checkpoint response (Laoukili et al. 2005). The mitotic kinase Plk1 has a pivotal function in all stages of mitosis such as regulation of centrosome maturation or the spindle assembly (van Vugt and Medema 2005; Petronczki et al. 2008). Most recently, kinesins that are required for the formation and function of the mitotic spindle, chromosome segregation and cytokinesis have been shown to be direct targets of the MMB (Cross and McAinsh 2014; Wolter et al. 2017).
Notably, deletion of FoxM1 has been reported to cause similar effects as Lin9 or B-Myb inhibition. FoxM1-deficient MEFs exhibited pleiotropic effects including defects in G2/M transition, chromosome segregation and cytokinesis (Laoukili et al. 2005). Deletion of FoxM1 *in vivo* resulted in cell cycle arrest and mitotic failures (Wang et al. 2005). Recent studies provide evidence that B-Myb is required for the recruitment of FoxM1 to promoters of late cell cycle genes (Down et al. 2012; Sadasivam et al. 2012; Chen et al. 2012). It would be interesting to know whether the activation of mitotic genes by B-Myb is, at least in part, mediated by FoxM1 rather than B-Myb. Furthermore, in Oesophageal adenocarcinoma, FoxM1 directly interacts with Lin9 (Wiseman et al. 2015). If this observation also applies for other cancer types needs to be investigated e.g. by immunoprecipitation assays.

Suppression of MMB components by RNAi is associated with a number of phenotypes including reduced proliferation, accumulation of cells in G2 and delayed entry into mitosis. Indeed, depletion of Lin9 or B-Myb caused changes in cell cycle distribution and lead to G2/M cell cycle arrest, cells with aberrant DNA content (polyploid cells) and impaired proliferation (Fig. 5B, 7). These findings implicate that proliferation of lung cancer cells strongly depends on functional MMB. In many studies comparable effects on cell cycle distribution were described (Osterloh et al. 2007; Schmit et al. 2009; Knight et al. 2009; Reichert et al. 2010; Esterlechner et al. 2013). For instance knockdown of MMB in hTERT immortalized human BJ fibroblasts by shRNA against Lin9 or B-Myb delayed progression from G2 to M (Osterloh et al. 2007). A similar phenotype was observed in the same cells after RNAi-mediated depletion of Lin54, another core member of MMB (Schmit et al. 2009). In MEFs, conditional Lin9 knockout results in formation of bi- and multinucleated cells with aberrant nuclei, multiple centrosomes and malformed spindle apparatus. As a consequence, cells arrest in G2/M, become polyploid and undergo premature senescence (Reichert et al. 2010). Likewise to somatic cells, studies in F9 murine embryonal carcinoma cells also described a G2/M arrest of cells and polyploidy after depletion of MMB components by shRNA. Furthermore, knockdown of Lin9 and B-Myb expression in murine embryonic stem cells was reported to induce G2/M arrest, mitotic spindle defects and centrosome failures leading to aneuploidy (Tarasov et al. 2008; Esterlechner et al. 2013). It would be of interest to know whether lung cancer cells accumulate in G2 because of failed progression into or due to delay in mitosis. This can be addressed by FACS staining with MPM-2 antibodies and calculation of the mitotic cell fraction.

In the present work, re-activation of p53 tumor suppressor function in K-Ras-driven lung adenocarcinoma cells led to suppression of mitotic gene expression (Fig 8B). Moreover, induction of p53 induced the formation of the repressive DREAM complex and resulted in enrichment of DREAM at mitotic gene promoters (Fig. 9A. 9C). Conversely, MMB was displaced from these promoters (Fig. 9C). One might assume that downregulation of mitotic genes could be a consequence of cell cycle arrest after p53 restoration. However, reduced gene expression was detected before cells arrest in G1 phase which is indicative that downregulation of mitotic genes is not an indirect effect due to cell cycle arrest. Together these findings strongly suggest that p53 inhibits MMB and promotes the formation of DREAM, thus yielding in reduced mitotic gene expression in lung adenocarcinoma cells. This corroborates published studies that demonstrate indirect repression of mitotic genes and formation of the repressive DREAM after p53 activation (Mannefeld et al. 2009; Quaas et al. 2012; Fischer et al. 2015; Fischer, Quaas, et al. 2016; Fischer, Grossmann, et al. 2016). For instance, experiments in human and murine cells showed that the MMB component B-Myb is bound to CHR elements before induction of p53. In the presence of high levels of p53 or its effector p21, protein binding at CHR sites shifts to DREAM (Müller et al. 2012; Fischer et al. 2015; Fischer, Quaas, et al. 2016). Similar findings were reported for Kif23, a kinesin of the kinesin-6 family and one subunit of the centraspindlin complex that is crucial for central spindle formation (White and Glotzer 2012). Upon induction of p53, DREAM assembles at CHR elements displacing MMB in the Kif23 promoter region thereby mediating repression (Fischer et al. 2013). Moreover, recent metaanalysis studies confirmed that quite a number of cell cycle genes are repressed by the p53-p21-DREAM-CDE/CHR signaling pathway. In addition, several of these genes are activated in G2/M by the MuvB core complex, B-Myb and FoxM1 (Fischer et al. 2015; Fischer, Quaas, et al. 2016; Fischer, Grossmann, et al. 2016). Inactivation of p53 in human BJ fibroblasts with different p53 status and cancer cell lines revealed that p53 negatively regulates FoxM1 (Pandit et al. 2009).
However, direct evidence if p53-dependent repression is also mediated by p21 and binding at CHR/CDE in lung cancer cells needs to be further elucidated. For instance, depletion assays of p21 by RNAi or in p21-deficient cells before and after p53 restoration could clarify if there is a p21 dependency for the repression of MMB targets in lung cancer cells. Thereby, immunoprecipitation assays and ChIP analysis at respective promoters could be used to monitor the switch between MMB and DREAM.

The finding that DREAM complex formation and DREAM-mediated repression of target genes is promoted by p53 after DNA damage suggests that inactivation of the p53 pathway could result in hyperactivation of MMB and increased expression of mitotic genes (Mannefeld et al. 2009). Consistent with this notion, immunohistochemical staining in NSCLC adenocarcinomas revealed an elevated expression of genes with function in mitosis which were known to be direct targets of

the MMB. In addition, phosphorylated B-Myb was detected within the tumors (Fig. 12B). These observations give rise to the assumption that MMB is responsible for overexpression of mitotic genes in K-Ras-driven lung adenocarcinomas with p53-negative background and might be the driver for tumorigenesis. The importance of MMB to tumorigenesis is further supported by the finding that deletion of B-Myb in the K-Ras-driven NSCLC mouse model resulted in a similar phenotype than observed after Lin9 knockout (Iltzsche et al. 2016). In many reports, overexpression of mitotic genes has been linked to CIN. For instance CENPA, a protein required for centromere formation and chromosome segregation, is overexpressed in many aneuploid colon cancers (Amato et al. 2009). High expression of the kinetochore protein Hec1 or the spindle checkpoint proteins MAD2 in mice have been demonstrated to be sufficient to generate aneuploidy and to induce tumorigenesis *in vivo* (Sotillo et al. 2007; Diaz-Rodríguez et al. 2008). Furthermore, the kinesin Kif14, which mainly functions during cytokinesis and interacts with PRC1, is overexpressed in a number of cancers including breast, lung and ovarian carcinomas. Recently, many mitotic genes have been reported to be part of published CIN signatures that associate with clinical outcome of various cancers (Carter et al. 2006; Cheng et al. 2013; Chibon et al. 2010). Strikingly, several MMB target genes as well as the MMB subunits B-Myb and FoxM1 were identified among these signatures. Although the present work is focused on the regulation of mitotic genes in lung cancer, the results may also be likely relevant for other tumor types.
Given the fact that a panel of mitotic genes regulated by MMB is overexpressed in NSCLC and linked with poor outcome, the mitotic signature might be used as prognostic biomarker. Although elevated expression levels of mitotic genes could be a consequence of the higher proliferation rate of cancer cells, a subset of the MMB-regulated genes could play a causal role in tumor initiation or progression. Notably, several MMB targets are already used as prognostic marker. The expression pattern of kinesin Kif4a, which is involved in chromosome segregation and essential for cytokinesis, is utilized as prognostic marker for cervical cancer and NSCLC (Taniwaki et al. 2007). Another kinesin, Kif14, regulates cytokinesis together with the citron kinase and is in clinical use as biomarker for cervical, breast and lung cancer (Gruneberg et al. 2006; Corson and Gallie 2006; Corson et al. 2007; W. Wang et al. 2016). Most recently, a MMB-dependent mitotic kinesin signature has been proposed as prognostic biomarker for breast cancer (Wolter et al. 2017). In addition, the MuvB core member Lin9 is part of the Mammaprint breast cancer prognostic gene signature (van ’t Veer et al. 2002).

Based on the effect of MMB knockout on cancer cell proliferation one might consider MMB-inhibition as an approach for lung cancer therapy. So far no enzymatic activity of the MMB complex has been identified and thus, inhibition with small molecules is challenging. Ligand-induced protein degradation of multidomain scaffold proteins by bifunctional ligands has been described as a promising tool (Winter et al. 2015). In that approach, one part of the bifunctional ligand is specific for the target protein, whereas the other part mediates the recruitment of a cellular E3 ligase to the target

protein thereby inducing proteasomal degradation. However, complete suppression of MMB might be difficult as deletion of Lin9 and B-Myb in mice has been found to be lethal and can cause severe side effects on healthy high proliferating tissues (e.g. intestine) (Tanaka et al. 1999; Reichert et al. 2010). Moreover, the circumstance that Lin9 might act in a dual role as tumor suppressor and oncogene has to be considered. Incomplete inhibition might lead to aneuploidy and increases the chance for chromosomal instability due to reduced expression rates of mitotic genes as published in several studies. Deletion of the MMB target Cenpe, a centromere associated kinesin-like motor protein, has been shown to enhance cell transformation and cause aneuploidy and chromosomal instability *in vitro* and *in vivo* (Weaver et al. 2007). During mitosis, Cenpe mediates the interaction between microtubules of the mitotic spindle and the chromosomes and triggers mitotic checkpoint signaling through interaction with the BubR1 kinase (Yen et al. 1992; Mao et al. 2003). Also the key mitotic kinesin Plk1 was demonstrated to induce tumorigenesis *in vivo* after reduced expression (Lu et al. 2008; Lu and Yu 2009). In contrast to their wildtype counterparts, Plk1 heterozygous mice depicted a 3-fold higher incidence for tumor development and displayed an elevated level of aneuploid in pre-malignant splenocytes. Considering the function of Plk1 during mitosis including regulation of centrosome maturation, spindle assembly, mitotic exit and cytokinesis it is conceivable that aberrant expression may induces failures during mitosis yielding in aneuploid cells.
Due to the missing enzymatic activity and the narrow therapeutic window of MMB one might alternatively concentrate on downstream targets of MMB. Focusing on targets with specialized functions in mitosis might allow a more precise therapy with better prognostic outcome and lesser production of side effects. On the other hand, only specific patient populations can be treated and further sub-classification of NSCLC in advance would be necessary. An example for an MMB target that is already investigated in phase I and II clinical trials as a cancer target is Survivin (Birc5) that is strongly overexpressed e.g. in human neuroblastoma tumors and correlates with poor outcome (Islam et al. 2000; Giaccone et al. 2009; Lamers et al. 2011). Silencing of Survivin within these tumors resulted in apoptosis via mitotic catastrophe. Inhibition of PRC1, a microtubule-associated non-motor protein, and Kif23, which is involved in the formation of the cleavage furrow, revealed a strong anti-proliferative effect on breast cancer cells *in vitro*. Moreover, deletion of Kif23 was shown to suppress lung tumor formation *in vivo* (Iltzsche et al. 2016). For successful targeted therapy further identification of up-regulated pathways should be conducted.

Taken together, the findings of this study provide evidence for the contribution of MMB to lung tumorigenesis *in vivo* in a p53-negative background and the potential of MMB and its downstream effectors as therapeutic target. According to the data presented the following model is proposed (Fig. 18): Mitogenic stimuli (e.g. Ras) drive the progression through the cell cycle by induction of cyclin/CDK complexes which foster the switch of DREAM to MMB and expression of mitotic MMB target

genes. However, in p53-negative cells safety mechanisms fail to revert the switch, hence leading to elevated expression of mitotic genes. This in turn might promote chromosome mis-segregation and cytokinesis failures and the induction of CIN (as a consequence of aneuploidy) which contributes to tumor development.

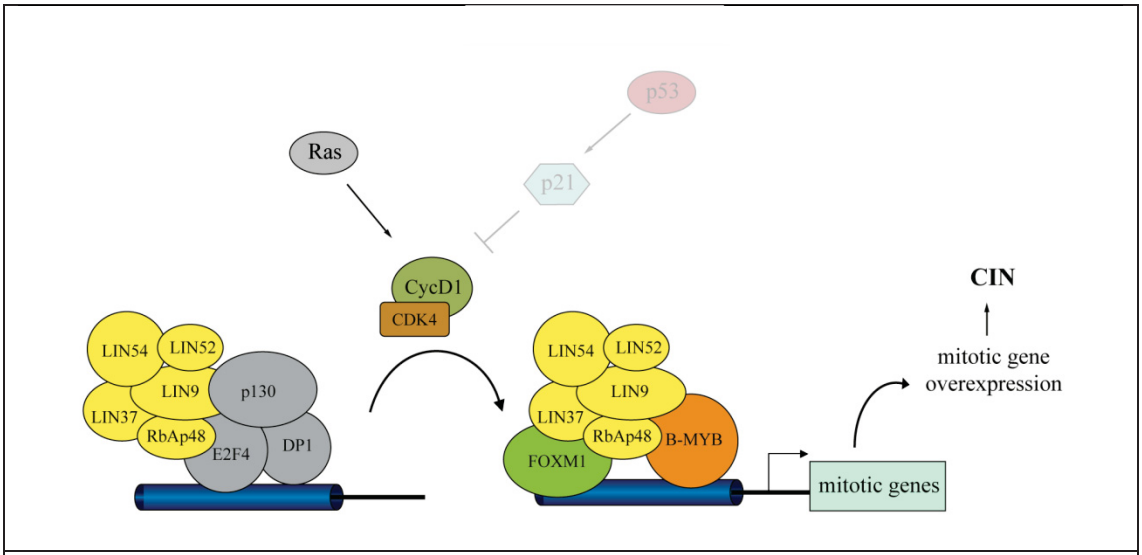

Figure 18: Model for MMB-induced mitotic gene overexpression and induction of CIN in p53-negative cells
Mitogenic stimuli can foster the switch of repressive DREAM to MMB, an activator of mitotic gene expression. In p53-negsative cells, the safeguard mechanism through the p53-p21 pathway fails to revert the switch to MMB, thus leading to overexpression of mitotic genes. This in turn, may promote chromosomal instability (CIN) and tumorigenesis.

5. Summary

The evolutionary conserved Myb-MuvB (MMB) multiprotein complex has an essential role in transcriptional activation of mitotic genes. MMB target genes as well as the MMB associated transcription factor B-Myb and FoxM1 are highly expressed in a range of different cancer types. The elevated expression of these genes correlates with an advanced tumor state and a poor prognosis. This suggests that MMB could contribute to tumorigenesis by mediating overexpression of mitotic genes. Although MMB has been extensively characterized biochemically, the requirement for MMB to tumorigenesis *in vivo* remains largely unknown and has not been tested directly so far.

In this study, conditional knockout of the MMB core member Lin9 inhibits tumor formation *in vivo* in a mouse model of lung cancer driven by oncogenic K-Ras and loss of p53. The incomplete recombination observed within tumors points towards an enormous selection pressure against the complete loss of Lin9. RNA interference (RNAi)-mediated depletion of Lin9 or the MMB associated subunit B-Myb provides evidence that MMB is required for the expression of mitotic genes in lung cancer cells. Moreover, it was demonstrated that proliferation of lung cancer cells strongly depends on MMB. Furthermore, in this study, the relationship of MMB to the p53 tumor suppressor was investigated in a primary lung cancer cell line with restorable p53 function. Expression analysis revealed that mitotic genes are downregulated after p53 re-expression. Moreover, activation of p53 induces formation of the repressive DREAM complex and results in enrichment of DREAM at mitotic gene promoters. Conversely, MMB is displaced at these promoters.
Based on these findings the following model is proposed: In p53-negative cells, mitogenic stimuli foster the switch from DREAM to MMB. Thus, mitotic genes are overexpressed and may promote chromosomal instability and tumorigenesis.

This study provides evidence that MMB contributes to the upregulation of G2/M phase-specific genes in p53-negative cells and suggests that inhibition of MMB (or its target genes) might be a strategy for treatment of lung cancer.

6. Zusammenfassung

Der evolutionär konservierte Myb-MuvB (MMB) Multiproteinkomplex hat eine wesentliche Rolle in der transkriptionellen Aktivierung mitotischer Gene. Zielgene des MMB sowie die MMB assoziierten Transkriptionsfaktoren B-Myb und FoxM1 sind hoch exprimiert in einer Bandbreite verschiedener Krebsarten. Die erhöhte Expression dieser Gene korreliert mit einem fortgeschrittenen Tumorstadium und einer geringen Prognose. Das weißt auf darauf hin, dass MMB an der Tumorentstehung beteiligt sein könnte indem es die Überexpression mitotischer Gene fördert. Obwohl MMB biochemisch eingehend untersucht wurde, ist die Erfordernis von MMB zur Tumorentstehung *in vivo* weitestgehend unbekannt und wurde bisher nicht direkt getestet.

In dieser Studie hemmt der konditionale Knockout der MMB Kerneinheit Lin9 die Tumorbildung *in vivo* in einem Lungenkrebs-Mausmodell angetrieben durch onkogenes K-Ras und den Verlust von p53. Die unvollständige Rekombination welche in Tumoren beobachtet wurde deutet auf einen starken Selektionsdruck gegen den kompletten Verlust von Lin9 hin. Die Verminderung von Lin9 und der MMB-assoziierten Untereinheit B-Myb durch RNAi-Interferenz (RNAi) liefert Beweise dafür, dass MMB für die Expression mitotischer Gene in Lungenkrebszellen notwendig ist. Zudem wurde gezeigt, dass das Zellwachstum von Lungenkrebszellen stark von MMB abhängig ist. Weiterhin wurde der Zusammenhang zwischen MMB und dem p53-Tumorsuppressor in einer primären Lungenkrebszelllinie mit wiederherstellbarer p53-Funktion untersucht. Expressionsanalysen zeigen, dass mitotische Gene nach Re-expression von p53 runterreguliert werden. Außerdem induziert die Aktivierung von p53 die Bildung des repressiven DREAM-Komplexes und führt zu einer Anreicherung von DREAM an Promotoren mitotischer Gene. Im Gegenzug wird MMB an den Promotoren verdrängt.
Basierend auf den Ergebnissen wird das folgende Model vorgeschlagen: In p53-negativen Zellen begünstigen mitogene Reize den Wechsel von DREAM zu MMB. Dadurch werden mitotische Gene überexprimiert und können so chromosomale Instabilität und Tumorentstehung fördern

Diese Studie liefert Hinweise, dass MMB an der Hochregulation G2/M-Phasenspezifischer Gene in p53-negativen Zellen beteiligt ist und dass die Hemmung von MMB (oder seiner Zielgene) eine Strategie zur Behandlung von Lungenkrebs sein könnte.

7. References

Adams, P. D. 2001. “Regulation of the Retinoblastoma Tumor Suppressor Protein by Cyclin/cdks.” *Biochimica et Biophysica Acta - Reviews on Cancer* 1471 (3): 123–33.

Amato, Angela, Tiziana Schillaci, Laura Lentini, and Aldo Di Leonardo. 2009. “CENPA Overexpression Promotes Genome Instability in pRb-Depleted Human Cells.” *Molecular Cancer* 8: 119..

American Cancer Society. 2017. “Cancer Facts & Figures 2017.” Atlanta. doi:10.1101/gad.1593107.

Bakhoum, Samuel F., William T. Silkworth, Isaac K. Nardi, Joshua M. Nicholson, Duane a. Compton, and Daniela Cimini. 2014. “The Mitotic Origin of Chromosomal Instability.” *Current Biology* 24 (4). Elsevier: R148–49.

Bakhoum, Samuel F, and Duane a Compton. 2012. “Chromosomal Instability and Cancer : A Complex Relationship with Therapeutic Potential.” *The Journal of Clinical Investigation* 122 (4): 1138–43.

Bar-Shira, Anat, Jehonathan H. Pinthus, Uri Rozovsky, Myriam Goldstein, William R. Sellers, Yuval Yaron, Zelig Eshhar, and Avi Orr-Urtreger. 2002. “Multiple Genes in Human 20q13 Chromosomal Region Are Involved in an Advanced Prostate Cancer Xenograft.” *Cancer Research* 62 (23): 6803–7.

Bartek, Jiri, and Jiri Lukas. 2001. “Pathways Governing G1/S Transition and Their Response to DNA Damage.” *FEBS Letters* 490 (3): 117–22.

Beall, Eileen L., Peter W. Lewis, Maren Bell, Michael Rocha, D. Leanne Jones, and Michael R. Botchan. 2007. “Discovery of tMAC: A Drosophila Testis-Specific Meiotic Arrest Complex Paralogous to Myb-Muv B.” *Genes and Development* 21 (8): 904–19.

Beijersbergen, Roderick L., Ron M. Kerkhoven, Liang Zhu, Leone Carlée, P. Mathijs Voorhoeve, and René Bernards. 1994. “E2F-4, a New Member of the E2F Gene Family, Has Oncogenic Activity and Associates with p107 in Vivo.” *Genes and Development* 8 (22): 2680–90..

Bektas, Nuran, Anette Ten Haaf, Jürgen Veeck, Peter Johannes Wild, Juliane Lüscher-Firzlaff, Arndt Hartmann, Ruth Knüchel, and Edgar Dahl. 2008. “Tight Correlation between Expression of the Forkhead Transcription Factor FOXM1 and HER2 in Human Breast Cancer.” *BMC Cancer* 8: 42..

Bertoli, Cosetta, Jan M Skotheim, and Robertus a M de Bruin. 2013. “Control of Cell Cycle Transcription during G1 and S Phases.” *Nature Reviews. Molecular Cell Biology* 14 (8). Nature Publishing Group: 518–28.

Bieging, Kathryn T, Stephano Spano Mello, and Laura D Attardi. 2014. “Unravelling Mechanisms of p53-Mediated Tumour Suppression.” *Nature Reviews. Cancer* 14 (5). Nature Publishing Group: 359–70.

Bowman, Brittany M, Katrina A Sebolt, Benjamin A Hoff, Jennifer L Boes, Danette L Daniels, Kevin A Heist, C J Galban, et al. 2015. “Phosphorylation of FADD by the Kinase CK1 Alpha Promotes KRAS(G12D)- Induced Lung Cancer.” *Science Signaling* 8 (361): 1–10.

Bracken, Adrian P., Marco Ciro, Andrea Cocito, and Kristian Helin. 2004. “E2F Target Genes: Unraveling the Biology.” *Trends in Biochemical Sciences*..

Bradford, M M. 1976. “A Rapid and Sensitive Method for the Quantitation of Microgram Quantities of Protein Using the Principle of Protein Dye Binding.” *Analytical Biochemistry* 72: 248–54.

Carter, Scott L, Aron C Eklund, Isaac S Kohane, Lyndsay N Harris, and Zoltan Szallasi. 2006. “A Signature of Chromosomal Instability Inferred from Gene Expression Profiles Predicts Clinical Outcome in Multiple Human Cancers.” *Nature Genetics* 38 (9): 1043–48.

Cartwright, P, H Müller, C Wagener, K Holm, and K Helin. 1998. “E2F-6: A Novel Member of the E2F Family Is an Inhibitor of E2F-Dependent Transcription.” *Oncogene* 17 (5): 611–23. .

Cellurale, Cristina, Guadalupe Sabio, Norman J Kennedy, Madhumita Das, Marissa Barlow, Peter Sandy, Tyler Jacks, and Roger J Davis. 2011. “Requirement of c-Jun NH(2)-Terminal Kinase for Ras-Initiated Tumor Formation.” *Molecular and Cellular Biology* 31 (7): 1565–76.

Ceol, Craig J., and H. Robert Horvitz. 2001. “Dpl-1 DP and Efl-1 E2F Act with Lin-35 Rb to Antagonize Ras Signaling in C. Elegans Vulval Development.” *Molecular Cell* 7 (3): 461–73..

Chan, G. K T, B. T. Schaar, and T. J. Yen. 1998. “Characterization of the Kinetochore Binding Domain of CENP-E Reveals Interactions with the Kinetochore Proteins CENP-F and hBUBR1.” *Journal of Cell Biology* 143 (1): 49–63.

Chen, X., G. a. Muller, M. Quaas, M. Fischer, N. Han, B. Stutchbury, a. D. Sharrocks, and K. Engeland. 2012. “The Forkhead Transcription Factor FOXM1 Controls Cell Cycle-Dependent Gene Expression through an Atypical Chromatin Binding Mechanism.” *Molecular and Cellular Biology* 33 (2): 227–36.

Cheng, Wei Yi, Tai Hsien Ou Yang, and Dimitris Anastassiou. 2013. “Biomolecular Events in Cancer Revealed by Attractor Metagenes.” *PLoS Computational Biology* 9 (2).

Chibon, F, P Lagarde, S Salas, G Perot, V Brouste, F Tirode, C Lucchesi, et al. 2010. “Validated Prediction of Clinical Outcome in Sarcomas and Multiple Types of Cancer on the Basis of a Gene Expression Signature Related to Genome Complexity.” *Nat Med* 16 (7): 781–87.

Cho, Kwang jin, Dharini van der Hoeven, and John F. Hancock. 2013. “Inhibitors of K-Ras Plasma Membrane Localization.” *Enzymes* 33: 249–65..

Chong, Jean-Leon, Pamela L Wenzel, M Teresa Sáenz-Robles, Vivek Nair, Antoney Ferrey, John P Hagan, Yorman M Gomez, et al. 2009. “E2f1-3 Switch from Activators in Progenitor Cells to Repressors in Differentiating Cells.” *Nature* 462 (7275): 930–34..

Cobrinik, David, Myung Ho Lee, Gregory Hannon, George Mulligan, Roderick T. Bronson, Nicholas Dyson, Ed Harlow, David Beach, Robert A. Weinberg, and Tyler Jacks. 1996. “Shared Role of the pRB-Related p130 and p107 Proteins in Limb Development.” *Genes and Development* 10 (13): 1633–44.

Corson, Timothy W., Qi Zhu Chang, Suzanne K. Lau, Frances A. Shepherd, Ming Sound Tsao, and Brenda L. Gallie. 2007. "KIF14 Messenger RNA Expression Is Independently Prognostic for Outcome in Lung Cancer." *Clinical Cancer Research* 13 (11): 3229–34.

Corson, Timothy W., and Brenda L. Gallie. 2006. "KIF14 mRNA Expression Is a Predictor of Grade and Outcome in Breast Cancer." *International Journal of Cancer* 119 (5):.

Cox, Adrienne D, Stephen W Fesik, Alec C Kimmelman, Ji Luo, and Channing J Der. 2014. "Drugging the Undruggable RAS: Mission Possible?" *Nature Reviews. Drug Discovery* 13 (11): 828–51.

Cross, Robert a., and Andrew McAinsh. 2014. "Prime Movers: The Mechanochemistry of Mitotic Kinesins." *Nature Reviews Molecular Cell Biology* 15 (4): 257–71.

Diaz-Rodríguez, Elena, Rocio Sotillo, Juan-Manuel Schvartzman, and Robert Benezra. 2008. "Hec1 Overexpression Hyperactivates the Mitotic Checkpoint and Induces Tumor Formation in Vivo." *Proceedings of the National Academy of Sciences of the United States of America* 105 (43): 16719–24.

Dick, Frederick a, and Seth M Rubin. 2013. "Molecular Mechanisms Underlying RB Protein Function." *Nature Reviews. Molecular Cell Biology* 14 (5). Nature Publishing Group: 297–306..

Dick, Frederick, and Joe S. Mymryk. 2011. "Sweet DREAMs for Hippo." *Genes and Development* 25 (9): 889–94..

Dow, Lukas E, Prem K Premsrirut, Johannes Zuber, Christof Fellmann, Katherine McJunkin, Cornelius Miething, Youngkyu Park, Ross a Dickins, Gregory J Hannon, and Scott W Lowe. 2012. "A Pipeline for the Generation of shRNA Transgenic Mice." *Nature Protocols* 7 (2). Nature Publishing Group: 374–93.

Down, Christin F., Julie Millour, Eric W.-F. F Lam, and Roger J. Watson. 2012. "Binding of FoxM1 to G2/M Gene Promoters Is Dependent Upon B-Myb." *Biochimica et Biophysica Acta (BBA) - Gene Regulatory Mechanisms* 1819 (8). Elsevier B.V.: 855–62.

Downward, Julian. 2003. "Targeting RAS Signalling Pathways in Cancer Therapy." *Nature Reviews* 3 (1): 11–22.

DuPage, Michel, Alison L Dooley, and Tyler Jacks. 2009. "Conditional Mouse Lung Cancer Models Using Adenoviral or Lentiviral Delivery of Cre Recombinase." *Nature Protocols* 4 (7): 1064–72.

Ehmer, Ursula, and Julien Sage. 2015. "Control of Proliferation and Cancer Growth by the Hippo Signaling Pathway." *Molecular Cancer Research : MCR*, 127–41.

Engeland, Kurt. 2016. "Stopping Cells from Dividing." *AGING* 8 (3): 425–26.

Errico, Alessia, Krupa Deshmukh, Yoshimi Tanaka, Andrei Pozniakovsky, and Tim Hunt. 2010. "Identification of Substrates for Cyclin Dependent Kinases." *Advances in Enzyme Regulation* 50 (1). Elsevier Ltd: 375–99.

Esterlechner, Jasmina, Nina Reichert, Fabian Iltzsche, Michael Krause, Florian Finkernagel, and Stefan Gaubatz. 2013. "LIN9, a Subunit of the DREAM Complex, Regulates Mitotic Gene Expression and Proliferation of Embryonic Stem Cells." *PLoS ONE* 8 (5).

Fang, Bingliang. 2014. “Development of Synthetic Lethality Anticancer Therapeutics.” *Journal of Medicinal Chemistry* 57 (19): 7859–73. .

Fang, Bingliang. 2015. “RAS Signaling and Anti-RAS Therapy: Lessons Learned from Genetically Engineered Mouse Models, Human Cancer Cells, and Patient-Related Studies.” *Acta Biochimica et Biophysica Sinica* 48 (1): 27–38.

Feldser, David M, Kamena K Kostova, Monte M Winslow, Sarah E Taylor, Chris Cashman, Charles a Whittaker, Francisco J Sanchez-Rivera, et al. 2010. “Stage-Specific Sensitivity to p53 Restoration during Lung Cancer Progression.” *Nature* 468 (7323). Nature Publishing Group: 572–75.

Fischer, Martin, and James A DeCaprio. 2015. “Does Arabidopsis Thaliana DREAM of Cell Cycle Control?” *The EMBO Journal* 34 (15): e201592196.

Fischer, Martin, Patrick Grossmann, Megha Padi, and James A. DeCaprio. 2016. “Integration of TP53, DREAM, MMB-FOXM1 and RB-E2F Target Gene Analyses Identifies Cell Cycle Gene Regulatory Networks.” *Nucleic Acids Res.* 44 (13): 6070–86..

Fischer, Martin, Inga Grundke, Sindy Sohr, Marianne Quaas, Saskia Hoffmann, Arne Knörck, Catalina Gumhold, and Karen Rother. 2013. “p53 and Cell Cycle Dependent Transcription of Kinesin Family Member 23 (KIF23) Is Controlled Via a CHR Promoter Element Bound by DREAM and MMB Complexes.” *PLoS ONE* 8 (5). doi:10.1371/journal.pone.0063187.

Fischer, Martin, Marianne Quaas, Annina Nickel, and Kurt Engeland. 2015. “Indirect p53-Dependent Transcriptional Repression of Survivin , CDC25C , and PLK1 Genes Requires the Cyclin-Dependent Kinase Inhibitor p21 / CDKN1A and CDE / CHR Promoter Sites Binding the DREAM Complex.” *Oncotarget* 6 (39): 41402–17.

Fischer, Martin, Marianne Quaas, Lydia Steiner, and Kurt Engeland. 2016. “The p53-p21-DREAM-CDE/CHR Pathway Regulates G2/M Cell Cycle Genes.” *Nucleic Acids Research* 44 (1): 164–74.

Fischer, Martin, Lydia Steiner, and Kurt Engeland. 2014. “The Transcription Factor p53 : Not a Repressor , Solely an Activator.” *Cell Cycle* 13 (19): 3037–58.

Forristal, Chantal, Shauna a Henley, James I MacDonald, Jason R Bush, Carley Ort, Daniel T Passos, Srikanth Talluri, et al. 2014. “Loss of the Mammalian DREAM Complex Deregulates Chondrocyte Proliferation.” *Molecular and Cellular Biology* 34: 2221–34.

Fung, Siau-Min, Gary Ramsay, and Alisa L Katzen. 2002. “Mutations in Drosophila Myb Lead to Centrosome Amplification and Genomic Instability.” *Development* 129: 347–59.

Furuno, Nobuaki, Nicole Den Elzen, and Jonathon Pines. 1999. “Human Cyclin A Is Required for Mitosis until Mid Prophase.” *Journal of Cell Biology* 147 (2): 295–306.

Gaubatz, S, J A Lees, G J Lindeman, and D M Livingston. 2001. “E2F4 Is Exported from the Nucleus in a CRM1-Dependent Manner.” *Molecular and Cellular Biology* 21 (4): 1384–92.

Gaubatz, S, J G Wood, and D M Livingston. 1998. “Unusual Proliferation Arrest and Transcriptional Control Properties of a Newly Discovered E2F Family Member, E2F-6.” *Proceedings of the National Academy of Sciences of the United States of America* 95 (16): 9190–95.

Georlette, Daphne, Soyeon Ahn, David M MacAlpine, Evelyn Cheung, Peter W Lewis, Eileen L Beall, Stephen P Bell, Terry Speed, J Robert Manak, and Michael R Botchan. 2007. “Genomic Profiling and Expression Studies Reveal Both Positive and Negative Activities for the Drosophila Myb MuvB/dREAM Complex in Proliferating Cells.” *Genes & Development* 21 (22): 2880–96.

Giaccone, Giuseppe, Petr Zatloukal, Jaromir Roubec, Karijn Floor, Jaromir Musil, Milan Kuta, Rob J. Van Klaveren, Subhash Chaudhary, Adrie Gunther, and Setareh Shamsili. 2009. “Multicenter Phase II Trial of YM155, a Small-Molecule Suppressor of Survivin, in Patients with Advanced, Refractory, Non-Small-Cell Lung Cancer.” *Journal of Clinical Oncology* 27 (27): 4481–86.

Giacinti, C, and a Giordano. 2006. “RB and Cell Cycle Progression.” *Oncogene* 25 (38): 5220–27.

Giam, Maybelline, and Giulia Rancati. 2015. “Aneuploidy and Chromosomal Instability in Cancer: A Jackpot to Chaos.” *Cell Division* 10 (3). 1-12.

Ginsberg, Doron, Gino Vairo, Thomas Chittenden, Zhi Xiong Xiao, Gangfeng Xu, Karen L. Wydner, James A. DeCaprio, Jeanne B. Lawrence, and David M. Livingston. 1994. “E2F-4, a New Member of the E2F Transcription Factor Family, Interacts with p107.” *Genes and Development* 8 (22): 2665–79.

Girard, F, U Strausfeld, a Fernandez, and N J Lamb. 1991. “Cyclin A Is Required for the Onset of DNA Replication in Mammalian Fibroblasts.” *Cell* 67 (6): 1169–79.

Green, Douglas R, and Guido Kroemer. 2009. “Cytoplasmic Functions of the Tumour Suppressor p53.” *Nature* 458 (7242): 1127–30.

Gruneberg, Ulrike, Rüdiger Neef, Xiuling Li, Eunice H Y Chan, Ravindra B. Chalamalasetty, Erich A. Nigg, and Francis A. Barr. 2006. “KIF14 and Citron Kinase Act Together to Promote Efficient Cytokinesis.” *Journal of Cell Biology* 172 (3): 363–72.

Guiley, Keelan Z, Tyler J Liban, Jessica G Felthousen, Parameshwaran Ramanan, Larisa Litovchick, and Seth M Rubin. 2015. “Structural Mechanisms of DREAM Complex Assembly and Regulation.” *Genes & Development*, 1–14.

Hanahan, Douglas, and Robert a Weinberg. 2011. “Hallmarks of Cancer: The next Generation.” *Cell* 144 (5). Elsevier Inc.: 646–74.

Harbour, J. William, and Douglas C. Dean. 2000. “The Rb/E2F Pathway: Expanding Roles and Emerging Paradigms.” *Genes and Development*..

Harbour, J. William, Robin X. Luo, Angeline Dei Santi, Antonio A. Postigo, and Douglas C. Dean. 1999. “Cdk Phosphorylation Triggers Sequential Intramolecular Interactions That Progressively Block Rb Functions as Cells Move through G1.” *Cell* 98 (6): 859–69.

Harrison, Melissa M, Craig J Ceol, Xiaowei Lu, and H Robert Horvitz. 2006. “Some C. Elegans Class B Synthetic Multivulva Proteins Encode a Conserved LIN-35 Rb-Containing Complex Distinct from a NuRD-like Complex.” *Proceedings of the National Academy of Sciences of the United States of America* 103 (45): 16782–87.

Haruki, N, T Harano, a Masuda, T Kiyono, T Takahashi, Y Tatematsu, S Shimizu, et al. 2001. “Persistent Increase in Chromosome Instability in Lung Cancer: Possible Indirect Involvement of p53 Inactivation.” *The American Journal of Pathology* 159 (4): 1345–52.

Hauser, S, T Ulrich, S Wurster, K Schmitt, N Reichert, and S Gaubatz. 2012. “Loss of LIN9, a Member of the DREAM Complex, Cooperates with SV40 Large T Antigen to Induce Genomic Instability and Anchorage-Independent Growth.” *Oncogene* 31 (14). Nature Publishing Group: 1859–68.

Hijmans, E M, P M Voorhoeve, R L Beijersbergen, L J van ’t Veer, and R Bernards. 1995. “E2F-5, a New E2F Family Member That Interacts with p130 in Vivo.” *Molecular and Cellular Biology* 15 (6): 3082–89.

Holland, Andrew J, and Don W Cleveland. 2009. “Boveri Revisited: Chromosomal Instability, Aneuploidy and Tumorigenesis.” *Nature Reviews. Molecular Cell Biology* 10. Nature Publishing Group: 478–87.

Holt, Sarah V, Mailys a S Vergnolle, Deema Hussein, Marcin J Wozniak, Victoria J Allan, and Stephen S Taylor. 2005. “Silencing Cenp-F Weakens Centromeric Cohesion, Prevents Chromosome Alignment and Activates the Spindle Checkpoint.” *Journal of Cell Science* 118: 4889–4900.

Horvath, Philippe, and Rodolphe Barrangou. 2010. “CRISPR/Cas, the Immune System of Bacteria and Archaea.” *Science (New York, N.Y.)* 327 (5962): 167–70.

Hsu, Patrick D., Eric S. Lander, and Feng Zhang. 2014. “Development and Applications of CRISPR-Cas9 for Genome Engineering.” *Cell* 157 (6): 1262–78.

Hunter, T, and J Pines. 1994. “Cyclins and Cancer .2. Cyclin-D and Cdk Inhibitors Come of Age.” *Cell* 79 (4): 573–82..

Hurford, Robert K., David Cobrinik, Myung Ho Lee, and Nicholas Dyson. 1997. “pRB and p107/p130 Are Required for the Regulated Expression of Different Sets of E2F Responsive Genes.” *Genes and Development* 11 (11): 1447–63..

Iltzsche, F, K Simon, S Stopp, G Pattschull, S Francke, P Wolter, S Hauser, et al. 2017. “An Important Role for Myb-MuvB and Its Target Gene KIF23 in a Mouse Model of Lung Adenocarcinoma.” *Oncogene*, 36 (1):110-121.

Inoue, Akira, and Toshihiro Nukiwa. 2005. “Gene Mutations in Lung Cancer: Promising Predictive Factors for the Success of Molecular Therapy.” *PLoS Medicine*. doi:10.1371/journal.pmed.0020013.

Islam, a, H Kageyama, N Takada, T Kawamoto, H Takayasu, E Isogai, M Ohira, et al. 2000. “High Expression of Survivin, Mapped to 17q25, Is Significantly Associated with Poor Prognostic Factors and Promotes Cell Survival in Human Neuroblastoma.” *Oncogene* 19 (5): 617–23..

Jackson, Erica L., Nicholas Willis, Kim Mercer, Roderick T. Bronson, Denise Crowley, Raymond Montoya, Tyler Jacks, and David a. Tuveson. 2001. "Analysis of Lung Tumor Initiation and Progression Using Conditional Expression of Oncogenic K-Ras." *Genes and Development* 15 (617): 3243–48..

Kastan, Michael B, and Jiri Bartek. 2004. "Cell-Cycle Checkpoints and Cancer." *Nature* 432 (7015): 316–23..

Katzen, Alisa L., Jean Jackson, Brian P. Harmon, Siau Min Fung, Gary Ramsay, and J. Michael Bishop. 1998. "Drosophila Myb Is Required for the G2/M Transition and Maintenance of Diploidy." *Genes and Development* 12 (6): 831–43.

Kimura, Masashi, Chiharu Uchida, Yukihiko Takano, Masatoshi Kitagawa, and Yukio Okano. 2004. "Cell Cycle-Dependent Regulation of the Human Aurora B Promoter." *Biochemical and Biophysical Research Communications* 316 (3): 930–36.

Kissil, Joseph L., Marita J. Walmsley, Linda Hanlon, Kevin M. Haigis, Carla F Bender Kim, Alejandro Sweet-Cordero, Matthew S. Eckman, et al. 2007. "Requirement for Rac1 in a K-Ras-Induced Lung Cancer in the Mouse." *Cancer Research* 67: 8089–94.

Kittler, Ralf, Laurence Pelletier, Anne-kristine Heninger, Mikolaj Slabicki, Mirko Theis, Lukasz Miroslaw, Ina Poser, et al. 2007. "Genome-Scale RNAi Profiling of Cell Division in Human Tissue Culture Cells." *Nature Cell Biology* 9 (12): 1401–12.

Knight, A S, M Notaridou, and R J Watson. 2009. "A Lin-9 Complex Is Recruited by B-Myb to Activate Transcription of G2/M Genes in Undifferentiated Embryonal Carcinoma Cells." *Oncogene* 28 (15). Nature Publishing Group: 1737–47.

Kobayashi, Kosuke, Toshiya Suzuki, Eriko Iwata, Norihito Nakamichi, Takamasa Suzuki, Poyu Chen, Misato Ohtani, et al. 2015. "Transcriptional Repression by MYB 3 R Proteins Regulates Plant Organ Growth." *The EMBO Journal* 34 (15): 1992–2007.

Korenjak, Michael, Barbie Taylor-Harding, Ulrich K. Binn, John S. Satterlee, Olivier Stevaux, Rein Aasland, Helen White-Cooper, Nick Dyson, and Alexander Brehm. 2004. "Native E2F/RBF Complexes Contain Myb-Interacting Proteins and Repress Transcription of Developmentally Controlled E2F Target Genes." *Cell* 119 (2): 181–93.

Laemmli, U K. 1970. "Cleavage of Structural Proteins during the Assembly of the Head of Bacteriophage T4." *Nature* 227 (5259): 680–85.

Lamers, Fieke, Ida Van Der Ploeg, Linda Schild, Marli E. Ebus, Jan Koster, Bo R. Hansen, Troels Koch, Rogier Versteeg, Huib N. Caron, and Jan J. Molenaar. 2011. "Knockdown of Survivin (BIRC5) Causes Apoptosis in Neuroblastoma via Mitotic Catastrophe." *Endocrine-Related Cancer* 18: 657–68..

Lane, D P. 1992. "Cancer. p53, Guardian of the Genome." *Nature*. 358, 15-16.

Laoukili, J, M R Kooistra, A Bras, J Kauw, R M Kerkhoven, A Morrison, H Clevers, and R H Medema. 2005. "FoxM1 Is Required for Execution of the Mitotic Programme and Chromosome Stability." *Nature Cell Biology* 7 (2): 126–36.

Lee, Bum Kyu, Akshay A. Bhinge, and Vishwanath R. Iyer. 2011. “Wide-Ranging Functions of E2F4 in Transcriptional Activation and Repression Revealed by Genome-Wide Analysis.” *Nucleic Acids Research* 39 (9): 3558–73.

Lengauer, C, K W Kinzler, and B Vogelstein. 1997. “Genetic Instability in Colorectal Cancers.” *Nature*. 386, 623–627.

Lewis, Peter W, Eileen L Beall, Tracey C Fleischer, Daphne Georlette, Andrew J Link, and Michael R Botchan. 2004. “Identification of a Drosophila Myb – E2F2 / RBF Transcriptional Repressor Complex,” 2929–40.

Li, Jing, Cong Ran, Edward Li, Faye Gordon, Grant Comstock, Hasan Siddiqui, Whitney Cleghorn, et al. 2008. “Synergistic Function of E2F7 and E2F8 Is Essential for Cell Survival and Embryonic Development.” *Developmental Cell* 14 (1): 62–75.

Liang, Xiao-Dong, Yue-Chu Dai, Zhao-Yun Li, Mei-Fu Gan, Shi-Rong Zhang, Yin-Pan, Hong-Sheng Lu, et al. 2014. “Expression and Function Analysis of Mitotic Checkpoint Genes Identifies TTK as a Potential Therapeutic Target for Human Hepatocellular Carcinoma.” *PLoS ONE* 9 (6): e97739.

Lim, Shuhui, and Philipp Kaldis. 2013. “Cdks, Cyclins and CKIs: Roles beyond Cell Cycle Regulation.” *Development* 140 (15): 3079–93.

Lipinski, M M, and T Jacks. 1999. “The Retinoblastoma Gene Family in Differentiation and Development.” *Oncogene* 18 (55): 7873–82.

Litovchick, Larisa, Laurence a. Florens, Selene K. Swanson, Michael P. Washburn, and James a. DeCaprio. 2011. “DYRK1A Protein Kinase Promotes Quiescence and Senescence through DREAM Complex Assembly.” *Genes and Development* 25 (8): 801–13.

Litovchick, Larisa, Subhashini Sadasivam, Laurence Florens, Xiaopeng Zhu, Selene K. Swanson, Soundarapandian Velmurugan, Runsheng Chen, Michael P. Washburn, X. Shirley Liu, and James A. DeCaprio. 2007. “Evolutionarily Conserved Multisubunit RBL2/p130 and E2F4 Protein Complex Represses Human Cell Cycle-Dependent Genes in Quiescence.” *Molecular Cell* 26 (4): 539–51.

Liu, M., B. Dai, S.-H. Kang, K. Ban, F.-J. Huang, F. F. Lang, K. D. Aldape, et al. 2006. “FoxM1B Is Overexpressed in Human Glioblastomas and Critically Regulates the Tumorigenicity of Glioma Cells.” *Cancer Research* 66 (7): 3593–3602.

Liu, Yu, Chong Chen, Zhengmin Xu, Claudio Scuoppo, Cory D Rillahan, Jianjiong Gao, Barbara Spitzer, et al. 2016. “Deletions Linked to TP53 Loss Drive Cancer through p53-Independent Mechanisms.” *Nature* 531 (7595). Nature Publishing Group: 471–75.

Lu, Lin-Yu, Jamie L Wood, Katherine Minter-Dykhouse, Lin Ye, Thomas L Saunders, Xiaochun Yu, and Junjie Chen. 2008. “Polo-like Kinase 1 Is Essential for Early Embryonic Development and Tumor Suppression.” *Molecular and Cellular Biology* 28 (22): 6870–76.

Lu, Lin-Yu, and Xiaochun Yu. 2009. “The Balance of Polo-like Kinase 1 in Tumorigenesis.” *Cell Division* 4: 4.

Malumbres, Marcos, and Mariano Barbacid. 2005. “Mammalian Cyclin-Dependent Kinases.” *Trends in Biochemical Sciences* 30 (11): 630–41.

Malumbres, Marcos, and Mariano Barbacid 2009. “Cell Cycle, CDKs and Cancer: A Changing Paradigm.” *Nature Reviews. Cancer* 9 (3): 153–66.

Manak, J Robert, Nesanet Mitiku, and Joseph S Lipsick. 2002. “Mutation of the Drosophila Homologue of the Myb Protooncogene Causes Genomic Instability.” *Proceedings of the National Academy of Sciences of the United States of America* 99 (11): 7438–43.

Mannefeld, M, E Klassen, and S Gaubatz. 2009. “B-MYB Is Required for Recovery from the DNA Damage-Induced G2 Checkpoint in p53 Mutant Cells.” *Cancer Research* 69 (9): 4073–80.

Mao, Xin, Guy Orchard, Debra M. Lillington, Robin Russell-Jones, Bryan D. Young, and Sean J. Whittaker. 2003. “Amplification and Overexpression of JUNB Is Associated with Primary Cutaneous T-Cell Lymphomas.” *Blood* 101 (4): 1513–19.

Mao, Yinghui, Ariane Abrieu, and Don W. Cleveland. 2003. “Activating and Silencing the Mitotic Checkpoint through CENP-E-Dependent Activation/inactivation of BubR1.” *Cell* 114 (1): 87–98.

Marceau, Aimee H., Jessica G. Felthousen, Paul D. Goetsch, Audra N. Iness, Hsiau-Wei Lee, Sarvind M. Tripathi, Susan Strome, Larisa Litovchick, and Seth M. Rubin. 2016. “Structural Basis for LIN54 Recognition of CHR Elements in Cell Cycle-Regulated Promoters.” *Nature Communications* 7. Nature Publishing Group: 12301: 1-11.

Maya, Ruth, Moshe Balass, Seong Tae Kim, Dganit Shkedy, Juan Fernando Martinez Leal, Ohad Shifman, Miri Moas, et al. 2001. “ATM-Dependent Phosphorylation of Mdm2 on Serine 395: Role in p53 Activation by DNA Damage.” *Genes and Development* 15 (9): 1067–77..

Moberg, K, M A Starz, and J A Lees. 1996. “E2F-4 Switches from p130 to p107 and pRB in Response to Cell Cycle Reentry.” *Molecular and Cellular Biology* 16 (4): 1436–49.

Molina, J R, P Yang, S D Cassivi, S E Schild, and A A Adjei. 2008. “Non-Small Cell Lung Cancer: Epidemiology, Risk Factors, Treatment, and Survivorship.” *Mayo Clinic Proceedings* 83 (5): 584–94.

Moon, Nam Sung, and Nicholas Dyson. 2008. “E2F7 and E2F8 Keep the E2F Family in Balance.” *Developmental Cell* 14 (1): 1–3.

Morgan, David O. 1997. “cyclin-dependent kinases : Engines , Clocks , and Microprocessors.” *Cell* 13, pp. 261–91

Morkel, M, J Wenkel, J Bannister, T Kouzarides, and C Hagemeier. 1997. “An E2F-like Repressor of Transcription.” *Nature* 390 (11): 567–68.

Müller, Gerd and Kurt Engeland. 2010. “The Central Role of CDE/CHR Promoter Elements in the Regulation of Cell Cycle-Dependent Gene Transcription.” *The FEBS Journal* 277 (4): 877–93.

Müller, Gerd, Axel Wintsche, Konstanze Stangner, Sonja J Prohaska, Peter F Stadler, and Kurt Engeland. 2014. "The CHR Site: Definition and Genome-Wide Identification of a Cell Cycle Transcriptional Element." *Nucleic Acids Research*, 1–20.

Müller, Gerd, Marianne Quaas, Michael Schümann, Eberhard Krause, Megha Padi, Martin Fischer, Larisa Litovchick, James a. Decaprio, and Kurt Engeland. 2012. "The CHR Promoter Element Controls Cell Cycle-Dependent Gene Transcription and Binds the DREAM and MMB Complexes." *Nucleic Acids Research* 40 (4): 1561–78.

Müller, Gerd, Konstanze Stangner, Thomas Schmitt, Axel Wintsche, and Kurt Engeland. 2016. "Timing of Transcription during the Cell Cycle: Protein Complexes Binding to E2F, E2F/CLE, CDE/CHR, or CHR Promoter Elements Define Early and Late Cell Cycle Gene Expression." *Oncotarget*. doi:10.18632/oncotarget.10888.

Musacchio, Andrea. 2011. "Spindle Assembly Checkpoint: The Third Decade." *Philosophical Transactions of the Royal Society B: Biological Sciences* 366 (1584): 3595–3604.

Musacchio, Andrea, and Edward D Salmon. 2007. "The Spindle-Assembly Checkpoint in Space and Time." *Nature Reviews. Molecular Cell Biology* 8 (5): 379–93.

Negrini, S, V G Gorgoulis, and T D Halazonetis. 2010. "Genomic Instability--an Evolving Hallmark of Cancer." *Nature Reviews Molecular Cell Biology* 11 (3): 220–28.

Nikitin, Alexander Yu, Ana Alcaraz, Miriam R Anver, Roderick T Bronson, Robert D Cardiff, Darlene Dixon, Armando E Fraire, et al. 2004. "Classification of Proliferative Pulmonary Lesions of the Mouse : Recommendations of the Mouse Models of Human Cancers Consortium Classification of Proliferative Pulmonary Lesions of the Mouse : Recommendations of the Mouse Models of Human Cancers Consorti," no. 6: 2307–16.

O'Hare, Michael, Mehdi Shadmand, Rania S. Sulaiman, Kamakshi Sishtla, Toshiaki Sakisaka, and Timothy W. Corson. 2016. "*Kif14* Overexpression Accelerates Murine Retinoblastoma Development." *International Journal of Cancer* 139 (8): 1752–58.

Obaya, A. J., and J. M. Sedivy. 2002. "Regulation of Cyclin-Cdk Activity in Mammalian Cells." *Cellular and Molecular Life Sciences*.

Ogawa, Hidesato, Kei-Ichiro Ishiguro, Stefan Gaubatz, David M Livingston, and Yoshihiro Nakatani. 2002. "A Complex with Chromatin Modifiers That Occupies E2F- and Myc-Responsive Genes in G0 Cells." *Science* 296 (5570): 1132–36.

Ohtsubo, M, a M Theodoras, J Schumacher, J M Roberts, and M Pagano. 1995. "Human Cyclin E, a Nuclear Protein Essential for the G1-to-S Phase Transition." *Molecular and Cellular Biology* 15 (5): 2612–24.

Olivier, Magali, Monica Hollstein, and Pierre Hainaut. 2010. "TP53 Mutations in Human Cancers: Origins, Consequences, and Clinical Use." *Cold Spring Harbor Perspectives in Biology* 2 (1): 1–17.

Osterloh, Lisa, Björn von Eyss, Fabienne Schmit, Lena Rein, Denise Hübner, Birgit Samans, Stefanie Hauser, and Stefan Gaubatz. 2007. "The Human synMuv-like Protein LIN-9 Is Required for Transcription of G2/M Genes and for Entry into Mitosis." *The EMBO Journal* 26 (1): 144–57.

Pandit, Bulbul, Marianna Halasi, and Andrei L. Gartel. 2009. "p53 Negatively Regulates Expression of FoxM1." *Cell Cycle*.

Pardee, a B. 1974. "A Restriction Point for Control of Normal Animal Cell Proliferation." *Proceedings of the National Academy of Sciences of the United States of America* 71 (4): 1286–90.

Pavletich, N P. 1999. "Mechanisms of Cyclin-Dependent Kinase Regulation: Structures of Cdks, Their Cyclin Activators, and Cip and INK4 Inhibitors." *Journal of Molecular Biology* 287 (5): 821–28.

Petronczki, Mark, Péter Lénárt, and Jan Michael Peters. 2008. "Polo on the Rise-from Mitotic Entry to Cytokinesis with Plk1." *Developmental Cell*.

Pilarsky, Christian, Michael Wenzig, Thomas Specht, Hans Detlev Saeger, and Robert Grützmann. 2004. "Identification and Validation of Commonly Overexpressed Genes in Solid Tumors by Comparison of Microarray Data." *Neoplasia (New York, N.Y.)* 6 (6): 744–50.

Pilkinton, Mark, Raudel Sandova, Julie Song, Scott a. Ness, and Oscar R. Colamonici. 2007. "Mip/LIN-9 Regulates the Expression of B-Myb and the Induction of Cyclin A, Cyclin B, and CDK1." *Journal of Biological Chemistry* 282 (1): 168–75.

Pilkinton, M, R Sandoval, and O R Colamonici. 2007. "Mammalian Mip/LIN-9 Interacts with Either the p107, p130/E2F4 Repressor Complex or B-Myb in a Cell Cycle-Phase-Dependent Context Distinct from the Drosophila dREAM Complex." *Oncogene* 26 (54): 7535–43.

Pylayeva-Gupta, Yuliya, Elda Grabocka, and Dafna Bar-Sagi. 2011. "RAS Oncogenes: Weaving a Tumorigenic Web." *Nature Reviews. Cancer* 11 (11). Nature Publishing Group: 761–74.

Quaas, Marianne, Gerd a. Müller, and Kurt Engeland. 2012. "p53 Can Repress Transcription of Cell Cycle Genes through a p21 WAF1/CIP1-Dependent Switch from MMB to DREAM Protein Complex Binding at CHR Promoter Elements." *Cell Cycle* 11: 4661–72.

Raemaekers, Tim, Katharina Ribbeck, Joël Beaudouin, Wim Annaert, Mark Van Camp, Ingrid Stockmans, Nico Smets, Roger Bouillon, Jan Ellenberg, and Geert Carmeliet. 2003. "NuSAP, a Novel Microtubule-Associated Protein Involved in Mitotic Spindle Organization." *Journal of Cell Biology* 162 (6): 1017–29.

Raschellá, G., A. Negroni, A. Sala, S. Pucci, A. Romeo, and B. Calabretta. 1995. "Requirement of B-Myb Function for Survival and Differentiative Potential of Human Neuroblastoma Cells." *Journal of Biological Chemistry* 270 (15): 8540–45.

Raschellà, Giuseppe, Vincenzo Cesi, Roberto Amendola, Anna Negroni, Barbara Tanno, Pierluigi Altavista, Gian Paolo Tonini, Bruno De Bernardi, and Bruno Calabretta. 1999. "Expression of B-Myb in Neuroblastoma Tumors Is a Poor Prognostic Factor Independent from MYCN Amplification." *Cancer Research* 59 (14): 3365–68.

Rayman, Joseph B., Yasuhiko Takahashi, Vahan B. Indjeian, Jan Hermen Dannenberg, Steven Catchpole, Roger J. Watson, Heinte Riele, and Brian David Dynlacht. 2002. "E2F Mediates Cell Cycle-Dependent Transcriptional Repression in Vivo by Recruitment of an HDAC1/mSin3B Corepressor Complex." *Genes and Development* 16 (8): 933–47.

Reichert, Nina, Sebastian Wurster, Tanja Ulrich, Kathrin Schmitt, Stefanie Hauser, Leona Probst, Rudolf Götz, et al. 2010. "Lin9, a Subunit of the Mammalian DREAM Complex, Is Essential for Embryonic Development, for Survival of Adult Mice, and for Tumor Suppression." *Molecular and Cellular Biology* 30 (12): 2896–2908.

Reilly, K M, D a Loisel, R T Bronson, M E McLaughlin, and T Jacks. 2000. "Nf1;Trp53 Mutant Mice Develop Glioblastoma with Evidence of Strain-Specific Effects." *Nature Genetics* 26 (1): 109–13.

Rowland, Benjamin D, and Daniel S Peeper. 2006. "KLF4, p21 and Context-Dependent Opposing Forces in Cancer." *Nature Reviews. Cancer* 6 (1): 11–23.

Sadasivam, S., S. Duan, and J. a. DeCaprio. 2012. "The MuvB Complex Sequentially Recruits B-Myb and FoxM1 to Promote Mitotic Gene Expression." *Genes & Development* 26 (5): 474–89.

Sadasivam, S, and J A DeCaprio. 2013. "The DREAM Complex: Master Coordinator of Cell Cycle-Dependent Gene Expression." *Nature Reviews. Cancer* 13: 585–95.

Schmit, Fabienne, Sarah Cremer, and Stefan Gaubatz. 2009. "LIN54 Is an Essential Core Subunit of the DREAM/LINC Complex That Binds to the cdc2 Promoter in a Sequence-Specific Manner." *FEBS Journal* 276: 5703–16.

Schmit, Fabienne, Michael Korenjak, Mirijam Mannefeld, Kathrin Schmitt, Claudia Franke, Björn Von Eyss, Sladjana Gagrica, Frank Hänel, Alexander Brehm, and Stefan Gaubatz. 2007. "LINC, a Human Complex That Is Related to pRB-Containing Complexes in Invertebrates Regulates the Expression of G2/M Genes." *Cell Cycle* 6: 1903–13.

Shen, Zhiyuan. 2011. "Genomic Instability and Cancer: An Introduction." *Journal of Molecular Cell Biology*.

Shepard, Jennifer L, James F Amatruda, Howard M Stern, Aravind Subramanian, David Finkelstein, James Ziai, K Rose Finley, et al. 2005. "A Zebrafish Bmyb Mutation Causes Genome Instability and Increased Cancer Susceptibility." *Proc Natl Acad Sci U S A* 102: 13194–99.

Sotillo, Rocío, Eva Hernando, Elena Díaz-Rodríguez, Julie Teruya-Feldstein, Carlos Cordón-Cardo, Scott W Lowe, and Robert Benezra. 2007. "Mad2 Overexpression Promotes Aneuploidy and Tumorigenesis in Mice." *Cancer Cell* 11 (1): 9–23.

Sozzani, R, C Maggio, S Varotto, S Canova, C Bergounioux, D Albani, and R Cella. 2006. "Interplay between Arabidopsis Activating Factors E2Fb and E2Fa in Cell Cycle Progression and Development." *Plant Physiol* 140 (4): 1355–66.

Stengel, Kristy R., Chellappagounder Thangavel, David A. Solomon, Steve P. Angus, Yi Zheng, and Erik S. Knudsen. 2009. "Retinoblastoma/p107/p130 Pocket Proteins. Proteins Dynamics and Interactions with Target Gene Promoters." *Journal of Biological Chemistry* 284 (29): 19265–71.

Stewart, B W, and C P Wild. 2014. “World Cancer Report 2014.” *World Health Organization*. Lyon Cedex. doi:9283204298.

Takashima, Asami, and Douglas V Faller. 2013. “Targeting the RAS Oncogene.” *Expert Opinion on Therapeutic Targets* 17 (5). Informa UK, Ltd.: 507–31.

Tanaka, Y, N P Patestos, T Maekawa, and S Ishii. 1999. “B-Myb Is Required for Inner Cell Mass Formation at an Early Stage of Development.” *J Biol Chem* 274 (40): 28067–70.

Taniwaki, Masaya, Atsushi Takano, Nobuhisa Ishikawa, Wataru Yasui, Kouki Inai, Hitoshi Nishimura, Eiju Tsuchiya, Nobuoki Kohno, Yusuke Nakamura, and Yataro Daigo. 2007. “Activation of KIF4A as a Prognostic Biomarker and Therapeutic Target for Lung Cancer.” *Clinical Cancer Research* 13 (22): 6624–31.

Tanner, Minna M., Seija Grenman, Anjila Koul, Oskar Johannsson, Paul Meltzer, Tanja Pejovic, Åke Borg, and Jorma J. Isola. 2000. “Frequent Amplification of Chromosomal Region 20q12-q13 in Ovarian Cancer.” *Clinical Cancer Research* 6 (5): 1833–39.

Tao, Deyou, Yihong Pan, Hongsheng Lu, Song Zheng, Hui Lin, Hongyan Fang, and Feilin Cao. 2014. “B-Myb Is a Gene Implicated in Cell Cycle and Proliferation of Breast Cancer” 7 (9): 5819–27.

Tarasov, Kirill V., Yelena S. Tarasova, Wai Leong Tam, Daniel R. Riordon, Steven T. Elliott, Gabriela Kania, Jinliang Li, et al. 2008. “B-MYB Is Essential for Normal Cell Cycle Progression and Chromosomal Stability of Embryonic Stem Cells.” *PLoS ONE* 3 (6).

Tetreault, Marie-Pier, Yizeng Yang, and Jonathan P Katz. 2013. “Krüppel-like Factors in Cancer.” *Nature Reviews. Cancer* 13 (10). Nature Publishing Group: 701–13.

Thompson, Sarah L., Samuel F. Bakhoum, and Duane A. Compton. 2010. “Mechanisms of Chromosomal Instability.” *Current Biology* 20 (6). Elsevier Ltd: R285–95.

Thorner, A R, K A Hoadley, J S Parker, S Winkel, R C Millikan, and C M Perou. 2009. “In Vitro and in Vivo Analysis of B-Myb in Basal-like Breast Cancer.” *Oncogene* 28 (5): 742–51.

Trimarchi, J M, B Fairchild, R Verona, K Moberg, N Andon, and J a Lees. 1998. “E2F-6, a Member of the E2F Family That Can Behave as a Transcriptional Repressor.” *Proceedings of the National Academy of Sciences of the United States of America* 95 (6): 2850–55.

Tschöp, Katrin, Andrew R. Conery, Larisa Litovchick, James a. DeCaprio, Jeffrey Settleman, Ed Harlow, and Nicholas Dyson. 2011. “A Kinase shRNA Screen Links LATS2 and the pRB Tumor Suppressor.” *Genes and Development* 25: 814–30.

van ’t Veer, Laura J, Hongyue Dai, Marc J van de Vijver, Yudong D He, Augustinus A M Hart, Mao Mao, Hans L Peterse, et al. 2002. “Gene Expression Profiling Predicts Clinical Outcome of Breast Cancer.” *Nature* 415 (6871): 530–36.

van den Heuvel, Sander, and Nicholas J Dyson. 2008. “Conserved Functions of the pRB and E2F Families.” *Nature Reviews. Molecular Cell Biology* 9 (9): 713–24.

van der Hoeven, Dharini, Kwang-jin Cho, Xiaoping Ma, Sravanthi Chigurupati, Robert G Parton, and John F Hancock. 2013. “Fendiline Inhibits K-Ras Plasma Membrane Localization and Blocks K-Ras Signal Transmission.” *Molecular and Cellular Biology* 33 (2): 237–51. .

van Vugt, M A, and R H Medema. 2005. “Getting in and out of Mitosis with Polo-like Kinase-1.” *Oncogene* 24 (17): 2844–59.

Vanden Bosch, An, Tim Raemaekers, Sarah Denayer, Sophie Torrekens, Nico Smets, Karen Moermans, Mieke Dewerchin, Peter Carmeliet, and Geert Carmeliet. 2010. “NuSAP Is Essential for Chromatin-Induced Spindle Formation during Early Embryogenesis.” *Journal of Cell Science* 123: 3244–55.

Vermeulen,K.,Van Bockstaele,D.R.,Berneman, Z.N., Katrien Vermeulen, Dirk R Van Bockstaele, and Zwi N Berneman. 2003. “The Cell Cycle:a Review of Regulation,deregulation and Therapeutic Targets in Cancer.” *Cell Proliferation* 36 (3): 131–49.

Verona, R, K Moberg, S Estes, M Starz, J P Vernon, and J A Lees. 1997. “E2F Activity Is Regulated by Cell Cycle-Dependent Changes in Subcellular Localization.” *Molecular and Cellular Biology* 17 (12): 7268–82.

Vogelstein, B, D Lane, and a J Levine. 2000. “Surfing the p53 Network.” *Nature* 408: 307–10.

Vogelstein, Bert, Nickolas Papadopoulos, Victor E Velculescu, Shibin Zhou, Luis A Diaz Jr., and Kenneth W Kinzler. 2013. “Cancer Genome Landscapes.” *Science* 339 (6127): 1546–58.

Wang, I-Ching, Yi-Ju Chen, Douglas Hughes, Vladimir Petrovic, Michael L Major, Hyung Jung Park, Yongjun Tan, Timothy Ackerson, and Robert H Costa. 2005. “Forkhead Box M1 Regulates the Transcriptional Network of Genes Essential for Mitotic Progression and Genes Encoding the SCF (Skp2-Cks1) Ubiquitin Ligase.” *Molecular and Cellular Biology* 25 (24): 10875–94.

Wang, W., Y. Shi, J. Li, W. Cui, and B. Yang. 2016. “Up-Regulation of KIF14 Is a Predictor of Poor Survival and a Novel Prognostic Biomarker of Chemoresistance to Paclitaxel Treatment in Cervical Cancer.” *Bioscience Reports* 36 (2): e00315–e00315.

Weaver, Beth A., and Don W. Cleveland. 2006. “Does Aneuploidy Cause Cancer?” *Current Opinion in Cell Biology* 18 (6): 658–67.

Weaver, Beth A A, Alain D Silk, Cristina Montagna, Pascal Verdier-pinard, and Don W Cleveland. 2007. “Aneuploidy Acts Both Oncogenically and as a Tumor Suppressor.” *Cancer Cell* 11 (January): 25–36.

Weaver, Robbyn L, Jazeel F Limzerwala, Ryan M Naylor, Karthik B Jeganathan, Darren J Baker, and Jan M van Deursen. 2016. “BubR1 Alterations That Reinforce Mitotic Surveillance Act against Aneuploidy and Cancer.” *eLife* 5 (3): 341–53.

Weijts, Bart Gmw, Walbert J Bakker, Peter Wa Cornelissen, Kuo-Hsuan Liang, Frank H Schaftenaar, Bart Westendorp, Charlotte Acmt De Wolf, et al. 2012. “E2F7 and E2F8 Promote Angiogenesis through Transcriptional Activation of VEGFA in Cooperation with HIF1.” *The EMBO Journal* 31: 3871–84.

Wen, Hong, Laura Andrejka, Jonathan Ashton, Roger Karess, and Joseph S. Lipsick. 2008. “Epigenetic Regulation of Gene Expression by Drosophila Myb and E2F2-RBF via the Myb-MuvB/dREAM Complex.” *Genes and Development* 22 (5): 601–14.

Wheatley, Sally P., Edward H. Hinchcliffe, Michael Glotzer, Anthony A. Hyman, Greenfield Sluder, and Yu Li Wang. 1997. “CDK1 Inactivation Regulates Anaphase Spindle Dynamics and Cytokinesis in Vivo.” *Journal of Cell Biology* 138 (2): 385–93.

White-Cooper, Helen. 2010. “Molecular Mechanisms of Gene Regulation during Drosophila Spermatogenesis.” *Reproduction* 139 (1): 11–21.

White, Erin A., and Michael Glotzer. 2012. “Centralspindlin: At the Heart of Cytokinesis.” *Cytoskeleton*. 69 (11) 882-829.

Winter, Georg E, Dennis L Buckley, Joshiawa Paulk, Justin M Roberts, Amanda Souza, Sirano Dhe-Paganon, and James E Bradner. 2015. “Phthalimide Conjugation as a Strategy for in Vivo Target Protein Degradation.” *Science (New York, N.Y.)* 348 (6241): 1376–81.

Wiseman, Elizabeth F, Xi Chen, Namshik Han, Aaron Webber, Zongling Ji, Andrew D Sharrocks, and Yeng S Ang. 2015. “Deregulation of the FOXM1 Target Gene Network and Its Coregulatory Partners in Oesophageal Adenocarcinoma.” *Molecular Cancer* 14: 1–14.

Wolter, Patrick, Steffen Hanselmann, Grit Pattschull, Eva Schruf, Stefan Gaubatz, Patrick Wolter, Steffen Hanselmann, Grit Pattschull, Eva Schruf, and Stefan Gaubatz. 2017. “Central Spindle Proteins and Mitotic Kinesins Are Direct Transcriptional Targets of MuvB, B-MYB and FOXM1 in Breast Cancer Cell Lines and Are Potential Targets for Therapy.” *Oncotarget* 5 (0). doi:10.18632/oncotarget.14466.

Yamauchi, Tomohiro, Takefumi Ishidao, Teruaki Nomura, Toshie Shinagawa, Yasunori Tanaka, Shigenobu Yonemura, and Shunsuke Ishii. 2008. “A B-Myb Complex Containing Clathrin and Filamin Is Required for Mitotic Spindle Function.” *The EMBO Journal* 27 (13): 1852–62.

Yee, Karen S., and Karen H. Vousden. 2005. “Complicating the Complexity of p53.” *Carcinogenesis* 26 (8): 1317–22.

Yen, T J, G Li, B T Schaar, I Szilak, and D W Cleveland. 1992. “CENP-E Is a Putative Kinetochore Motor That Accumulates Just before Mitosis.” *Nature* 359 (6395): 536–39.

Yochum, Gregory S. 2012. “AXIN2: Tumor Suppressor, Oncogene or Both in Colorectal Cancer?” *Journal of Cancer Science and Therapy* 4 (7): 2. doi:10.4172/1948-5956.1000e109.

Yoon, Dae-Sung, Robert P Wersto, Weibo Zhou, Francis J Chrest, Elizabeth S Garrett, Teag Kyu Kwon, and Edward Gabrielson. 2002. “Variable Levels of Chromosomal Instability and Mitotic Spindle Checkpoint Defects in Breast Cancer.” *The American Journal of Pathology* 161 (2): 391–97.

Zhan, Ming, Daniel R. Riordon, Bin Yan, Yelena S. Tarasova, Sarah Bruweleit, Kirill V. Tarasov, Ronald A. Li, Robert P. Wersto, and Kenneth R. Boheler. 2012. "The B-MYB Transcriptional Network Guides Cell Cycle Progression and Fate Decisions to Sustain Self-Renewal and the Identity of Pluripotent Stem Cells." *PLoS ONE* 7 (8).

Zhu, Wencheng, Paloma H Giangrande, and Joseph R Nevins. 2004. "E2Fs Link the Control of G1/S and G2/M Transcription." *The EMBO Journal* 23 (23): 4615–26.

Zondervan, P. E., J. Wink, J. C. Alers, J. N. Ijzermans, S. W. Schalm, R. A. De Man, and H. Van Dekken. 2000. "Molecular Cytogenetic Evaluation of Virus-Associated and Non-Viral Hepatocellular Carcinoma: Analysis of 26 Carcinomas and 12 Concurrent Dysplasias." *Journal of Pathology* 192 (2): 207–15.

Zwicker, J, F C Lucibello, L A Wolfraim, C Gross, M Truss, K Engeland, and R Müller. 1995. "Cell Cycle Regulation of the Cyclin A, cdc25C and cdc2 Genes Is Based on a Common Mechanism of Transcriptional Repression." *The EMBO Journal* 14 (18): 4514–22.

8. Appendix

8.1. List of figures

8.2. Abbreviations

Ad-Cre	Adenoviral Cre recombinase
APC/C	Anaphase promoting complex/cylcosome
Birc5	Baculoviral inhibitor of apoptosis repeat-containing 5
CDE	Cell cycle-dependent element
CDK	Cyclin-dependent kinase
CDKi	CDK inhibitor
Cenpf	Centromere protein F
ChIP	Chromatin immunoprecipitation
CHR	Cell cycle genes homology
Co-IP	Co-immunopreciptation
Ctrl	Control
DNA	Deoxyribonucleic acid
DREAM	Drosophila RBF, dE2F2 and dMyb-interacting proteins
EC	Embryonic carcinoma
e.g.	Example
ESC	Embryonic stem cell
FACS	Fluorescence activated cell sorting
FBS	FoxM1 binding site
Fig	Figure
GAPDH	Glyceraldehyde-3-phosphate dehydrogenase
G0, G1, G2	Gap phase
h	Hours
HDAC	Histone deacetylase
HPRT	Hypoxanthine-guanine phosphoribosyltransferase
ICM	Inner cell mass
IF	Immunofluorescence
IgG	Immunoglobulin G
IP	Immunoprecipitation
kd	Knock down
kda	kilodalton
Kif	Kinesin
lenti-Cre	Lentiviral Cre recombinase
MAPK	Mitogen-activated protein kinase
MBS	Myb binding site
MEF	Mouse embryonic fibroblasts
MMB	Myb-MuvB
MMB-FoxM1	Myb-MuvB-FoxM1
M-phase	Mitosis
MPM2	Mitotic protein #2
Myb	Myeloblastosis
Nusap1	Nucleolar spindle–associated protein

o/n	Over night
PCR	Polymerase chain reaction
Plk1	Polo-like kinase 1
pRB	Retinoblastoma
qRT-PCR	Quantitative real-time PCR
RNA	Ribonucleic acid
RNAi	RNA interference
RT	Room temperature/Reverse transcriptase
SDS-PAGE	SDS-polyacrylamide gel electrophoresis
shRNA	Short-hairpin RNA
siRNA	Small interfering RNA
S-phase	Synthesis phase
Wt	Wild type
+/+	Homozygous, wild type
+/-	Heterozygous
-/-	Homozygous, knock out
Δ	Delta/Deletion

8.3. Own publications and conference contributions

Iltzsche F.*, Simon K.*, Stopp S*., Pattschull G.*, Francke S., Wolter P., Hauser S., Murphy DJ., Garcia P., Rosenwald A., Gaubatz S. (2017) „**An important role for Myb-MuvB and its target gene KIF23 in a mouse model of lung adenocarcinoma**"; *Oncogene*; 36(1):110-121

*These authors contributed equally to this work.

Esterlechner J., Reichert N., Iltzsche F., Krause M., Finkernagel F., Gaubatz S. (2013) "**LIN9, a subunit of the DREAM complex, regulates mitotic gene expression and proliferation of embryonic stem cells**" PLoS One; 8(5):e62882

Conference contributions (Talks and Posters)

03/2014	Genes & Cancer 30th Anniversary Meeting, Cambridge, UK *Poster*: Role of DREAM-mediated gene expression in tumorigenesis
10/2013	8th International GSLS Symposium. "Scientific Crosstalk" held at RVZ, Würzburg, Germany *Talk*: Role of DREAM-mediated gene expression downstream of mutated K-Ras in lung cancer
09/2013	Retreat of the Integrated Graduate College of the SFB Transregio 17, Pommersfelden, Germany *Talk*: Role of DREAM-mediated gene expression downstream of K-Ras in lung cancer
06/2013	Gordon Research Conference "Cell Growth and Proliferation", West Dover, USA Poster: Role of DREAM-mediated gene expression downstream of mutated K-Ras in lung cancer
02/2012	Retreat of the Integrated Graduate College of the SFB Transregio 17, Schöntal, Germany *Talk*: Role of DREAM-mediated gene expression in lung cancer
04/2011	Joint meeting of SFB Transregio 17 & LOEWE, Marburg, Germany *Poster*: Role of DREAM-mediated gene expression in lung cancer
10/2010	Retreat of the Integrated Graduate College of the SFB Transregio 17, Würzburg, Germany

8.4. Curriculum vitae

The *Curriculum vitae* will not be published for data protection reasons.

8.5. Acknowledgments

First and foremost, I convey my gratitude and sincere thanks to my supervisor Prof. Dr. Stefan Gaubatz for giving me the opportunity to work in his lab and for supervising my PhD thesis. I appreciate all the scientific support and guidance during my PhD project.

Besides my supervisor, I extend my gratitude and thanks to other members of my thesis committee: Dr. Katrin Paeschke and Dr. Daniel J. Murphy for their encouragement and insightful comments during our meetings.

I thank all the current and former lab members for the cheerful atmosphere and their advice and support: Katja Simon, Dr. Sabine Stop, Grit Patschull, Dr. Marc Fackler, Dr. Jasmina Esterlchener, Dr. Patrick Wolter, Dr. Geeta Kumari, Dr. Tanja Ulrich and Piero Ocone.

Special thanks to the technical assistants Adelgunde Wolpert and Susanne Spahr who always supported my practical research. I learned a lot of them!

Special thanks to Katja, Denise, Janna, Caro and Pascal who always have a friendly ear. I spend a lot of pleasant moments with you at many wine fests.

Finally, I want to thank my parents and my siblings who were supporting me my whole life.

8.6. Affidativ

I hereby confirm that my thesis entitled "The Role of DREAM/MMB-mediated mitotic gene expression downstream of mutated K-Ras in lung cancer" is the result of my own work. I did not receive any help or support from commercial consultants. All sources and / or materials applied are listed and specified in the thesis.

Furthermore, I confirm that this thesis has not yet been submitted as part of another examination process neither in identical nor in similar form.

Place, Date Signature

Eidesstattliche Erklärung

Hiermit erkläre ich an Eides statt, die Dissertation “Die Rolle DREAM/MMB-vermittelter mitotischer Genexpression unterhalb von mutiertem K-Ras in Lungenkrebs” eigenständig, d.h. insbesondere selbständig und ohne Hilfe eines kommerziellen Promotionsberaters, angefertigt und keine anderen als die von mir angegebenen Quellen und Hilfsmittel verwendet zu haben.

Ich erkläre außerdem, dass die Dissertation weder in gleicher noch in ähnlicher Form bereits in einem anderen Prüfungsverfahren vorgelegen hat.

Ort, Datum Unterschrift